Multisensory logic of infant-directed aggression by males

Yoh Isogai, Zheng Wu, Michael I. Love, Michael Ho-Young Ahn, Dhananjay Bambah-Mukku, Vivian Hua, Karolina Farrell, Catherine Dulac

PII: S0092-8674(18)31557-5
DOI: doi:10.1016/j.cell.2018.11.032
Reference: CELL 10572

Published in: *Cell*

Received date: 28 October 2017
Revised date: 11 October 2018
Accepted date: 20 November 2018

Cite this article as: Isogai Y, Wu Z, Love MI, Ho-Young Ahn M, Bambah-Mukku D, Hua V, Farrell K, Dulac C, Multisensory logic of infant-directed aggression by males, *Cell*, doi:10.1016/j.cell.2018.11.032

Identification of Infant Cues Driving Attacks by Males

Multi-sensory detection of pups

	Shape	Salivary gland extracts	Attack by ♂
=	=	+	Yes
≠	≠	+	No

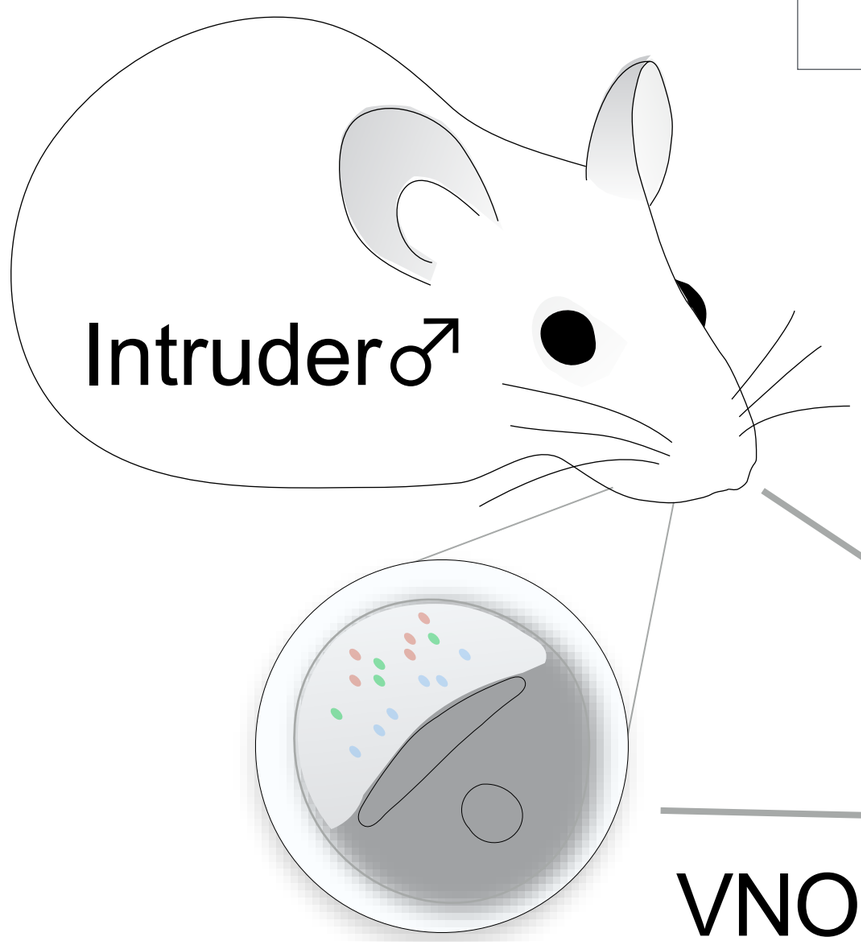

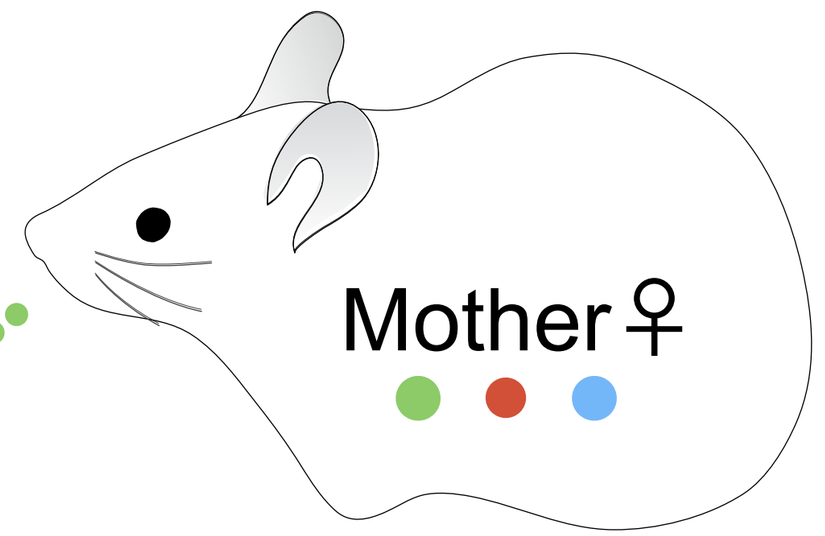

VNO receptors
- Vmn2r88,Vmn2r122/123
- Vmn2r65
- V1rc1, V1rc30, V1ri9

Origin of pup-associated chemosignals
- Hemoglobins
- Submandibular gland protein C
- V1R ligands

Nesting material

Highlights

- Reconstituted pup shape and chemosignals trigger aggression by virgin males
- Repertoire of 7 VNO receptors activated by pups is also stimulated by adult cues
- Deletion of receptors to salivary protein and hemoglobin shows role in pup attack
- Complex recognition involves pup's shape and chemosignals from infants and parents

-

Multisensory logic of infant-directed aggression by males

Yoh Isogai[1,2,*], Zheng Wu[1,4], Michael I. Love[3,5], Michael Ho-Young Ahn[1], Dhananjay Bambah-Mukku[1], Vivian Hua[1], Karolina Farrell[2], Catherine Dulac[1,6,*]

[1]Howard Hughes Medical Institute, Department of Molecular and Cellular Biology, Harvard University, Cambridge, MA 02138, USA

[2]Sainsbury Wellcome Centre for Neural Circuits and Behaviour, University College London, London W1T 4JG, United Kingdom

[3]Dana Farber Cancer Institute, Harvard Medical School, Boston, MA 02215, USA

[4]Present address: Howard Hughes Medical Institute, Department of Neuroscience, Columbia University, New York, NY 10027, USA

[5]Present address: Department of Biostatistics and Department of Genetics, University of North Carolina-Chapel Hill, Chapel Hill, NC 27516, USA

[6]Lead Contact

[*]Authors for correspondence: y.isogai@ucl.ac.uk, dulac@fas.harvard.edu

Summary

Newborn mice emit signals that promote parenting from mothers and fathers, but trigger aggressive responses from virgin males. Although pup-directed attacks by males require vomeronasal function, the specific infant cues that elicit this behavior are unknown. We developed a behavioral paradigm based on reconstituted pup cues and showed that discrete infant morphological features combined with salivary chemosignals elicit robust male aggression. Seven vomeronasal receptors were identified based on infant-mediated activity, and the involvement of two receptors, Vmn2r65, and Vmn2r88, in infant-directed aggression was demonstrated by genetic deletion. Using the activation of these receptors as readouts for biochemical fractionation, we isolated two pheromonal compounds, the submandibular gland protein C and hemoglobins. Unexpectedly, none of the identified vomeronasal receptors and associated cues were specific to pups. Thus, infant-mediated aggression by virgin males relies on the recognition of pup's physical traits in addition to parental and infant chemical cues.

Introduction

In natural environments, animals receive a barrage of sensory information from which salient features trigger behavioral actions (Tinbergen, 1969; Stowers et al., 2002). In turn, sensory information and behavioral decisions are gated by the animal's internal state, enabling sensory inputs to generate motor outputs that are adapted to a given context (Beach, 1942a; Marder, 2012; Chen and Hong, 2018).

The behavioral responses of adult mice to infant cues provide a dramatic example of behavioral variation according to the animal's internal state. When presented with pups, virgin females, mothers and fathers exhibit parental care, which includes nest building, grooming, crouching over pups, aggression towards intruders, and nursing in females. By contrast, virgin males display infanticidal behavior, in which they attack and kill infants (McCarthy and vom Saal, 1985). Previous studies have demonstrated the critical roles of olfactory, somatosensory and auditory cues in maternal behavior (Beach and Jaynes, 1956; Stern, 1990; Marlin et al., 2015). By contrast, vomeronasal function appears largely dispensable for parenting (Kimchi et al., 2007; Tachikawa et al., 2013; Wu et al., 2014). In virgin males, however, genetic and surgical inactivation of the vomeronasal organ (VNO) leads to the loss of pup-directed aggressive behavior, and to the robust expression of parental care (Mennella and Moltz, 1988; Tachikawa et al., 2013; Wu et al., 2014), demonstrating the essential role of VNO cues in eliciting infanticide and in repressing parenting behavior. However, the identity of infant cues that trigger male attacks and the specific vomeronasal receptors (VRs) that detect these cues remain uncharacterized.

To uncover the nature of pup signals leading to aggressive responses in males, we developed a behavioral paradigm in which mice were exposed to reconstituted chemical and physical features of a mouse infant. Remarkably, in addition to pup

chemosignals, discrete morphological traits emerged as an essential trigger to infant-directed aggression. To further dissect the molecular basis of VNO-mediated infant recognition, we identified the entire repertoire of 7 VNO receptors (VRs) detecting pup cues, and exploited these findings to purify two new pheromonal compounds, the submandibular gland protein C, and hemoglobin beta, which activate the Vmn2r65 receptor and the Vmn2r88 and Vmn2r122/123 receptors, respectively. Single and double knockout of *Vmn2r65* and *Vmn2r88* demonstrated their role in male infanticide. Unexpectedly, neither the pup-associated cues nor the receptors responsive to these cues were pup-specific, and instead were shared with adult conspecific cues and their receptors. Altogether, our data suggest that infant-mediated attack by virgin males relies on the detection of multiple pheromonal compounds of broad specificity together with distinctive infant morphological traits.

The surprising lack of VRs and corresponding chemosignals unique to pup contrasts with the large number and high specificity of VRs sensing adult mouse and predator cues and suggests that integrative circuit mechanisms rather than labeled line pathways may drive stereotyped instinctive behaviors such as infanticide by males. Moreover, this vomeronasal “stealth” may point to the conflicting needs of infants to be both concealed and advertised to adults in order to survive and be nurtured.

Results

Reconstitution of signals for pup-directed aggression

Virgin males attack dead pups vigorously, indicating that vocalization, body temperature and movement are not essential cues for pup-directed aggression (Figure 1A, B). Further, pup-directed male aggression occurs in full darkness, suggesting that

vision is also dispensable (not shown). This prompted us to design silicone pup dummies recapitulating the morphological traits of a mouse pup, such as its size, shape, and texture (Figure 1A).

Pup dummies conditioned for an hour with scents from a cage containing a mother and pups elicited robust attacking behavior (Supplemental video 1). Intriguingly, the majority of males attacking pup dummies displayed the stereotypical behaviors seen in aggressive episodes with live or dead pups, such as chemo-investigation, rough handling, aggressive grooming, and biting. We compared aggression directed against dead or dummy pups swabbed with pup salivary gland extracts and established that, dummies conditioned with pup scents (*e.g.,* pup salivary extracts) provoked naturalistic pup-directed aggression (Figure 1B; Supplemental video 1,2), such that the initial investigation of pups by males switches to quickly alternating chemo-investigation and biting. Occasionally, males grab dummies by the mouth, and carry them within the cage with jerky movements, before repeatedly biting them on the ground (Supplemental video 1). Compared to dummies swabbed with pup scents, dead pups provoked more sustained attacks and shorter latency to the first attack (Figure 1B-D), suggesting that additional cues emitted by dead pups intensify male aggression. However, the aggressive behavior of males toward silicone dummies conditioned with pup scents closely mimics attacks of real pups.

To further characterize the minimal set of stimuli required for pup-directed aggression, we swabbed dummies with pup salivary extracts as a source of pup cues; phosphate buffered saline (PBS) as negative control; and adult male urine, a source of chemosignals known to trigger male-directed attacks (Chamero et al., 2007).

Interestingly, dummies coated with PBS alone elicited some low level of attacks (Figure 1E). However, swabbing dummies with pup salivary extracts significantly

increased the duration of aggressive bouts and chemoinvestigative contacts compared to PBS or adult male urine swabbed dummies (Figure 1F). The initial 3 min of the behavior assay contained the highest frequency of aggressive events, and salivary extracts led to significantly higher attack duration and contact time in this period compared to PBS or urine swabbed dummies (Figure 1G).

Collectively, these experiments demonstrated that signals required for pup-directed attacks can be reconstituted using inanimate cues. Importantly, specific chemical cues produced in pup salivary glands significantly enhanced pup-directed aggression, while cues known to be involved in adult-adult aggression, such as adult male urine, did not.

Specific morphological features elicit pup-directed aggression

Next we asked whether specific physical features were instrumental in triggering male attacks during interactions with pups.

Fast-frame videography of adult males investigating pups indicated that males made extensive orofacial contact with pups (Supplemental video 3), prompting us to examine the effect of infant morphological traits in dummy-directed aggression. We tested three additional dummy shapes: the brick, an unnatural object of similar size with sharp edges; the blob, a legless dummy with pup-like head and body curvature; and the hybrid, which combined the brick with limbs and a tail (Figure 1A). Exposure of males to a brick failed to induce aggression, even when painted with pup salivary extracts ($p < 0.001$, Student's *t*-Test, N = 15; Figure 1H-J, Supplemental figure 1). Likewise, the blob did not elicit aggression ($p = 0.12$, Student's *t*-Test, N = 15). Strikingly, however, the hybrid shape with hind and front legs and tail partially restored aggression ($p < 0.01$,

Student's *t*-Test, N = 15), although to a smaller extent than the more realistic dummy shape ($p < 0.05$, Student's *t*-Test, N = 15; Figure 1J).

These results revealed that the identification of pups by aggressive males is a multi-sensory process, involving the recognition of specific physical and chemical signals.

A discrete set of seven VRs detect pup chemosignals

We next aimed to analyze in more detail the contribution of VNO detection in this behavior. To search for VRs activated by pups, we assessed the induction of the immediate early gene *Egr1*, a sensitive molecular readout of VNO neural activity (Isogai et al., 2011), and visualized the activation of subpopulations of VNO neurons following encounters of adult virgin males and females with C57BL6/J pups (Figure 2A,B).

Because pups are taken from the mother's cage and transferred to the behavioral arena, we tested the potential contribution of maternal odor in our assays, and sampled bedding from cages in which mothers had been separated from their pups and housed alone for 2 days. This exposure resulted in the activation of about 4-fold fewer *Egr1*$^+$neurons than from pup exposure (Figure 2A,B), suggesting that our assay robustly monitors VNO activation by pup cues, even in the context of mother-infant cohabitation.

Following exposure to pups, significantly fewer *Egr1*$^+$ cells were detected in the VNO of virgin females and non-aggressive virgin males compared to aggressive virgin males ($p < 0.001$ by Student's *t*-Test, virgin females N = 9, non-aggressive males N = 3; Figure 2B). This is consistent with a previous report showing that VNOs of fathers have reduced *c-fos* activation following pup exposure compared to virgin males (Tachikawa et

al., 2013), and it extends this observation to males lacking aggressive display towards pups, irrespective of their status as virgin or fathers.

Next, we used an *in situ* hybridization-based screen to uncover the identity of VRs expressed in *Egr1*$^{+}$ neurons following pup encounters by aggressive males (Star Methods; Isogai et al., 2011). Five VRs were identified: Vmn2r88 (representing 43.4 ± 0.8 % of *Egr1*$^{+}$ cells; mean ± SEM), V1rc1 or V1rc30 (15.6 ± 1.5 %; our probe does not distinguish between these 2 closely related transcripts), Vmn2r65 (11.2 ± 1.6 %), and V1ri9 (9.0 ± 1.7 %) (Figure 2C,H).

Approximately 20 % of *Egr1*$^{+}$ cells were not covered by the pool of five VR probes, suggesting that one or few additional VRs to pup cues may exist that were not identified in this candidate-based screen (Figure 2C bottom panel, green arrows). We therefore performed a second, unbiased, screen of transcripts associated with the phosphorylated ribosomal protein S6 (pS6) in activated neurons (Knight et al., 2012). Control experiments confirmed that the phosphorylation of the S6 is robustly induced in *Egr1*$^{+}$ neurons upon pup exposure (Figure 2D). Next, we captured the transcriptome of neurons activated by pup cues or fresh bedding by immunopurification of phospho-ribosome associated RNAs (Figure 2E). Data from RNA-seq of pS6 pulled down transcripts were analyzed and searched for transcripts enriched in VNOs from animals exposed to pup cues.

Among these transcripts were genes encoding VRs, but no genes encoding odorant receptors or other classes of known chemosensory receptors (Figure 2F), as well as V1rc1, V1rc30, Vmn2r65, and Vmn2r88, *i.e.*, four out of five VR transcripts identified in our earlier screen (Figure 2G). Two closely related genes V1rc1 and V1rc30, which could not be distinguished from each other by *in situ* hybridization, encoded receptors that are both activated by pup cues. In addition, a VR sequence annotated as

pseudogene Vmn2r-ps159 emerged from the pS6 screen. Upon closer examination, these reads matched perfectly with the sequences of Vmn2r122 and Vmn2r123, previously cloned but not mapped to the genome (Matsunami and Buck, 1997; Ryba and Tirindelli, 1997). We confirmed that VNO neurons expressing Vmn2r122 or 123 (denoted as Vmn2r122/123 since they could not be distinguished by *in situ* hybridization) were robustly activated by pup cues, accounting for 14.0 ± 2.2 % of *Egr1*$^{+}$ neurons (Figure 2H). Overall, the expression of the seven VR genes identified here accounted for 92.2 ± 1.2 % of the VNO neurons activated by pups (Figure 2I), suggesting that we reached a nearly comprehensive identification of VRs to infant cues.

Surprisingly, published work as well as our data revealed that none of the identified VRs were specific to pup cues (Figure 2J), such that they were each also stimulated by either adult male or female cues (Figure 2J). Thus, none of the receptors activated by pup cues conveyed specific information about infants – although they may do so as a group.

Identifying the sources of infant chemosignals

Next, we sought to exploit the identification of VRs activated by pups to search for the corresponding molecular cues. Over 50 % of VNO neurons activated by pups express V2Rs, among which the majority express either Vmn2r65 or Vmn2r88, prompting us to focus on the specific compounds recognized by these two VRs.

Since Vmn2r65 and Vmn2r88 were robustly activated by both adult and pups cues, we first tested the ability of tissue homogenates from organs previously implicated in pheromone production and release, *i.e.*, adult salivary and lacrimal glands (Figure

3A), as well as that of urine, to stimulate Vmn2r65- and Vmn2r88-expressing VNO neurons.

Interestingly, Vmn2r65-expressing neurons were exclusively stimulated by extracts of adult female submaxillary and sublingual glands but not by extracts from any other tissues, or by female urine (Figure 3B,C). Moreover, this activity was exclusively present in female but not male tissues (Figure 3F). In contrast, the ligand activity for Vmn2r88 was detected in extracts from multiple tissues in both males and females, most strongly in salivary and lacrimal glands (Figure 3B,D,F). Salivary extracts from C57BL/6J pup also activated Vmn2r65- and Vmn2r88-expressing neurons (Figure 3B,E). In addition, salivary extracts from both male and female pups from four distinct mouse strains stimulated Vmn2r65, Vmn2r88, and Vmn2r122/123-expressing neurons (Supplemental figure 3).

Thus, both adults and pups produce ligands for Vmn2r65 and Vmn2r88, further strengthening our initial observation that receptors identified based on their activation by pup cues also recognize adult cues. Moreover, our data suggest that responses of Vmn2r65, 88, and Vmn2r122/123 neurons to pup cues are neither sex nor strain specific.

Biochemical purification of compounds associated with pup recognition

We performed biochemical fractionations of tissue homogenates from adult C57BL/6J salivary glands to isolate compounds stimulating Vmn2r65 and Vmn2r88 expressing neurons (Figure 4A, 5A). First, we used size exclusion chromatography to separate molecules by size, then exposed animals to individual fractions and quantified the percentage of activated (*Egr1*$^{+}$) cells among Vmn2r65- or Vmn2r88-expressing VNO

neurons. Our initial analysis revealed that ligands for Vmn2r65 and Vmn2r88 were likely macromolecules with molecular weight of 60-80 kDa and 30-40 kDa, respectively (Figure 4B; Figure 5B). We further purified these samples by ion exchange chromatography (Figure 4C,D; Figure 5D,E), and analyzed active fractions by mass spectrometry (MS, Methods).

This strategy provided us with short lists of candidate ligands for Vmn2r65 and Vmn2r88, which were further narrowed down based on our earlier identification of the strain-, sex-, and salivary gland specificity of ligand activities (Supplemental figure 4A, 5A). Control homogenates from different tissues, strains (C57B6/J and 129S1/SvImJ) and sexes were subjected to identical purification procedures. Specifically, fractionation from male salivary glands was used as a negative control for the Vmn2r65-stimulating activity, which we had earlier identified in gland extracts from pups and adult females only. Likewise, salivary gland extracts from adult males of the 129S1/SvImJ strain had no or only very weak activity on neurons expressing Vmn2r88 and thus served as a negative control for this activity. As further described below, the combination of *Egr1* induction to monitor ligand activity on specific VNO neurons, together with our MS-based screening provided a powerful and efficient platform to identify novel pheromone ligands.

Vmn2r65 is activated by the submandibular gland protein C (Smgc)

Based on previously identified ligands of the large metabotropic glutamate receptor subfamily, we assumed that Vmn2r65 ligands would likely consist of polypeptides (Liberles, 2014). Moreover, the protein(s) of interest should be secreted in order to act as pheromone(s).

The highly purified, active fraction from female salivary glands was strikingly enriched in submandibular gland protein C (Smgc), a large 70 kDa protein previously identified from rat and mouse salivary glands (Zinzen et al., 2004) (Figure 4C,D; Supplemental figure 4A). Interestingly, Smgc is expressed by juveniles of both sexes but exclusively by adult females (Zinzen et al., 2004), consistent with the specificity of activation of Vmn2r65 by juvenile and adult tissue extracts shown earlier (Figure 3E,F; Supplemental figure 3).

We produced full-length recombinant Smgc in *E. coli* and confirmed its biological activity on Vmn2r65-expressing neurons in virgin males, thus demonstrating Smgc as a ligand for Vmn2r65 (Figure 4E,F). Importantly, Smgc was also identified by MS of partially fractionated pup salivary glands (Figure 4G; Supplemental figure 4B), confirming that adult females and pups commonly produce Smgc as a pheromone.

Vmn2r88 is activated by specific paralogs of hemoglobin

We next compared MS datasets obtained with active fractions of salivary gland extracts from C57BL/6J males and females with equivalent (but largely inactive) fractions obtained from 129S1/SvImJ mice. This strategy resulted in a list of secreted proteins that are candidate Vmn2r88 ligands (Supplemental figure 5A). We also noticed that the active purified fractions had a red tint (Supplemental figure 5B). Intriguingly, MS identified hemoglobins (Hbs) among the top candidate Vmn2r88 ligands (Supplemental figure 5A), and the Vmn2r88-stimulating activity was indeed present in blood lysate (Figure 5C). The purified active fraction from salivary gland extracts visualized on a SDS-PAGE gel showed prominent 14 kDa bands (Figure 5D,E), which matches the molecular weight of the monomeric Hb subunits alpha and beta.

Beta subunits of mouse Hb are strain specific (Weaver et al., 1981), and Hbb-bt (also known as Hbbt1; Supplemental figure 5A), the C57BL/6J-specific Hb beta subunit identified by MS satisfied the expected strain-specificity of the Vmn2r88 ligand activity. To reconstitute Hb complexes occurring *in vivo*, we co-expressed recombinant alpha and beta subunits in *E. coli* and purified the resulting complexes (Figure 5F), the vast majority of which proved to be heterodimers of Hbb-bt and Hba-a1 with a minor contribution of tetramers (Supplemental figure 5F,G). We then presented the reconstituted Hb complexes to virgin male mice in order to test if they displayed Vmn2r88 ligand activity.

Indeed, VNO neurons expressing Vmn2r88 showed robustly activation after exposure of virgin males to the Hbb-bt/Hba-a1 complexes (Figure 5G). Interestingly, neurons expressing Vmn2r122/123 were also activated by Hbb-bt/Hbb-a1 (Figure 5G). Finally, Hbb-bt was also identified by MS in pup salivary gland extract fractions with Vmn2r88 ligand activity (Supplemental figure 5C,D,E), demonstrating that Hb represents the Vmn2r88 ligand activity in both adults and pups.

The Hb beta gene locus in mice exists in two major haplotypes, Hbb^s and Hbb^d. The Hbb^s haplotype of the C57BL/6J strain is defined by the Hbb-bt gene while the Hbb^d haplotype of the 129S1/SvImJ strain is represented by the Hbb-b1 and Hbb-b2 genes (Hempe et al., 2007). Because Hbb-bt and Hbb-b1 sequences differ in only three amino acids, we wondered if Vmn2r88 can discriminate between these two ligands. We expressed Hbb-b1 and Hbb-b2, each complexed with Hba-a1 in *E. coli,* and exposed virgin male mice to these purified protein complexes at the same concentration as in our initial test with Hbb-bt/Hba-a1 (0.4 mg at 4 mg/ml). Notably, this concentration is over an order of magnitude below the reported concentration of Hb in the blood of adult mice (~140 mg/ml) (Raabe et al., 2011) and therefore likely falls within a physiological range

as a VNO stimulus. Interestingly, in contrast to the robust activation by Hbb-bt/Hba-a1 (Figure 5G), we observed a much weaker activation of Vmn2r88-expressing neurons by Hbb-b1/Hba-a1 and no apparent activation by Hbb-b2/Hba-a1 (Figure 5H): *Egr1* signals in Vmn2r88-expressing neurons in VNOs of animals exposed to Hbb-b2/Hba-a1 did not significantly exceed the background (1.77 ± 0.13 σ above background, N = 3~4 per stimulus), and this activity was significantly weaker than the activities of Hbb-bt/Hba-a1 and Hbb-b1/Hba-a1 as Vmn2r88 ligands ($p < 0.001$; Figure 5I). These results suggest that Hbs emitted by several mouse strains may act as VNO cues, and that the strength of signaling through Vmn2r88-expressing neurons is strain-dependent. In addition, the specificity of the Vmn2r88 stimulating activity seems to reside in the beta subunit of the Hb complex.

The finding that Vmn2r88 is activated by Hb is highly unexpected, since Hb , although reported to be expressed in tissues other than mature and immature red blood cells (Gomes et al., 2010), is not known to be actively secreted outside the body in the absence of bleeding. Moreover, because attacks by males will naturally release Hb through pup wounding, activation of Vmn2r88 may result from, rather than be the cause of, male aggression. We have shown that Vmn2r88 is also robustly activated in virgin females exposed to pups, suggesting that Hb is naturally presented by pups even in the absence of male attacks (Supplemental figure 2B). These considerations prompted us to further examine the origin of this chemosignal.

Blood from both male and female adult C57BL/6J mice strongly activated Vmn2r88 expressing neurons (Figure 5C). In addition, several lines of evidence suggest that Hb is constitutively deposited in mouse bedding in absence of overt bleeding. First, the Vmn2r88 ligand is enriched in the mixed bedding of adult male mice from five strains (Isogai et al., 2011). Second, we found that bedding from group-housed adult C57BL/6J

males, but not from adult virgin C57BL/6J females, activates Vmn2r88 neurons (Figure 5J). Third, strong Vmn2r88 ligand activity was found in bedding of co-housed pups and mothers, and in pups presented alone, while the ligand activity is not detectable in the bedding of C57BL/6J mothers after they were transferred to new cages with fresh bedding and without pups for two days (Figure 5J).

Strikingly, we consistently identified Hbs in the beddings of mothers cohoused with P1 pups by western blot, while Hbs were not detected in the bedding of similarly single housed non-pregnant females and males (Figure 5L). The observation that Vmn2r88-stimulating activity is found in the bedding of mother with pups could indicate the presence of remnant blood following parturition. This hypothesis prompted us to test the stability of Hb over days. Indeed, we found that hemoglobin's ability to activate Vmn2r88 remains stable for at least three weeks (Figure 5M, N), consistent with the notion of Hb signals able to persist from parturition until weaning.

Finally, in order to determine whether Hbs found in the bedding of co-housed pups and mothers originate from pups, mothers, or both, we tested bedding from cross-fostered pups. Since Hbb-b1, expressed by the 129S1/SvImJ strain, is less active in stimulating Vmn2r88 neurons than Hbb-bt, expressed by C57BL/6J mice, transfer of Hbs from C57BL/6J pups should be detectable in bedding of 129S1/SvImJ mother's cages. However, cross-fostering C57BL/6J pups with 129S1/SvImJ mothers did not increase Vmn2r88 stimulating activity of bedding, while bedding of cross-fostered 129S1/SvImJ pups with C57BL/6J mothers did (Figure 5K). This indicates that mothers, might be a more significant source of Hbs than pups, likely deposited during parturition.

Hbs thus emerge as a new class of chemosignals which, since highly correlated with the birth and continuing presence of pups until weaning, can be exploited by males. Hbs, together with Smgc, are the first compounds isolated based on their participation in

pup signaling to males. However, our attempts to swab recombinant Hbs and Smgc alone and together onto pup dummies did not result in any apparent increase in male aggression. This result indicated that the sole or combined activation of Vmn2r65, Vmn2r88 and Vmn2r122/123-expressing neurons from the seven receptor populations detecting pup cues is insufficient to fully represent the complex blend of pup signals leading to infanticide. Future studies may take advantage of the experimental system developed here to identify ligands corresponding to the other pup-activated VRs, *i.e.*, V1rc1, V1rc30 and V1ri9.

Contribution of two V2Rs in pup-directed aggression

To further assess the significance of Hbs and Smgc as pheromonal compounds, we genetically tested the involvement of the corresponding receptors in pup-directed aggression and generated loss-of-function alleles for the two major receptors activated by Smgc and Hbs, Vmn2r65 and Vmn2r88 (Methods). While not fully abrogating pup detection, combined mutations in these two VR genes, out of the seven VRs responding to infant cues, should reduce the number of VNO neurons activated by pup cues by more than 50% (Figure 2H), and may thus lead to observable effects on pup-mediated behavior compared to wild type animals.

Vmn2r65$^{-/-}$ and Vmn2r88$^{-/-}$ alleles lacking the seven trans-membrane domain were generated by homologous recombination (Figure 6A,B), resulting in complete absence of Vmn2r65 and Vmn2r88 transcripts in mutant VNOs (Figure 6C,D). We tested the resulting virgin male mutants for pup-directed behaviors.

The behavior of Vmn2r65$^{-/-}$ males differed significantly from littermate controls ($p < 0.05$, Fisher's Exact Test, N = 36 for wild type males; N = 35 for Vmn2r65$^{-/-}$ males; Figure 6E), with a decrease in pup-directed aggression in Vmn2r65$^{-/-}$ compared to

Vmn2r65$^{+/+}$ and Vmn2r65$^{+/-}$ virgin males. In addition, an increased number of Vmn2r65$^{-/-}$ animals compared to littermate controls displayed parenting, a response rarely observed in wild type virgin males (2.8 % of wild type males, N = 36 versus 28.6 % of Vmn2r65$^{-/-}$ males, N = 35; Figure 6E).

By contrast, we found no significant difference in pup-mediated attack versus ignoring or retrieving pups in Vmn2r88$^{-/-}$ compared to Vmn2r88$^{+/+}$ and Vmn2r88$^{+/-}$ virgin males (p = 0.11, Fisher's Exact Test; N = 31 for wild type males; N = 29 for Vmn2r88$^{-/-}$ male, p = 0.48, Fisher's Exact Test; N = 29 for Vmn2r88$^{+/-}$ males; N = 29 for Vmn2r88$^{-/-}$ males; Figure 6E). Because Hbs were found to activate both Vmn2r88 and Vmn2r122/123, (Figure 5G) the deletion of the sole Vmn2r88 gene may thus be insufficient to abrogate detection of these cues and impair infanticide.

Next, we analyzed the pup-directed behaviors of double mutant virgin males (Vmn2r65$^{-/-}$;Vmn2r88$^{-/-}$), and found that they dramatically differed from those of wild type males (p < 0.01, Fisher's Exact Test; Figure 6E). Vmn2r65$^{-/-}$;Vmn2r88$^{-/-}$ virgin males displayed a robust reduction in pup-directed aggression compared to wild type controls (53.4 % of wild type males combined for Vmn2r65 and Vmn2r88 groups, N = 67, versus 16.7 % of Vmn2r65$^{-/-}$;Vmn2r88$^{-/-}$ males, N = 30; Figure 6E), while acquiring a significant but modest increase in parental behavior (3.0 % of wild type males combined for Vmn2r65 and Vmn2r88 groups, N = 67, versus 23.3 % of double knockout males, N = 30). Further, 60.0 % of the double mutants (N = 30) failed to exhibit either aggressive or parental behaviors after 30 minutes, even though they extensively chemo-investigated the pups (Figure 6E). Moreover, the difference in the behaviors towards pups between Vmn2r88$^{-/-}$ and Vmn2r65$^{-/-}$;Vmn2r88$^{-/-}$ mice was statistically significant (p = 0.003, Fisher's Exact Test), and non-parental behaviors of Vmn2r65$^{-/-}$ and Vmn2r65$^{-/-}$;Vmn2r88$^{-/-}$ virgin males were also significantly different between the two groups (p = 0.041,

Fisher's Exact Test; Figure 6F), with fewer aggressive animals in the Vmn2r65$^{-/-}$;Vmn2r88$^{-/-}$ cohort than Vmn2r65$^{-/-}$ alone. These results point to a contribution of the Vmn2r88 deletion in pup-directed aggression when combined with the Vmn2r65$^{-/-}$ mutation, and suggest an additivity of receptor functions in the control of pup-directed behavior.

Importantly, we noted that the phenotype of Vmn2r65$^{-/-}$;Vmn2r88$^{-/-}$ virgin males was not equivalent to that of animals completely deprived of VNO function, such as Trpc2$^{-/-}$ (Wu et al., 2014) and VNO-ablated males (Tachikawa et al., 2013), which, in addition to the lack of pup directed attack, display robust parental behaviors. Because infant signals are still detected in Vmn2r65$^{-/-}$;Vmn2r88$^{-/-}$ males through the remaining VRs detecting pups, full display of parenting behavior in these mutants may be hindered by residual VNO signaling.

Detailed analysis of pup-directed behavior in mutants compared to controls (Figure 6G; Supplemental figure 6A) showed that, while the number of animals attacking versus ignoring and parenting was significantly different between genotypes (Figure 6E), there was no quantitative difference for several other measures such as attack latency, duration and latency of parental behaviors (pup retrieval, nest building, crouching over pups, and chemo-investigation of animals showing neither aggression nor retrieval) (Figure 6G; Supplemental figure 6A). This suggests that pheromone inputs may affect the initial behavioral choice rather than the parameters of behavior execution.

Next, we tested Vmn2r65$^{-/-}$;Vmn2r88$^{-/-}$ double mutants for deficits in other social behaviors. VNO neurons expressing Vmn2r65 are activated by female bedding (Isogai et al., 2011), prompting us to test Vmn2r65$^{-/-}$ males for deficits in mating behavior. However, we found no apparent deficit in a variety of parameters associated with mating, such as chemo-investigation, mounting and intromission (Supplemental figure

6B), suggesting that Vmn2r65 is not essential for male-female interactions. Further, we assayed inter-male aggression in double knockout males using a resident intruder test (Supplemental figure 6C). The percentage of Vmn2r65$^{-/-}$;Vmn2r88$^{-/-}$ males attacking intruders in 30 min sessions showed a slight but not statistically significant decrease from that of control animals (p = 0.20, Fisher's Exact Test; 70.0 % for double knockouts, 92.3 % for wild type controls, N = 13 wild type, N = 20 Vmn2r65$^{-/-}$;Vmn2r88$^{-/-}$). In addition, attack duration was indistinguishable from wild type control males (p = 0.36, Student's t-Test, N = 13 wild type, N = 20 Vmn2r65$^{-/-}$;Vmn2r88$^{-/-}$). Further, we found minor effects in the latency of aggression and duration of chemoinvestigative interactions in these animals, including sniffing and grooming. These results suggest that, in contrast to their strong impairment in pup-mediated aggression, Vmn2r65$^{-/-}$;Vmn2r88$^{-/-}$ males only display minor defects in aggression towards adult males.

Taken together, virgin males lacking the ability to sense two specific sets of VNO ligands associated with pups exhibit impaired pup-directed aggression, with a seemingly additive effect of the two receptor mutations. These results suggest an unexpected but efficient solution to the challenge of pup-recognition by virgin males: VNO cues emitted by pups are ambiguous and males must thus rely on the detection of multiple chemosensory cues, together with additional sources of information associated with the presence of pups. Our study demonstrates and identifies the integration of multiple cues – VNO receptor inputs and information about shape – in generating the appropriate response of virgin males towards infants.

Discussion

In this study, we examined the sensory triggers of infanticide by adult males, a dramatic yet poorly understood behavior observed throughout the animal kingdom. Aggression toward infants is displayed by sexually mature intruder males in many species of mammals, and has been extensively studied by ethologists and evolutionary biologists in the context of sexual selection (Hausfater and Hrdy, 1984). This physiological and evolutionary framework, initially developed from the observation of langurs (Sugiyama, 1965; Hrdy, 1974), and further expanded to a variety of primates, lions, rodents, and about half of mammalian species (Lukas and Huchard, 2014), postulates that males seek to increase their reproductive success by killing the offspring of rival males. In turn, the newly infant-deprived mother re-enters the estrus cycle (Hausfater and Hrdy, 1984; McCarthy and Vom Saal, 1986), enabling the intruder male to sire its own offspring.

In mice and rats, existing literature suggests that different types of infant signals initiate either parental care or infanticide (Beach and Jaynes, 1956; Stern, 1990; Tachikawa et al., 2013; Fraser and Shah, 2014; Wu et al., 2014; Marlin et al., 2015). In these species infant olfactory, auditory, and tactile cues can elicit maternal responses (Beach and Jaynes, 1956) (Stern, 1990) (Marlin et al., 2015). Interestingly, deprivation of a single sensory modality has little effect on maternal responses, while deprivation of two or more senses has more severe effects, suggesting that pup recognition by mothers involves the identification of multiple and partially redundant infant signals (Beach and Jaynes, 1956). By contrast, female and male mice in which VNO function is genetically or surgically impaired display largely normal parental behaviors, suggesting that VNO inputs are not required, although they may still participate in infant recognition (Kimchi et al., 2007; Fraser and Shah, 2014).

In mice, the understanding of pup recognition by infanticidal males, although scant, points to a set of cues distinct from those required to trigger parenting. Male mice lacking VNO activity display dramatically reduced aggression towards pups and instead frequently adopt parental behaviors (Mennella and Moltz, 1988; Tachikawa et al., 2013; Wu et al., 2014). This indicates that VNO-mediated infant cues and their cognate receptors, although not required for parental responses, are essential for pup-directed male aggression.

Here, we have used an immediate early gene-based high-throughput assay (Isogai et al., 2011), as well as an independent method based on the phosphorylation of the ribosomal protein S6 in activated neurons (Knight et al., 2012), to uncover the repertoire of seven VRs that together encompass 92.2% of the response to pup cues in aggressive virgin males. Moreover, we demonstrated genetically that two of these receptors, representing over 50% of the VNO response to pup signals, are involved in an additive manner in the sensory detection leading to pup-mediated aggression. These data uncovered an intriguing paradox: although VNO activation by pup cues is required to trigger typical pup-directed aggression by virgin males, the corresponding receptors are promiscuous, additionally recognizing cues from adult males or females, which convey very different types of social information associated with distinct behavioral responses.

These findings provide novel insights into the neurobiology of infant recognition (Figure 7; Supplemental figure 7). First, it appears that neonates do not emit any infant-specific VNO ligands. This is perhaps unsurprising since unambiguous pup-specific identification by the VNO would be predicted to lead to increased attack by virgin males and thus likely be selected against. Instead, VNO cues associated with pups seem to result from mother-infant cohabitation. We found that Smgc and hemoglobins are

abundant in nests of mothers nurturing infants. These chemosignals could therefore be directly transferred to pups.

Despite the absence of non-ambiguous, pup-specific VNO ligands, VNO activation is required for the expression of infanticide (Tachikawa et al., 2013; Wu et al., 2014). Two models may explain the specificity of behavioral responses by aggressive males. It is possible that the simultaneous activation of receptors identifying adult males and females conveys an unusual signal that triggers attack. Alternatively, or in addition to, aggressive males may detect additional non-VNO cues that lead to the unequivocal recognition of infants and attack.

Indeed, a reductionist behavioral paradigm based on pup-shaped silicone dummies, showed that the combined detection of chemical and shape-mediated signals triggers robust expression of pup-directed aggression. By contrast, several other sensory modalities, such as auditory, motion and temperature cues appear dispensable for pup-directed aggression, although these signals may help in further strengthening the aggressive response of males to pups, as suggested by the higher intensity of attacks triggered by live compared to dead infants and scented dummies.

Works by classical ethologists on instinctive behaviors in rats, particularly male mating and female parenting (Beach, 1942b; Beach and Jaynes, 1956) have suggested that, in contrast with the unimodal sign stimuli described by Tinbergen in insects, fish and birds (Tinbergen, 1969), information originating from multiple cues and sensory modalities is required to drive innate behavior in mammals. Similarly, we have uncovered the sensory integration of multiple pheromonal cues, none of which unique to pups, together with pup-mediated somatosensory inputs, as underlying instinctive male infanticide. A model of simple stimuli driving specific behaviors through dedicated labeled-line neuronal pathways may therefore not easily apply to mammals.

In mice, a handful of monomolecular chemical cues have been identified that play important roles in VNO pheromonal responses (Chamero et al., 2007; Haga et al., 2010; Ferrero et al., 2013; Fu et al., 2015). However, with the exception of major urinary proteins promoting territorial marking by males (Kaur et al., 2014), live animals are in many cases necessary to trigger pheromonal actions, thus leaving intact the contribution of multiple sensory cues in triggering behavior output. The reductionist approach developed here should allow for the identification of a comprehensive set of sensory information required to elicit distinct social behaviors.

The discovery of hemoglobins (Hbs) as a new family of VNO receptor ligands is both highly unexpected and intriguing. Hb beta t chain (Hbb-bt) is ubiquitously expressed in C57BL/6J mice at all stages of development and in both sexes (Weaver et al., 1981). Surprisingly, the activity of Vmn2r88 and Vmn2r122/123 mediated by Hbb-bt is found in C57BL/6J pups and in the bedding of adult C57BL/6J males and that of mothers and pups, but not of virgin females. The origin of Hbs in mouse bedding may be two-fold. It is possible that the Hbs deposited in bedding that stimulate Vmn2r88 and Vmn2r122/123 are metabolized byproducts from mothers, pups, or both. Indeed, it has been reported that secreted peptides derived from Hbs play physiological roles (Gomes et al., 2010). In addition, bleeding occurs in a number of related social contexts, particularly parturition. Indeed, blood spots in bedding of mothers who recently delivered pups can often be observed, likely originating from extraembryonic tissues. Importantly, these events take place independently from bleeding from pups resulting from male aggression. Therefore, somewhat unexpectedly, Hbs are ubiquitous in certain social environments and may be exploited as pheromones. Finally, pup bleeding caused by male attacks may further elevate the responses of Vmn2r88 and Vmn2r122/123 expressing neurons, and thus escalate aggressive responses of males to wounded pups. The high sensitivity of the

Vmn2r88 and Vmn2r122/123 receptors in turn appears sufficient for the detection of Hbs at concentrations well below its level in blood.

In conclusion, our study opens new avenues to study the circuit basis underlying the recognition of pups leading to infanticide by males, it uncovers precise physical and chemical features underlying this behavioral response, highlights the combination of multiple sensory modalities in eliciting a stereotyped but physiologically flexible instinctive behavior, and uncovers unusual sensory signaling from infants in a species in which adults can be both nurturing or aggressive.

Acknowledgement

We thank members of the Dulac lab for critical reading of the manuscript, Drs. J. Sanes, M. Yamagata, X. Duan, and P. Liu for recombineering plasmids, the Harvard Genome Modification Facility for generating mouse mutants, the Harvard Proteomics Facility for mass spectrometry, Harvard FAS Bauer Core for Illumina sequencing. We thank Drs. R. Irizarry for assistance with statistics, J. Moore for helping silicone pup fabrication, and D. Lessing for experimental help. We are particularly grateful for S. Sullivan's expert assistance with animal experiments and procedures. We also thank Dr. R. Axel for advice on the manuscript. M.I.L. is supported by NIH grants CA142538-08 and 5T32CA009337-35, Y.I. by a Charles A. King Trust fellowship and funds from the Gatsby Charitable Foundation and Wellcome Trust. C.D. is supported by HHMI and by NIH grants R01DC013087, R01DC003903, and R01HD082131.

Author contributions

Y.I. and C.D. designed the study. Y.I. performed all the experiments except those mentioned below. Z.W. constructed targeting vectors, M.I.L. designed pS6 experiments and analyzed the RNA-seq data, M.H.Y.A. scored the behavioral results and performed mating assays, and D.B.M. performed mating assays. V.H. helped construct the dummy assay and scored Egr1 in situ hybridization data, and K.F. scored dummy experiment data and produced recombinant hemoglobins. Y.I. and C.D. wrote the paper with inputs from other authors.

Declaration of interests

The authors declare no competing interests associated with this study.

References

Beach, F.A. (1942a). Analysis of factors involved in the arousal, maintenance and manifestation of sexual excitement in male animals. Psychosomatic Medicine *4*, 173-198.

Beach, F.A. (1942b). Analysis of the stimuli adequate to elicit mating behavior in the sexually inexperienced rat. Journal of Comparative Psychology *33*, 163-207.

Beach, F.A., and Jaynes, J. (1956). Studies of Maternal Retrieving in Rats. III. Sensory Cues Involved in the Lactating Female's Response To Her Young. Behaviour *10*, 104-124.

Chamero, P., Marton, T.F., Logan, D.W., Flanagan, K., Cruz, J.R., Saghatelian, A., Cravatt, B.F., and Stowers, L. (2007). Identification of protein pheromones that promote aggressive behaviour. Nature *450*, 899-902.

Chan, W., Costantino, N., Li, R., Lee, S.C., Su, Q., Melvin, D., Court, D.L., and Liu, P. (2007). A recombineering based approach for high-throughput conditional knockout targeting vector construction. Nucleic Acids Res *35*, e64.

Chen, P., and Hong, W. (2018). Neural Circuit Mechanisms of Social Behavior. Neuron *98*, 16-30.

Ferrero, D.M., Moeller, L.M., Osakada, T., Horio, N., Li, Q., Roy, D.S., Cichy, A., Spehr, M., Touhara, K., and Liberles, S.D. (2013). A juvenile mouse pheromone inhibits sexual behaviour through the vomeronasal system. Nature *502*, 368-371.

Fraser, E.J., and Shah, N.M. (2014). Complex chemosensory control of female reproductive behaviors. PLoS One *9*, e90368.

Fu, X., Yan, Y., Xu, P.S., Geerlof-Vidavsky, I., Chong, W., Gross, M.L., and Holy, T.E. (2015). A Molecular Code for Identity in the Vomeronasal System. Cell *163*, 313-323.

Gomes, I., Dale, C.S., Casten, K., Geigner, M.A., Gozzo, F.C., Ferro, E.S., Heimann, A.S., and Devi, L.A. (2010). Hemoglobin-derived peptides as novel type of bioactive signaling molecules. AAPS J *12*, 658-669.

Haga, S., Hattori, T., Sato, T., Sato, K., Matsuda, S., Kobayakawa, R., Sakano, H., Yoshihara, Y., Kikusui, T., and Touhara, K. (2010). The male mouse pheromone ESP1 enhances female sexual receptive behaviour through a specific vomeronasal receptor. Nature *466*, 118-122.

Hausfater, G., and Hrdy, S.B. (1984). Infanticide : comparative and evolutionary perspectives (New York: Aldine Pub. Co.).

Hempe, J.M., Ory-Ascani, J., and Hsia, D. (2007). Genetic variation in mouse beta globin cysteine content modifies glutathione metabolism: implications for the use of mouse models. Exp Biol Med (Maywood) *232*, 437-444.

Hrdy, S.B. (1974). Male-male competition and infanticide among the langurs (Presbytis entellus) of Abu, Rajasthan. Folia Primatol (Basel) *22*, 19-58.

Isogai, Y., Si, S., Pont-Lezica, L., Tan, T., Kapoor, V., Murthy, V.N., and Dulac, C. (2011). Molecular organization of vomeronasal chemoreception. Nature *478*, 241-245.

Kaur, A.W., Ackels, T., Kuo, T.H., Cichy, A., Dey, S., Hays, C., Kateri, M., Logan, D.W., Marton, T.F., Spehr, M.*, et al.* (2014). Murine pheromone proteins constitute a context-dependent combinatorial code governing multiple social behaviors. Cell *157*, 676-688.

Kimchi, T., Xu, J., and Dulac, C. (2007). A functional circuit underlying male sexual behaviour in the female mouse brain. Nature *448*, 1009-1014.

Knight, Z.A., Tan, K., Birsoy, K., Schmidt, S., Garrison, J.L., Wysocki, R.W., Emiliano, A., Ekstrand, M.I., and Friedman, J.M. (2012). Molecular profiling of activated neurons by phosphorylated ribosome capture. Cell *151*, 1126-1137.

Liberles, S.D. (2014). Mammalian pheromones. Annu Rev Physiol *76*, 151-175.

Love, M.I., Huber, W., and Anders, S. (2014). Moderated estimation of fold change and dispersion for RNA-seq data with DESeq2. Genome Biol *15*, 550.

Lukas, D., and Huchard, E. (2014). Sexual conflict. The evolution of infanticide by males in mammalian societies. Science *346*, 841-844.

Marder, E. (2012). Neuromodulation of neuronal circuits: back to the future. Neuron *76*, 1-11.

Marlin, B.J., Mitre, M., D'Amour J, A., Chao, M.V., and Froemke, R.C. (2015). Oxytocin enables maternal behaviour by balancing cortical inhibition. Nature *520*, 499-504.

Matsunami, H., and Buck, L.B. (1997). A multigene family encoding a diverse array of putative pheromone receptors in mammals. Cell *90*, 775-784.

McCarthy, M.M., and vom Saal, F.S. (1985). The influence of reproductive state on infanticide by wild female house mice (Mus musculus). Physiol Behav *35*, 843-849.

McCarthy, M.M., and Vom Saal, F.S. (1986). Inhibition of infanticide after mating by wild male house mice. Physiol Behav *36*, 203-209.

Mennella, J.A., and Moltz, H. (1988). Infanticide in the male rat: the role of the vomeronasal organ. Physiol Behav *42*, 303-306.

Raabe, B.M., Artwohl, J.E., Purcell, J.E., Lovaglio, J., and Fortman, J.D. (2011). Effects of weekly blood collection in C57BL/6 mice. J Am Assoc Lab Anim Sci *50*, 680-685.

Ryba, N.J., and Tirindelli, R. (1997). A new multigene family of putative pheromone receptors. Neuron *19*, 371-379.

Stern, J.M. (1990). MULTISENSORY REGULATION OF MATERNAL-BEHAVIOR AND MASCULINE SEXUAL-BEHAVIOR - A REVISED VIEW. Neuroscience and Biobehavioral Reviews *14*, 183-200.

Stowers, L., Holy, T.E., Meister, M., Dulac, C., and Koentges, G. (2002). Loss of sex discrimination and male-male aggression in mice deficient for TRP2. Science *295*, 1493-1500.

Sugiyama, Y. (1965). On the social change of hanuman langurs (Presbytis entellus) in their natural condition. Primates *6*, 381-418.

Tachikawa, K.S., Yoshihara, Y., and Kuroda, K.O. (2013). Behavioral transition from attack to parenting in male mice: a crucial role of the vomeronasal system. J Neurosci *33*, 5120-5126.

Tinbergen, N. (1969). The study of instinct, 1st edn (Oxford,: Clarendon P.).

Weaver, S., Comer, M.B., Jahn, C.L., Hutchison, C.A., 3rd, and Edgell, M.H. (1981). The adult beta-globin genes of the "single" type mouse C57BL. Cell *24*, 403-411.

Wu, Z., Autry, A.E., Bergan, J.F., Watabe-Uchida, M., and Dulac, C.G. (2014). Galanin neurons in the medial preoptic area govern parental behaviour. Nature *509*, 325-330.

Zinzen, K.M., Hand, A.R., Yankova, M., Ball, W.D., and Mirels, L. (2004). Molecular cloning and characterization of the neonatal rat and mouse submandibular gland protein SMGC. Gene *334*, 23-33.

Main figure titles and legends

Figure 1: Combination of physical and chemical signals triggers pup-directed aggression.

(A) Images of real pup and four silicone pup decoys used in these experiments

(B) Raster plots of behaviors by virgin males (N = 19) presented with dummies swabbed with C57BL/6J salivary extract (top) or dead C57BL/6J pups (bottom). Red: aggressive encounters with biting, blue: chemo-investigative bouts.

(C) Total aggression per 5 min assay is significantly longer when males are exposed to dead pups compared to dummies ($p < 0.001$ by *t*-Test). N = 19.

(D) Latency to attack is significantly shorter when males are exposed to dead pups compared to dummies ($p < 0.01$ by *t*-Test). N = 19.

(E,F) Durations of aggressive interactions and all contacts in the initial 3 min of encounters in which males are presented with dummies swabbed with PBS (blue), pup salivary extracts (red) and adult male urine (yellow). *$p < 0.05$, **$p < 0.01$ by paired *t*-Test, N = 15. Connected circles represent data obtained with the same males.

(G) Sliding window analysis of aggressive interactions between males and dummies swabbed with various chemical cues. Top graph shows the cumulative duration of aggressive bouts in 2 min sliding windows. Bottom graph shows the *p* values of the paired *t*-Test for differences in aggressive bout durations between dummies swabbed with PBS and pup salivary extracts (blue) or between dummies swabbed with male urine and pup salivary extracts (brown) in 2 min sliding windows. N = 15.

(H) Raster plots of behaviors by virgin males exposed to various silicone dummies. Each event marks an interaction between males and the introduced pup decoy swabbed with

pup salivary extract, with events categorized as aggressive (red) or non-aggressive (blue). N = 15.

(I) *p*-values of the paired *t*-Test for the differences in aggressive bout durations between decoys of various shapes swabbed with PBS and pup salivary extracts (blue) or between decoys swabbed with male urine and pup salivary extracts (brown) tested in 2 min sliding windows. Note the late attack against the "hybrid" decoy. N = 15.

(J) Cumulative aggression times by virgin males presented with pup decoys of four different shapes swabbed with pup salivary extract $*p < 0.05$, $**p < 0.01$, $***p < 0.001$ by paired *t*-Test. N = 15.

Figure 2: Pup cues activate seven VRs in the adult VNO

(A,B) *Egr1* induction in the VNO of virgin male and female mice upon pup exposure. The number of *Egr1*$^+$ VNO neurons identified in these experiments is shown in **(B)**. Each data point represents one animal. Number of animals used is indicated in the graph. $***p < 0.001$ by *t*-Test. Dark lines indicate the mean, and light lines indicate the quartiles.

(C) Top four panels: double FISH with RNA probes to *Egr1* and candidate *VRs* led to the identification of five VRs responding to pup cues. Arrows indicate cells in which *Egr1* (green) and VR signals (red) co-localize. Bottom panel: double FISH with RNA probes to *Egr1* (green) and a mix of the five VR probes shown in panels above. White arrows point to co-labeled neurons, and green arrows indicate *Egr1*$^+$ neurons that express none of the 5 identified VRs.

(D) Immunofluorescence with anti-pS6 antibody and *in situ* hybridization with RNA probe to *Egr1* demonstrates co-expression (arrows) in VNO neurons activated by pup cues (94.7 ± 2.2 % of *Egr1*$^+$ neurons are pS6$^+$; mean ± SEM; 699 *Egr1*$^+$ cells from 3 animals examined).

(E) Experimental pipeline for immuno-purification of phospho-ribosome associated RNAs from VNOs of animals exposed to pup cues.

(F) MA (log_2 difference over signal strength) plot showing the enrichment of specific VR in the VNOs of virgin males exposed to pup stimuli compared to fresh bedding. Red dots represent genes significantly ($p < 0.1$) over-represented in pup-exposed VNO samples. Green dots represent enriched VR genes.

(G) List of VRs identified in the pS6-based screen. The screen failed to identify the sparsely represented V1ri9 identified by the candidate VR screen (shown in C).

(H) Comprehensive set of VRs activated by pup cues. Double FISH with individual *VR* and *Egr1* probes. Are shown the percentages of co-labeled neurons (N = 3 animals with total number of VR^+ cells analyzed indicated in parentheses).

(I) Double RNA FISH with probes to *Egr1* and the mix of 7 receptor probes shown in H (N = 3 animals).

(J) Summary of responses by VRs, identified based on their recognition of pup cues, to non-pup cues, from data by Isogai et al. 2011 and data shown in Supplemental figure 2A.

All scale bars represent 100 µm unless indicated otherwise.

Figure 3: The origins of pup stimuli

(A) Schematic diagram depicting the location of various exocrine glands (green: lacrimal, orange: salivary, pink: preputial) used to test Vmn2r65 and Vmn2r88 ligand activity.

(B) Summary of VR activity using gland extracts from adults and pups, and adult urine. n/d: not determined.

(C) Vmn2r65 ligand activity is found exclusively in female submaxillary gland extract. RNA FISH with *Egr1* and *Vmn2r65* probes on virgin male VNOs after exposure to urine

and gland extracts from adult virgin females. Arrows mark Egr1 and Vmn2r65 co-expression.

(D) Vmn2r88 ligand activity is found in extracts of multiple glands. RNA FISH with *Egr1* and *Vmn2r88* probes on VNOs from virgin males after exposure to urine and gland extracts from adult virgin males. Arrows mark Egr1 and Vmn2r88 co-expression.

(E-F) Vmn2r88 and Vmn2r65 ligand activities are found in both pup and adult tissue extracts. All experiments were performed on 2 animals per stimulus, and the mean percentage of $VR^{+}Egr1^{+}$ neurons in VR^{+} cells in virgin male VNOs is indicated, along with the number of cells analyzed. All errors are in SEM.

All scale bars represent 100 µm.

Figure 4: The submandibular gland protein C (Smgc) activates neurons expressing Vmn2r65.

(A) Purification strategy of compound(s) activating Vmn2r65 neurons (see Methods). The mass spectrometry profile of the peak activity fractions obtained from adult female salivary gland extracts was compared to the most homologous fractions obtained from male gland extracts.

(B) Activity profile of gel filtration chromatography fractions using female C57BL/6J salivary gland extract as a starting material. The ligand activity for Vmn2r65 was assayed by exposure of virgin males to selected fractions. Each dot represents the mean percentage of $Vmn2r65^{+}Egr1^{+}$ neurons among all $Vmn2r65^{+}$ neurons from quantified on at least four VNO sections. Molecular weight for each fraction was estimated by SDS-PAGE. The ligand activity appears to elute broadly from this column, spanning 60 to 90 kDa.

(C) Activity profile of anion exchange chromatography fractions using Sepharose DEAE peak activity fractions as the input. The arrow marks the peak activity fraction (assayed in **D**), which was further analyzed by mass spectrometry.

(D) RNA FISH showing that Vmn2r65 neurons are activated by the exposure of virgin males to the peak fraction of anion exchange chromatography.

(E) SDS-PAGE gel of recombinant histidine-FLAG double-tagged Smgc produced in *E. coli*.

(F) Exposure of virgin males to recombinant Smgc results in specific activation of *Vmn2r65*$^{+}$ VNO neurons. RNA FISH of VNO sections from virgin males exposed to recombinant Smgc shows co-localization of *Egr1* and *Vmn2r65* (arrows) (84.2 ± 5.0% of *Vmn2r65*$^{+}$ neurons; Error in SEM; 166 *Vmn2r65*$^{+}$ neurons from 3 animals examined).

(G) Fractionated C57BL6/J pup salivary gland extracts activate Vmn2r65-expressing neurons.

All scale bars represent 100 µm.

Figure 5: Hemoglobins are polymorphic ligands of Vmn2r88 and Vmn2r122/123

(A) Purification scheme of the Vmn2r88 ligand (see Methods).

(B) Activity profile of C57BL6/J male salivary gland extracts after gel filtration chromatography. The activity was assessed as the percentage of Vmn2r88-expressing neurons with *Egr1* signal.

(C) Adult C57BL/6J blood activates Vmn2r88-expressing VNO neurons (Male blood: 92.5 ± 1.8 % of Vmn2r88 neurons; Error in SEM; 161 Vmn2r88 neurons from 2 animals; Female blood: 97.3 ± 0.4 % of Vmn2r88 neurons; 152 Vmn2r88 neurons from 2 animals examined).

(D) Vmn2r88-stimulating activity of the purified Poros HQ peak fraction confirmed by RNA FISH. Arrows mark colocalization between *Egr1* and *Vmn2r88*.

(E) Protein gel of the Poros HQ active peak fraction used for mass spectrometry.

(F) Recombinant hemoglobin produced in *E. coli* is red, indicating the presence of heme.

(G) Recombinant Hbb-bt/Hba-a1 robustly activates Vmn2r88-expressing neurons (94.1 ± 0.9 % of Vmn2r88 neurons; mean ± SEM; 240 Vmn2r88 neurons from 4 animals examined) and Vmn2r122/123-expressing neurons (63.4 ± 16.4 % of Vmn2r122/123 neurons; 184 Vmn2r122/123 neurons, 3 animals). Virgin males were exposed to recombinant Hbs and their VNOs were analyzed for the activation of *Egr1* in Vmn2r88 or Vmn2r122/123 neurons. **(H,I)** Specificity of Vmn2r88 activation by Hbs. Virgin males were exposed to recombinant Hbb-b1/Hba-a1 and Hbb-b2/Hba-a1, and their VNOs were analyzed by RNA FISH with *Egr1* and *Vmn2r88* probes. The intensities of the *Egr1* signals in Vmn2r88 neurons in Figure 5G,H, represented as fold increase from the standard deviation of image background, are plotted in a graph in Figure 5I. Each dot represents one cell. ***$p < 0.001$ by *t*-Test.

(J) Vmn2r88 ligand activity is deposited in bedding of males and in bedding of mothers cohabitating with infants. Mother/pup bedding robustly excites Vmn2r88 neurons, as evidenced by RNA FISH showing the colocalization of *Egr1* and *Vmn2r88* signals in the VNO of animals exposed to these cues (arrows). All experiments used 3 or 4 animals, and the percentage of $Vmn2r88^{+}Egr1^{+}$ cells in $Vmn2r88^{+}$ neurons are indicated, along with the total number of cells analyzed. All errors are in SEM.

(K) Plot of *Egr1* signals (represented as fold increase from the standard deviation of image background) in Vmn2r88 neurons, stimulated by bedding of cross-fostered cages. Bedding from cross-fostered cages (one 129S1/SvImJ mother with C57BL/6J pups, one 129S1/SvImJ mother with 129S1/SvImJ pups, one C57BL/6J mother with 129S1/SvImJ pups, N = 3 each). **$p < 0.01$ by Student's *t*-Test.

(L) Hemoglobin is readily detectable in the cage of pregnant and post-partum females with pups. Shown is a protein blot of bedding extracts probed by anti-Hb beta antibody.

Bedding from three females (A, B, C) for each condition and males (D,E,F) are used for this panel.

(M,N) Recombinant Hbb-bt/Hba-a1 was stored at room temperature for indicated period of time and tested for its ability to stimulate Vmn2r88-expressing neurons. Two CD-1 virgin males were used for this test per sample. The box plot in **(N)** shows the quantification of the *Vmn2r88* neurons co-labeled with *Egr1*. 4 sections from 2 animals were quantified for each time point.

All scale bars represent 100 µm unless otherwise indicated.

Figure 6: Vmn2r88 and Vmn2r65 contribution to pup-directed aggression by virgin adult males.

(A, B) Schematic of VR knockout constructs. The targeted **(A)** Vmn2r65 and **(B)** Vmn2r88 loci lack the transmembrane domain of the corresponding receptor.

(C, D) RNA FISH using probes specific to Vmn2r65 and Vmn2r88 (Isogai et al., 2011) confirms the loss of Vmn2r65 and Vmn2r88 expression in the VNO of $Vmn2r65^{-/-}$ and $Vmn2r88^{-/-}$ mice, respectively.

(E) Pup directed behaviors are altered in receptor knockout virgin males. Each circle represents a single animal, and the assignment of each animal in three behavioral outcomes is unique. *$p < 0.05$, **$p < 0.01$ by Fisher's Exact Test.

(F) Number of non-parental animals is significantly different between mice in which specific receptor inputs are deleted. *$p < 0.05$, **$p < 0.01$ by Fisher's Exact Test.

(G) Detailed quantitative analysis of pup-directed behaviors. The full analysis from all genotypes is presented in Supplemental figure 6A.

All scale bars represent 100 µm.

Figure 7: Pup recognition by virgin males involves multi-sensory inputs.

A model of vomeronasal signals associated with pups. Chemical signals associated with the presence of infants in fact originates from both pups and mothers.

Supplemental figure title and legends

Supplemental figure 1 (in relation to Figure 1):

(A-D) Raster plots of behavioral events by virgin males exposed to various types of silicone shapes swabbed with pup salivary extract, PBS, or male urine. The aggressive and non-aggressive bouts are marked by red and blue boxes, respectively. Below each raster plot is a sliding window analysis (2 min), using the same procedure as in Figure 1I. N = 15.

Supplemental figure 2 (in relation to the figure 2): Responses of Vmn2r122/123 and Vmn2r88 to various social stimuli.

(A) *Egr1* is robustly induced in VNO neurons expressing *Vmn2r122/123* in virgin males exposed to male C57BL/6J submaxillary gland extracts (82.2 ± 6.0% of Vmn2r122/123 cells are $Egr1^{+}$; Error in SEM; 38 $Vmn2r122/123^{+}$ neurons from 2 animals examined).

(B) Response of Vmn2r88 neurons to pups in virgin females exhibiting maternal behaviors. 78.9 ± 6.2% of Vmn2r88 neurons overlap with *Egr1* (245 Vmn2r88 neurons examined, N = 3 animals). Arrow marks the overlap of *Egr1* and *VR* signals.

The scale bar represents 100 μm.

Supplemental figure 3 (in relation to the Figure 3): V2R receptors detecting pups are sex and strain independent.

(A-D) In situ hybridization with probes of *Egr1* and vomeronasal receptors on VNOs of virgin CD-1 males exposed to salivary gland extracts of male or female pups from 4 different strains (n =2 animals per stimulus).

(**E**) Quantification of in situ hybridization signals. The percentage of VR^+ neurons that also co-express *Egr1* was quantified in the above experiments. The errors are in SEM, and total numbers of VR^+ neurons quantified are indicated in parentheses.

Supplemental figure 4 (in relation to the figure 4): Additional data for the identification of Smgc as a ligand for Vmn2r65.

(A) List of proteins identified by mass spectrometry that are exclusively enriched in ion exchange column fractions derived from female salivary gland.

(B) Smgc peptides identified by mass spectrometry of the partially fractionated preparation of pup salivary glands.

Supplemental figure 5 (in relation to the figure 5): Additional data for the identification of hemoglobins as ligands for Vmn2r88.

(A) List of proteins identified by mass spectrometry in purified active fraction derived from C57BL/6J male salivary gland extracts. Hemoglobin Hbb-bt (in this diagram denoted as Hbbt1, per Uniprot nomenclature) emerges as a top candidate.

(B) The peak activity fraction of Poros HQ chromatography is red.

(C) Silver stained gel of the peak activity fraction derived from pup salivary gland extracts showed a unique 14 kDa band.

(D) *In situ* hybridization of *Vmn2r88* and *Egr1* in the VNO of animals exposed to the peak fraction shown in (C).

(E) Peptides corresponding to hemoglobins identified by mass spectrometry analysis of the purified pup fractions. This analysis confirmed that Hbb-bt (or Hbbt1) is a top candidate.

(F) Gel filtration chromatography of recombinant hemoglobin Hbb-bt/Hba-a1. Purified recombinant hemoglobin appeared predominantly as a dimer rather than tetramer.

Endogenous hemoglobin tetramer in C57BL/J male blood extracts has a significantly shorter retention time than the major recombinant hemoglobin peak. Note that the Hba-a1 subunit in the recombinant hemoglobin is 11 amino acids longer than the native protein, resulting in a shorter retention time.

(G) Quantitative analysis of the retention times of hemoglobins in gel filtration chromatography. The table shows the mean retention time of the tetramer and dimer peaks (shown as arrows in F) (N = 3 technical replicates).

Supplemental figure 6 (in relation to the figure 6): Quantification of social behaviors in receptor knockout mice.

(A) Analysis of pup-directed behaviors of mutants including the attack latency of the aggressive animals ($Vmn2r65^{+/+}$, N = 19; $Vmn2r65^{+/-}$, N = 20; $Vmn2r65^{-/-}$, N = 13; $Vmn2r88^{+/+}$, N = 17; $Vmn2r88^{+/-}$, N = 15; $Vmn2r88^{-/-}$, N = 17; dKO, N = 5), the total chemoinvestigative events of ignoring animals, ($Vmn2r65^{+/+}$, N = 16; $Vmn2r65^{+/-}$, N = 9; $Vmn2r65^{-/-}$, N = 12; $Vmn2r88^{+/+}$, N = 13; $Vmn2r88^{+/-}$, N = 12; $Vmn2r88^{-/-}$, N = 7; dKO, N =18), and a repertoire of parental behavior ($Vmn2r65^{+/+}$, N = 1; $Vmn2r65^{+/-}$, N = 1; $Vmn2r65^{-/-}$, N = 10; $Vmn2r88^{+/+}$, N = 1; $Vmn2r88^{+/-}$, N = 4; $Vmn2r88^{-/-}$, N = 5; dKO, N = 7). Comparisons yield no statistically significant difference between genotypes by t-Test.

(B) The analysis of mating behavior in $Vmn2r65^{-/-}$ males ($Vmn2r65^{+/+}$ or $Vmn2r65^{+/-}$, N = 13; $Vmn2r65^{-/-}$, N = 14). $Vmn2r65^{-/-}$ virgin males were presented with hormonally primed estrus females and individual behaviors representative of mating response were quantified.

(C) Resident intruder assay with $Vmn2r65^{-/-}$;$Vmn2r88^{-/-}$ virgin males. The table shows the overall counts of the attacked animals in 1 hr behavioral bout ($p = 0.20$ by Fisher Exact Test). *$p < 0.05$ by *t*-Test. The graphs show the analysis of territorial aggression of $Vmn2r65^{-/-}Vmn2r88^{-/-}$ males (WT males, N = 13; $Vmn2r65^{-/-}Vmn2r88^{-/-}$, N = 20). Several

parameters such as the total time in chemoinvestigation, grooming and attack latency exhibited statistically significant difference. *$p < 0.05$ by Student's *t*-Test.

Supplemental figure 7 (in relation to Figure 7): Summary of the sensory requirements for pup-directed aggression by virgin males.

STAR METHODS

KEY RESOURCES TABLE

CONTACT FOR REAGENT AND RESOURCE SHARING

Further information and requests for resources and reagents should be directed to, and will be fulfilled by, Catherine Dulac (dulac@fas.harvard.edu).

EXPERIMENTAL MODEL AND SUBJECT DETAILS

Mice

Animals were maintained on 12 hr:12hr light/dark cycle with food and water provided ad libitum. Care of animals and experiments were performed in accordance with NIH guidelines and approved by the Harvard University Institutional Animal Care and Use Committee (IACUC). Only healthy animals were used for this study. Behavior experiments were performed in the dark phase of the light/dark cycle. In addition, all animals were initially group-housed in single sex cages post weaning and subsequently single housed prior to behavior experiments. For experiments described in Figure 1, male TrpC2$^{+/-}$ mice were used. These animals were single housed starting at 4 months old. For stimulus exposure experiments described in Figures 2,3,4, and 5, CD-1 males and females older than 4 weeks were used. For experiments described in Figure 6, all behavioral tests with receptor knockout mice, knockouts and littermate controls, including wild types and heterozygotes were performed with 3 to 6 month old animals. Vmn2r65 and Vmn2r88 single knockout males as well as littermate wild type and heterozygous control males were generated by heterozygous crosses**.** Vmn2r65$^{-/-}$;Vmn2r88$^{-/-}$ mice were generated using homozygous as well as heterozygous crosses.

METHOD DETAILS

RNA ANALYSIS

RNA *in situ* hybridization

Chromogenic in situ hybridization developed with NBT/BCIP was performed as previously described (Isogai et al., 2011). Fluorescence RNA *in situ* hybridization was performed as previously detailed (Isogai et al., 2011), except for use of either FITC or Dinitrophenyl (DNP) labeled *Egr1* probe and DIG labeled vomeronasal receptor probes. Sequences of probe targets are found in the Supplemental Table 1. Reagents used for RNA *in situ* hybridization are also listed in the Key Resources Table.

Phospho-S6 pulldown

The immunoprecipitation of phosphorylated polysomes from vomeronasal organs was performed as described in Knight et al. 2012. Briefly, VNOs were pooled from as many as five CD-1 adult males (Charles River) exhibiting pup directed aggression, and tissue homogenates were prepared in the presence of RNase inhibitors (RNasin, Promega; SUPERase•In, Life Technologies) and Protease and Phosphatase Inhibitors (Halt, Pierce; Calyculin A, Santa Cruz Biotechnology). The extract cleared by detergent (DHPC and NP-40) treatment and high-speed centrifugation was mixed with Protein A Dynabeads (Invitrogen), pre-incubated with anti-pS6 (240/244) antibody (Cell Signaling Technology) and incubated for 10 min at 4 ℃. After high salt washes, the bound polysomes were eluted and purified using Absolutely RNA Nanoprep Kit (Agilent). The blocking peptide for Phospho-S235/236 was not included, since antibodies specific to Phospho-S235/236 of the ribosomal protein S6 did not label any neurons in the VNO unless the cells were stimulated. As controls for this assay, pulldowns were performed

with VNOs from animals presented with fresh bedding. The experiments were done in triplicates.

RNA sequencing

SMARTer Ultra Low Input RNA for Illumina Sequencing - HV and Low Input Library Prep Kit (Clontech) were used to prepare RNA sequencing libraries. The cDNA libraries were sequenced by Illumina HiSeq 2500 using 50 bp paired end, rapid flow cells, which produced 15~20 million reads per sample.

PURIFICATION OF VOMERONASAL LIGANDS

Extract preparation

Salivary glands (containing both submaxillary and sublingual glands but not preputial gland) were dissected from adult (5 weeks to 1 year old) mice of strains such as C57BL/6J. The glands from males and females were collected separately and served for extract preparation. Pup glands were dissected from C57BL/6J pups (P1~P6), which consisted of both males and females. 129S1/SvImJ salivary glands were also dissected and processed identically. Approximately 1 gram of tissue was homogenized in 2 ml of 1x PBS supplemented with cOmplete EDTA-free Protease Inhibitor Cocktail tablet (Roche), 0.25 μM PMSF, 10 μg/ml AEBSF and 0.5 mM DTT in 4 ℃. After centrifugation in 15,000 rpm for 30 min, the supernatant was transferred to a beaker in which a bulk of the proteins was precipitated with ammonium sulfate (below).

Ammonium sulfate precipitation

Ammonium sulfate precipitation was performed using standard procedures. Briefly, 0.23 grams of ammonium sulfate were added to achieve 40 % saturation at 4 ℃. After the crystals were completely dissolved upon a 1 hr mixing on ice, the precipitate was

pelleted by centrifugation at 4 ℃. Since the super natant retained the activity, this fraction was filtered using 0.45 µm PES syringe filter (Millipore) and the ammonium sulfate was removed by either dialysis to 1x PBS or by buffer exchange using a spin column (Amicon Ultra-0.5 mL Centrifugal Filters, 10 kDa cutoff, Millipore).

Gel filtration chromatography

Sephacryl S100HR (GE Healthcare Life Sciences) was connected to PerSeptive Biosystems BioCAD Vision Workstation (Applied Biosystems) and 1x PBS was used as the column buffer. Approximately 1~2 ml of supernatant after the ammonium sulfate step was concentrated by Amicon Ultra-0.5 mL Centrifugal Filters and injected into the column. The protein compositions of every third fractions of this column were analyzed on SDS-PAGE gel. Subsequently select fractions were assayed for ligand activity by the exposure of 10 µl fractions to mice (details below).

Analytical gel filtration chromatography shown in the Supplemental figure 5 was carried out in Infinity II 1260 system (Agilent) with Bio Sec-3 (300A, 78x300 mm, Agilent) column with 1x PBS (pH 7.4) at room temperature as a mobile phase (1 ml/min). 5 µl of hemoglobins were injected into the column with an autosampler, and hemoglobins were monitored using 405 and 561 nm.

Ni Sepharose binding of Vmn2r88 ligand activity

The peak activity fractions from the gel filtration step were incubated with Ni Sepharose 6 Fast Flow resin (GE Healthcare) for 3 hrs at 4 ℃ with gentle mixing. After >10 column volume wash with 1x PBS/0.1 % NP-40, bound proteins were eluted using a step elution 20 mM, 50 mM, and 100 mM imidazole in 1x PBS, 4 column volume each. Most of the Vmn2r88 stimulating activity eluted in 50 mM imidazole fractions, and these fractions were pooled and buffer exchanged for further purification by Poros HQ column.

Ion exchange chromatography

For DEAE chromatography, 1 ml HiTrap DEAE Fast Flow (GE Healthcare) and 50 mM Tris pH 7.5 were used as the column binding buffer. The supernatant from the ammonium sulfate precipitation step was buffer exchanged to 50 mM Tris pH 7.5 and concentrated using Amicon Ultra-0.5 mL Centrifugal Filters. The bound proteins were eluted by the salt gradient to 2 M NaCl in the same buffer, and 200 µl fractions were collected.

For strong anion exchange chromatography to fractionate the Vmn2r65 ligand activity, we used Poros HQ/M column (1.7 ml, 20 µm, ThermoFisher Scientific) and 50 mM Tris pH 7.5 as a binding buffer at room temperature. For the purification of Vmn2r88 ligand activity, we used 50 mM Tris pH 8.8 at 4 ℃ for bin ding. Bound proteins were eluted using the gradient to 2 M NaCl in binding buffers. 200 µl fractions were collected and served for the analysis by SDS-PAGE and activity assays.

Activity testing

Throughout the chromatographic steps, 10 µl of fractions were presented to adult CD-1 male mice. Their VNOs were analyzed for the *Egr1* induction in Vmn2r65, Vmn2r88, or Vmn2r122/123 expressing cells.

Mass spectrometry

The mass spectrometry was conducted at the Harvard University FAS Mass Spectrometry Facility. The following conditions were used to identify proteins in purified chromatographic fractions. The samples were first buffer exchanged to 0.1 mM tetraethylammonium bicarbonate. The fractions were then treated with TCEP and iodoacetamide, followed by digestion with trypsin in solution overnight at 37 ℃. Digested

samples were submitted for LC-MS/MS performed by LTQ Orbitrap Elite (ThermoFisher Scientific) equipped with Waters NanoAcquity HPLC pump. The mass spectrometry survey scan was performed in the Orbitrap in the range of 395 –1,800 m/z at a resolution of 6×10^4, followed by the selection of the twenty most intense ions (TOP20) for CID-MS2 fragmentation in the Ion trap using a precursor isolation width window of 2 m/z, AGC setting of 10,000, and a maximum ion accumulation of 200 ms. Singly charged ion species were not subjected to CID fragmentation. Normalized collision energy was set to 35 V and an activation time of 10 ms, AGC was set to 50,000, the maximum ion time was 200 ms. Ions in a 10 ppm m/z window around ions selected for MS2 were excluded from further selection for fragmentation for 60 s.

Raw data were submitted for analysis in Proteome Discoverer 2.1.0.81 (ThermoFisher Scientific) software. Assignment of MS/MS spectra was performed using the Sequest HT algorithm by searching the data against a protein sequence database including all entries from the Mouse Uniprot Database and other known contaminants such as human keratins and common lab contaminants. Sequest HT searches were performed using a 20 ppm precursor ion tolerance and requiring each peptides N/C termini to adhere with Trypsin protease specificity while allowing up to two missed cleavages. Cysteine carbamidomethyl (+57.021) was set as static modifications while methionine oxidation (+15.99492 Da) was set as variable modification. MS2 spectra assignment false discovery rate (FDR) of 1% on protein level was achieved by applying the target-decoy database search. Filtering was performed using a Percolator (64bit version, reference 6). For quantification, a 0.02 m/z window centered on the theoretical m/z value of each the six reporter ions and the intensity of the signal closest to the theoretical m/z value was recorded. Reporter ion intensities were exported as excel tables. All fold changes were analyzed after normalization between samples based on total unique peptides ion signal.

Expression and purification of recombinant Smgc

A codon optimized cDNA corresponding to the isoform 3 of murine Smgc (Uniprot ID: Q6JHY2-2) lacking the signal peptide sequence (aa1-20) was synthesized (Genscript) and inserted as N-terminal histidine and C-terminal flag tags into pET28a vector (Novagen). The expression of Smgc was carried out in Rosetta (DE3) cells (Novagen) and was induced with 100 µM IPTG overnight at 20 ℃. The pellet was resuspended in 1x PBS containing 0.25 µM PMSF and lysed using lysozyme and repeated sonication. The lysate was cleared by centrifugation, adjusted to 25 mM imidazole, and incubated with Ni Sepharose 6 Fast Flow resin (GE Healthcare Life Sciences) for at least 3 hours at 4 ℃. After >20x column volume wash with 1x PBS added with 30 mM imidazole and 300 mM NaCl, bound proteins were eluted with 250 mM imidazole in 1x PBS at pH8. The peak fractions were subsequently incubated with Flag M2 magnetic beads (Sigma) for 3 hrs to overnight at 4 ℃. Subsequent ten washes with 1x PBS/0.1 % NP-40 (Calbiochem), bound proteins were eluted with one bead volume of 0.4 mM of FLAG peptide (Genscript) in 1x PBS three times by room temperature incubation for 30 min with gentle mixing. The purity and the molecular weight of the protein were analyzed by SDS-PAGE.

Expression and purification of recombinant hemoglobins

Codon optimized cDNAs comprising of C terminal histidine tagged Hba-a1 (Uniprot ID: P01942), a linker containing Shine-Dalgarno sequence (TGActgcagctacatggagattaactcaatctAGAGGGtattaataatgtatcgcttaaataAGGAGGAataacat), and either mouse Hbb-bt (Uniprot ID: A8DUK4), Hbb-b1 (Uniprot ID: P02088), or Hbb-b2 (Uniprot ID: P02089) were synthesized (IDT) and inserted to pET28a. The protein expression was induced in Rosetta (DE3) cells (Novagen) by 0.25 mM IPTG for 3 hours at 30 ℃. Notably, the recombinant proteins had a reddish color, suggesting that

recombinant hemoglobins are bound by endogenous heme-like molecules. We found the yield and activity of the recombinant Hba-a1/Hbb-bt comparable whether or not hemin was added to the culture. The lysate from the induced culture was purified similarly using the condition for Smgc using Ni Sepharose 6 Fast Flow and the purified proteins were analyzed by SDS-PAGE. The concentration of the purified proteins was adjusted to 4 mg/ml in 1x PBS.

Western blot

Western blot was carried out using bedding extracts of 129S1/SvImJ. One male and female were paired for breeding, and just prior to the parturition, the male was separated from the cage and we refreshed nesting material (a cotton pad). On the day pups are born, we sampled the bedding exclusively the nest. Especially, to enrich the protein concentration of the bedding extract, we limited the sampling to visibly stained materials (~40 µl in volume). We then used 40 µl of 1x PBS to extract proteins from these bedding by 15 min incubation at room temperature. Pregnant female bedding was collected one to two days prior to parturition. Therefore, the nesting material was in contact with the females for 1~2 days. Control bedding samples from non-pregnant females and males (all single housed) was sampled similarly after one to two days of exposure to the nesting material. 15 % SDS-PAGE. The proteins were subsequently transferred to nitrocellulose membranes (Amersham Protran Premium Western Blotting Membranes, GE Healthcare). Western blots were performed using 1:3000 rabbit anti-HBB (Invitrogen, PA5-48233) in 5 % powdered milk/1xPBST as the primary antibody and 1:10000 anti-rabbit IgG HRP-linked antibody (Cell Signaling Technologies, 7074P2) in 5 % powdered milk/1xPBST as the secondary antibody. The chemiluminescence was developed using SuperSignal West Pico PLUS Chemiluminescent Substrate (Thermo Fisher) and was captured using Azure Imager c400 (Azure Biosystems).

BEHAVIOR TESTS

Odor exposure assays

Vomeronasal stimulation via odor and pup exposure was conducted using methods already described (Isogai et al., 2011). The odor exposure experiments were performed in single housed cages. For bedding or pup exposure, we introduced bedding materials or pups into the cage, which induced frequent direct sniffing. For the presentation of liquids, 10 µl of the solutions were directly spotted to the nostril. VNOs were dissected after 40 min post stimulus presentation and were embedded to OCT and frozen in dry ice. For the experiments conducted in Figure 2D, 30 min was chosen for the exposure duration. These samples were subsequently served for RNA in situ hybridization analysis. Experiments in Figure 2A-C used TrpC2$^{+/-}$ mice whereas all other experiments used sexually naive CD-1 male and female mice (Charles River, adults older than at least 4 weeks). The induction of *Egr1* was used as a molecular marker for neural activity in the VNO.

Stimulus sampling for odor exposure assays

Bedding: Bedding consists of ground corncob and shredded cotton pads, which mice use to build their nest. For adult mouse bedding, soiled bedding was collected from cages that socially housed 4 to 5 adult mice of specific strains for 1 week. Then the bedding of 50 ml in volume, making sure that both urinary, fecal and other nest-associated excretions were equally represented, was used for each experiment. To sample chemosignals associated with mothers co-housed with pups, bedding specifically around their nests was used. The cage typically housed two C57BL/6J lactating mothers, which gave birth to C57BL/6J in a new cage with fresh bedding without mated males, and P1~P4 pups. For mother's bedding, C57BL/6J mothers were

single housed for 2 days and the nesting materials with which mothers had extensive contact as well as soiled bedding for exposure experiments were selectively sampled and used for the exposure.

Pups: C57BL/6J pups (P1 to P5) were exclusively used for the experiments. Pregnant C57BL/6J females previously mated with C57BL/6J males were transferred to a new cage with fresh bedding. Notably, these cages did not come in contact with adult males, to eliminate the contribution of adult male-derived chemosignals on pups. All experiments used 1 male and 1 female pups.

Cross-fostered bedding: first, 129S1/SvImJ females were mated with 129S1/SvImJ males and C57BL/6J females were mated with C57BL/6J males. Pregnant females were single housed prior to parturition. Pups in these cages were then introduced to either 129S1/SvImJ or C57BL/6J mother's cages for cross-fostering. Each cage received 5 to 8 pups and the pups were cross-fostered for 4 to 5 days. The bedding from the nest area was collected and exposed to CD-1 males. 3 independent bedding samples were tested per group.

Gland extracts: Gland extracts were made by homogenization of select glands (Harderian, extraorbital lacrimal, parotid, submaxillary, sublingual, and preputial glands) in adult (more than 5 week old) C57BL/6J male or female mice. 2x tissue volumes of 1x PBS supplemented with cOmplete EDTA-free Protease Inhibitor Cocktail tablet was used to grind tissues using disposable pestles in 1.5 ml tubes, and spun down the insoluble at 4 ℃ at 15,000 rpm for 30 min. 10 µl of supernatant was served for the exposure to two CD-1 males per extract. We have similarly prepared salivary gland extracts from different strains of pups, including Balb/c, FVB, and ID.

Urine and blood: Urine was freshly collected from adult mice of multiple strains including C57BL/6J and CD-1 in both gender. Blood was collected from some of these animals

and stored at -80 ℃ until the date of the exposure experiments to two CD-1 males per stimulus.

Chromatographic fractions and recombinant pheromones: 10 µl of chromatographic fractions at various stages of purifications as well as recombinant pheromones were used for exposure assays. To test the stability of recombinant hemoglobins, the hemoglobin solution (4 mg/ml) was stored at room temperature (21~23 ℃) for varying length of time, before exposure to mice.

Generation of Vmn2r65 and Vmn2r88 null mice

The Vmn2r65 and Vmn2r88 null alleles were produced using the homologous recombination of targeting vector containing self-excision neomycin resistance cassette using a published protocol (Chan et al., 2007). We designed the targeting vector to excise out the transmembrane domain (corresponding to the exon 6) of these V2R genes. BAC RP23-221O21 and BAC RP24-161J9 were used for the construction of Vmn2r65 and Vmn2r88 homology arms (long arm: 5 kb, short arm: 2 kb), respectively. Vmn2r65 targeting construct was designed to replace the exon 6 of the gene with ires-tau-EYFP and *neo* expression cassette, and Vmn2r88 targeting vector was design to replace a small piece of the exon 5 and entire exon 6 of the gene with ires-tau-tdTomato and *neo* expression cassette. The linearized targeting vectors were electroporated into V6.5 ES cells by Harvard Genome Modification Facility. ES cell clones which successfully recombined were examined by PCR spanning long arm and short arm integration sites. The ES cells in which successful targeting occurred were injected to blastocysts. The original insertion in these ES cells contained the self-excision *neo* cassette, which was subsequently removed in the germ line of the animal, leaving one loxP site at the end. Germ line transmissions of the mutant allele in F1 mice were confirmed by PCR genotyping. Finally, there was no expression of Vmn2r65 and

Vmn2r88 genes by RNA *in situ* hybridization using probes specific to these genes. The F1 mice were subsequently backcrossed these null nice to C57BL/6J for 5 generations (1 male, and 4 female C57BL/6J crosses) before preparing the cohorts for behavioral testing.

Monitoring of pup-directed behaviors

Male mice (wild type, Vmr2r65 heterozygous and homozygous, Vmn2r88 heterozygous and homozygous, Vmn2r65;Vmn2r88 double mutants) were socially housed until at least 10 days before they were tested for pup-directed behaviors, at which point they were single housed. A pair of C57BL/6J pups (one males and one female, P1 to P4) was introduced to each cage, and the behaviors of resident males were video recorded using over the cage CCTV cameras under red light illuminations. When males exhibited pup-directed aggression, the pups were immediately removed, and the experiments were stopped. When the resident males exhibited parental behaviors, the behavioral monitoring was extended for another 30 min from the onset of pup retrieval. Approximately one half of wild type males neither attacked nor retrieved, even though they extensively chemoinvestigated the pups. In this scenario, the experiment was stopped after 30 min from when the pups were introduced and scored as ignoring. The marking of the individual events of social behaviors were performed using Noldus Observer XT software by independent scorers blind to the genotypes. Several behavioral parameters were monitored: chemoinvestigation with direct contact, attack latency, parental behaviors such as grooming, pup retrieval latency, and nest building. In several occasions, virgin males made nest around the pups and exhibited parental behaviors. These mice therefore did not retrieve pups, in which case, the onset of the nest building was recorded as pup retrieval latency.

Resident-Intruder assays

The intruders were prepared by swabbing 100 µl freshly sampled adult (more than 5 weeks) CD-1 male urine, to whole body, especially anogenital and neck and facial areas of castrated CD-1 males (castrated at 4 weeks). Each intruder mouse was immediately introduced into a resident cage housing wild type or double mutant males. These behaviors were video recorded for 1 hr. Social interaction events during the behavior experiments such as chemoinvestigation, tail rattling, grooming, and attacking bouts were marked by an independent scorer blind to genotypes using Noldus Observer XT software.

Mating assay

All behavioral testing was carried out within 4 hours of the onset of the dark cycle. Male sexual behavior was tested as described previously (Stowers et al., 2002; Kimchi et al., 2007). Adult virgin wild type, heterozygous and homozygous mutant littermates were individually housed for 5-7 days before conducting resident-intruder assays. On the day of the test, ovariectomized females, hormonally primed to be in estrous, were introduced into the cage and allowed to freely interact with the resident males for 60 minutes. Video recordings of social interactions were analyzed using Noldus Observer XT software. Mice were scored on standard behavioral parameters including duration of chemoinvestigation as well as latency, number and total duration of mounting, intromission and ejaculation.

Female intruders were hormonally primed as follows. Ovariectomized adult females (C57BL/6J at 8 to 9 weeks) were injected with 10 µg (in 100 µl sesame oil) of 17β-estradiol benzoate (Sigma) on 2 consecutive days preceding the test day. On the test day, mice received a subcutaneous injection of 50 µg (in 50 µl sesame oil) of progesterone, at least 6 hours before testing.

Production of silicone dummies

Rubber dummy pups were manufactured by casting of Body Double Standard Set (Smooth-On) in P1 pup mold. In this study, four different shapes were made: “dummy” as faithful pup shape, “brick” using the square cutouts of slab silicone rubber, “blob” with pup body shape without limbs or tail, and “hybrid” with brick body shape but with limbs and a tail.

Behavioral experiments with silicone dummies

A cohort of male TrpC2$^{+/-}$ mice was used for this experiment. We chose this genetic background since we found that a high proportion (>90 %) of these mice exhibited aggressive behaviors (Wu et al., 2014). To ensure we start the behavioral assays with homogenous pool of males, these animals were single housed at 4 months old and pre-screened the males by testing their behavior towards pups in 5 min tests at least a month prior to the dummy testing. Each male was presented with one silicone object (“dummy”, “brick”, “blob”, and “hybrid” as shown in the Figure 1A) for 10 min per day for three consecutive days. These objects were swabbed with one of the chemicals (40 µl of 1x PBS, adult CD-1 male urine, or P2~6 C57BL/6J pup salivary extracts) in a random order. These sessions were video recorded, and the male behaviors were subsequently quantified as described in the Quantification and Statistical Analysis section. The experiments were performed in double blind fashion both to the experimenter and the scorers. The same animals were tested for different shapes at least leaving one week in between to minimize potential effects of prior experiences on behavioral outcomes.

QUANTIFICATION AND STATISTICAL ANALYSIS

RNA-seq data analysis

RNA-seq analysis was perform as shown in Figure 3E. The Illumina RNA-seq reads (in triplicates per group) were aligned using RNA-STAR to *M. musculus* reference genome mm10 (Ensembl). The number of fragments aligning to each gene was quantified using summarizeOverlaps from the GenomicRanges Bioconductor package. Statistical analysis of potential enrichments was performed using DESeq2 (Love et al., 2014), with multiple test correction producing a gene set with expected FDR ≤ 0.05. RNA-seq results are available at the Gene Expression Omnibus (accession number, GSE122138).

Quantification of the *Egr1* activity

We used the same procedure as our previously published study (Isogai et al. 2011). To quantify the activity of different exposures, we identified *Egr1*$^+$ cells in labeled *VR*$^+$ neurons and calculated the fraction of co-localization in *VR*$^+$ cells. At least 4 vomeronasal sections (14 or 16 µm in thickness) per animal were quantified, except for experiments involving mother's bedding in Figure 5J, in which three sections per animal were counted for 3 animals. To perform the hierarchical screen of VRs responsive to pup stimuli in Figure 2, we initially used clade specific probes that cover all the VR clades as well as non-canonical VNO receptors such as formyl peptide receptors to narrow down the putative receptors to pup odors (N = 2 animals for each receptor clade) (Isogai et al., 2011). We then used probes that can specifically detect single to a few receptor genes to identify receptors for pup cues. The final confirmation of the receptors used three animals quantifying at least four sections. To quantify the intensity difference of the *Egr1* signals observed in the activation of Vmn2r88 positive neurons by hemoglobins (Figure 5I), the intensities of *Egr1* signals in Vmn2r88 expressing neurons were measured using an 87.9 µm^2 circular mask, which corresponds to an approximate dimension of Vmn2r88 neurons. We also quantified pixel intensities and standard deviation of 4 to 5 neighboring non-Vmn2r88 neurons, which had background signals. Then the intensity of the *Egr1*

signal of each neuron was plotted as fold σ (standard deviation of the background signals). The statistical tests were performed using 2-tailed Student's *t*-Test assuming unequal variances. Exact sample sizes including quantified cell numbers and the number of animals used for these tests are reported in corresponding text and figure legends.

Quantification and analysis of dummy-directed behaviors

As important criteria for the analysis of the behaviors of males towards "artificial pups," we initially noticed that the males interact with dummies in a characteristic structure, which begins with initial approach to the dummy and subsequent chemoinvestigation with direct contact. Each interaction bout finishes with the male leaving the area. Therefore, this set of behavior was defined as one chemoinvestigative event and classified them as non-aggressive or aggressive. Non-aggressive bouts only had sniffing and grooming, while aggressive bouts contained biting interleaving with chemoinvestigation. Using Noldus Observer XT software the duration and frequency of aggressive and total (*i.e.,* aggressive plus non-aggressive) chemoinvestigative bouts were subsequently quantified by a human observer blind to the nature of chemosignals swabbed on the dummies. The sliding window analysis was performed using 2 min as the window. The statistical tests were performed using paired *t*-Test using R and GraphPad Prism. The number of animals used is described in the corresponding figure legends.

Analysis of receptor knockout mice

The distribution of the males that attacked or parent, or ignored in different genotypes were analyzed using Fisher's Exact Test, as performed previously (Wu et al. 2015). The significance of quantified behavioral parameters in Supplemental figure 6 was analyzed

by two-tailed *t*-Test assuming unequal variance. The number of animals in each test is indicated in the corresponding text and figure legends.

DATA AND SOFTWARE AVAILABILITY

The raw and processed RNA-seq data in this study have been deposited in the Gene Expression Omnibus (GEO:GSE122138, https://www.ncbi.nlm.nih.gov/geo/query/acc.cgi?acc=GSE122138).

Supplemental video and legends

Supplemental video 1. Related to Figure 1

Video showing virgin male interactions with a pup dummy, which was previously scented by co-housing with a mother and pups.

Supplemental video 2. Related to Figure 1

Video showing virgin male interactions with a pup dummy swabbed with pup salivary extracts.

Supplemental video 3. Related to Figure 1

Video (0.25x real time) captured by a high-speed camera showing the initial investigation of a mouse pup by a virgin male.

Supplemental table legend

Supplemental table 1: The target sequences of RNA FISH probes (in Excel format)

A

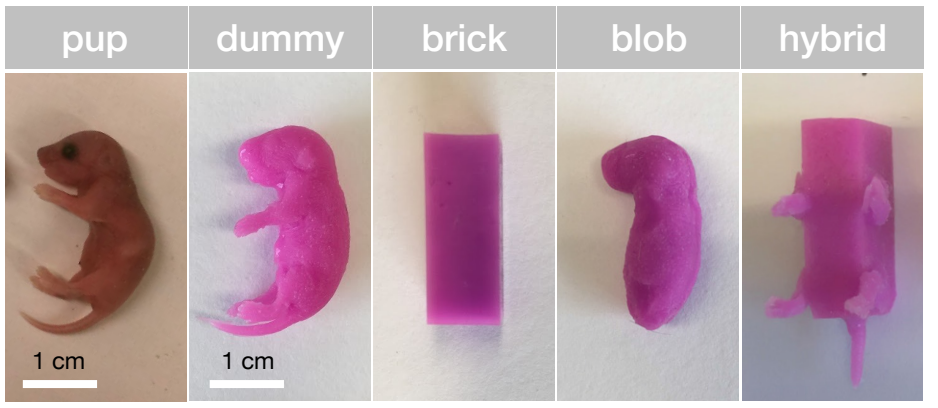
pup
dummy
brick
blob
hybrid
1 cm
1 cm

B

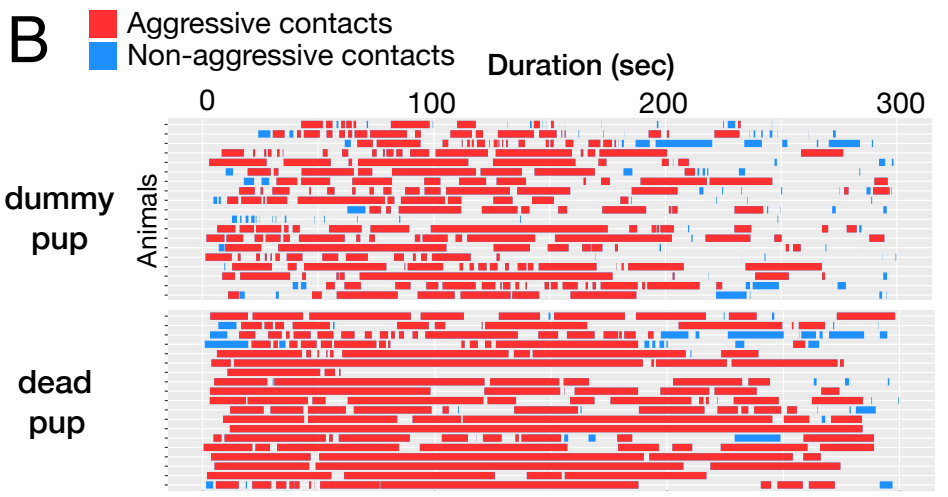
Aggressive contacts
Non-aggressive contacts
Duration (sec)
0
100
200
300
Animals
dummy pup
dead pup

C

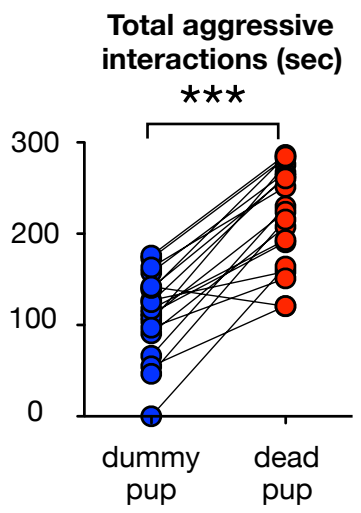
Total aggressive interactions (sec)
***
300
200
100
0
dummy pup
dead pup

D

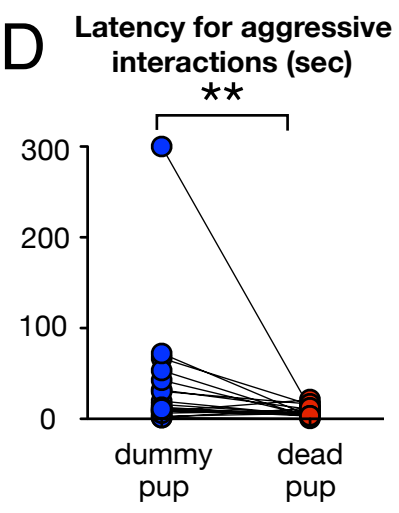
Latency for aggressive interactions (sec)
**
300
200
100
0
dummy pup
dead pup

E

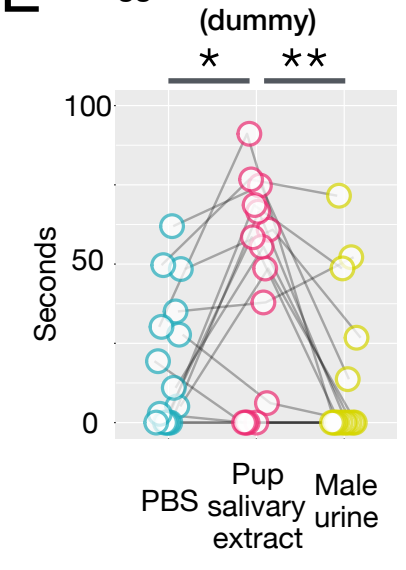
Aggressive interactions (dummy)
*
**
100
50
0
Seconds
PBS
Pup salivary extract
Male urine

F

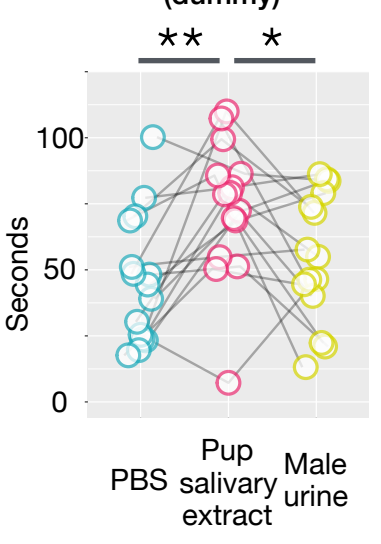
All contacts (dummy)
**
*
100
50
0
Seconds
PBS
Pup salivary extract
Male urine

G

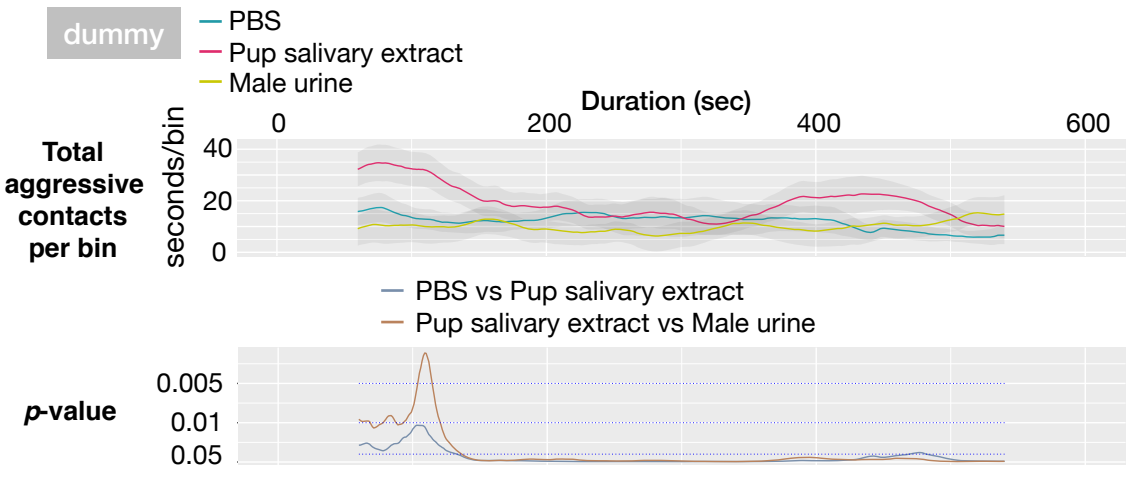
dummy
PBS
Pup salivary extract
Male urine
Duration (sec)
0
200
400
600
Total aggressive contacts per bin
seconds/bin
40
20
0
PBS vs Pup salivary extract
Pup salivary extract vs Male urine
p-value
0.005
0.01
0.05

H

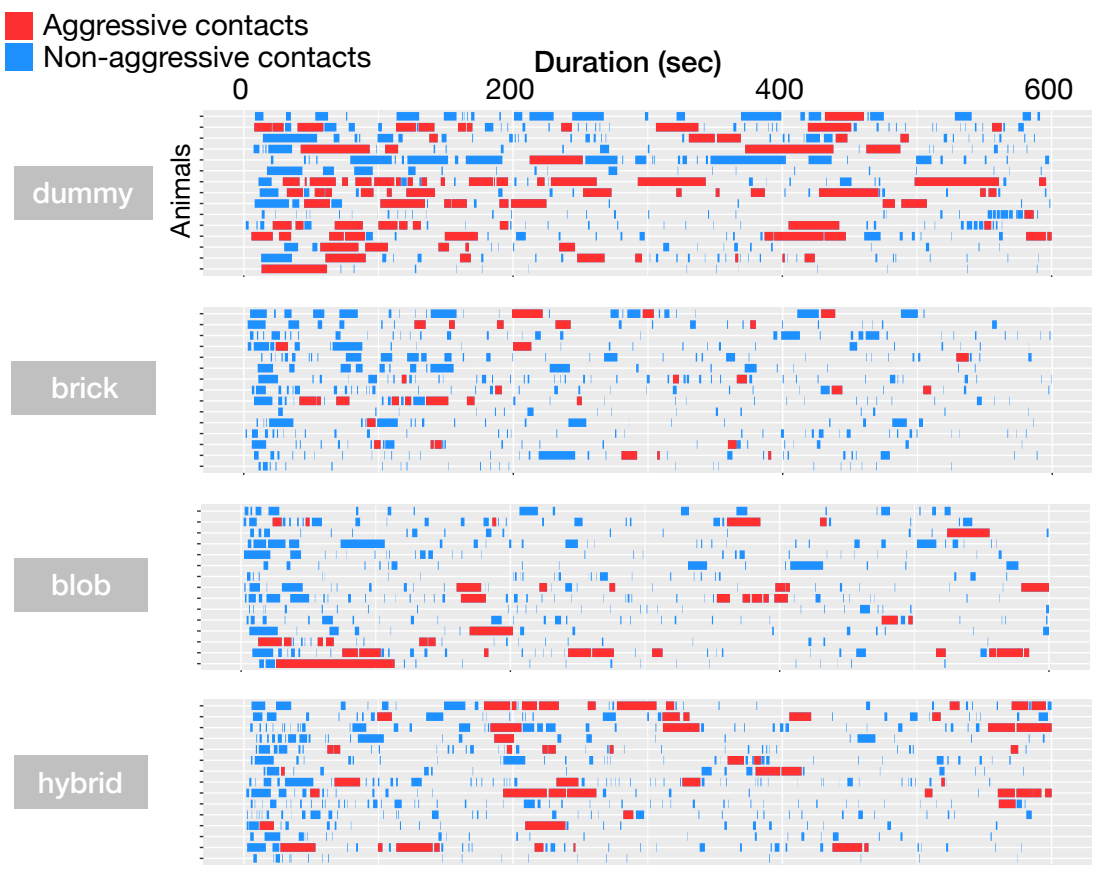
Aggressive contacts
Non-aggressive contacts
Duration (sec)
0
200
400
600
Animals
dummy
brick
blob
hybrid

I

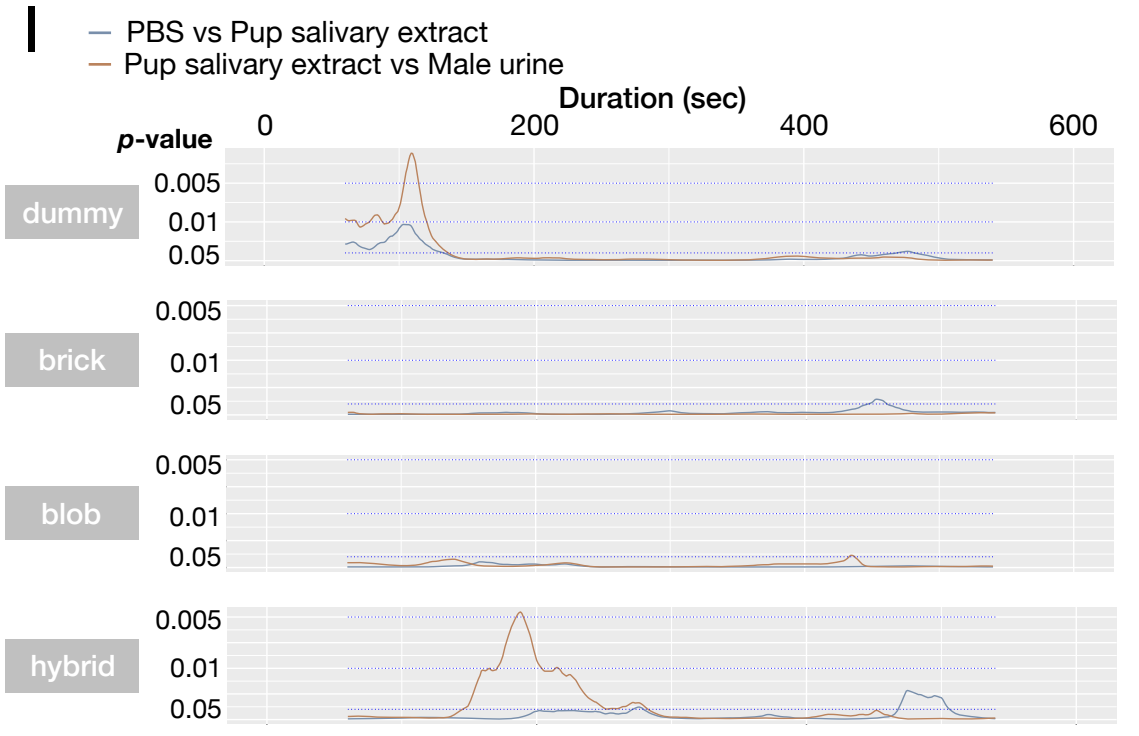
PBS vs Pup salivary extract
Pup salivary extract vs Male urine
Duration (sec)
0
200
400
600
p-value
dummy
brick
blob
hybrid
0.005
0.01
0.05

J

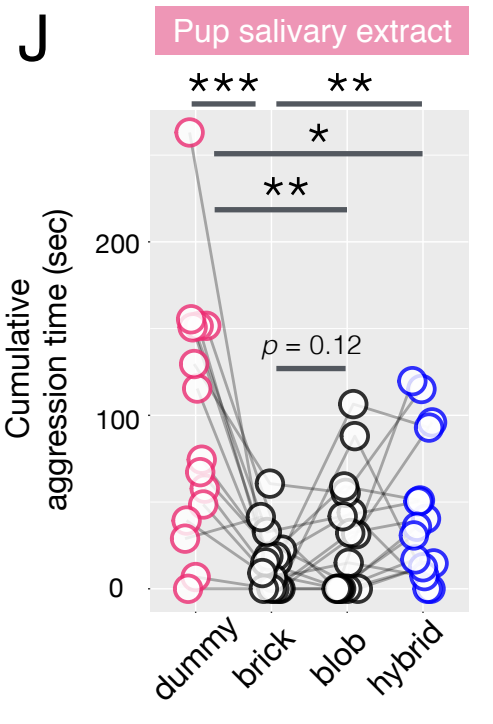
Pup salivary extract
***
**
*
**
p = 0.12
Cumulative aggression time (sec)
200
100
0
dummy
brick
blob
hybrid

A

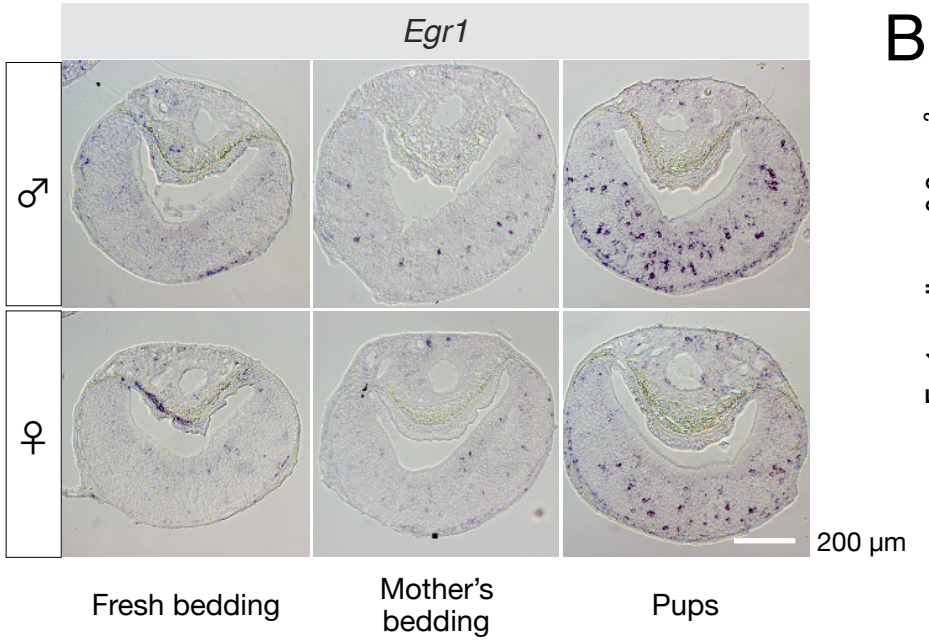

B

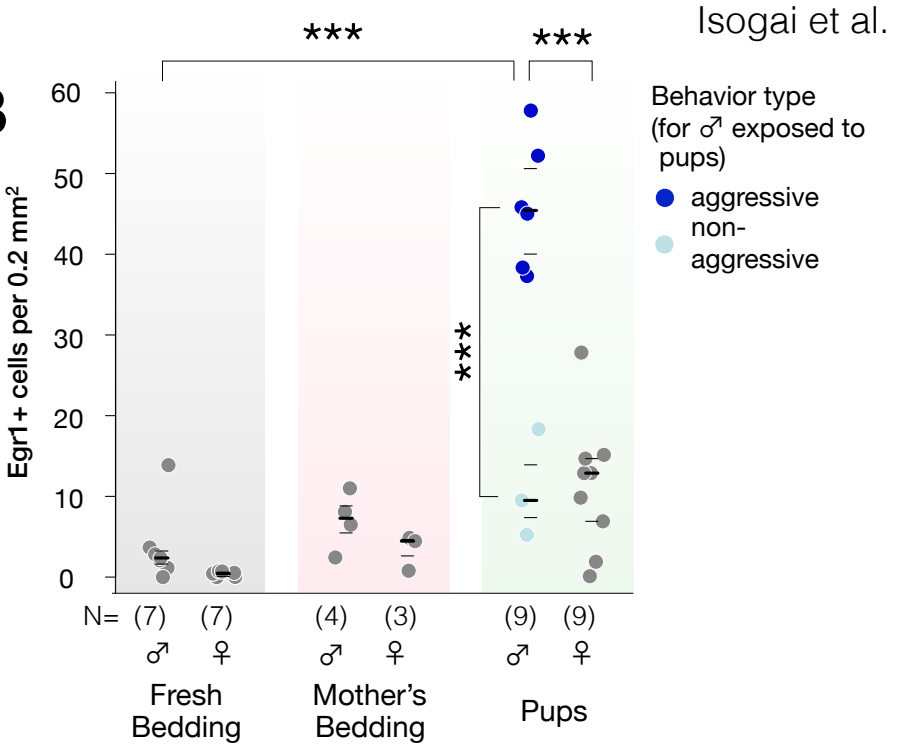

C

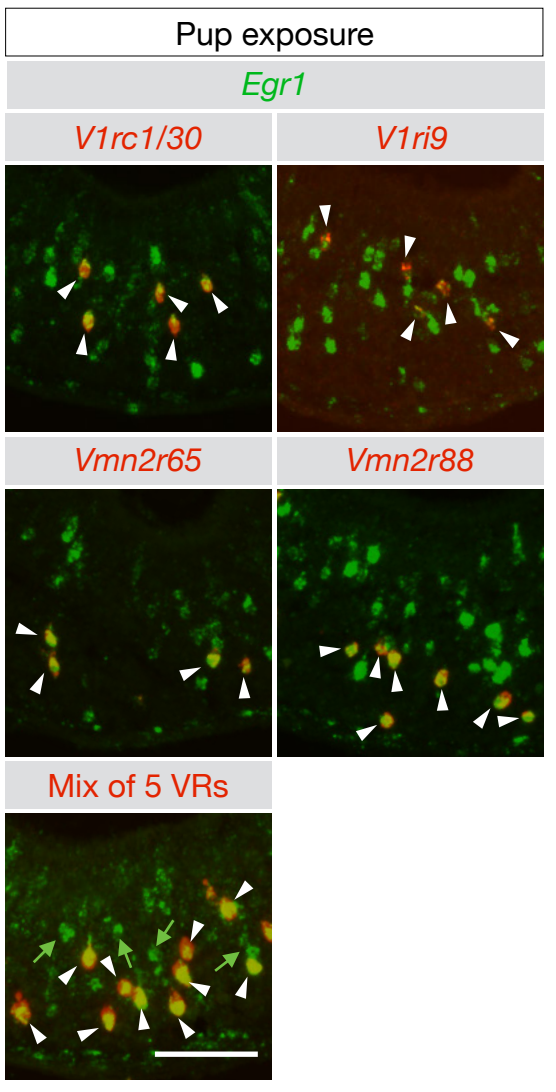

D

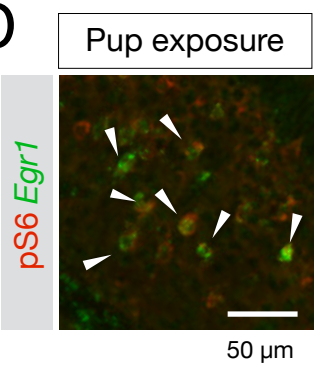

E

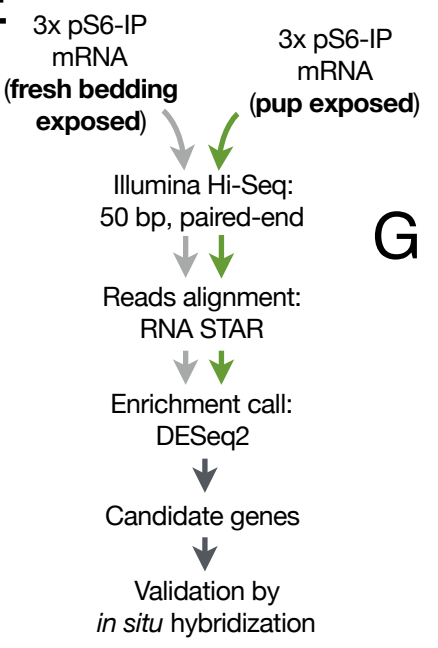

F

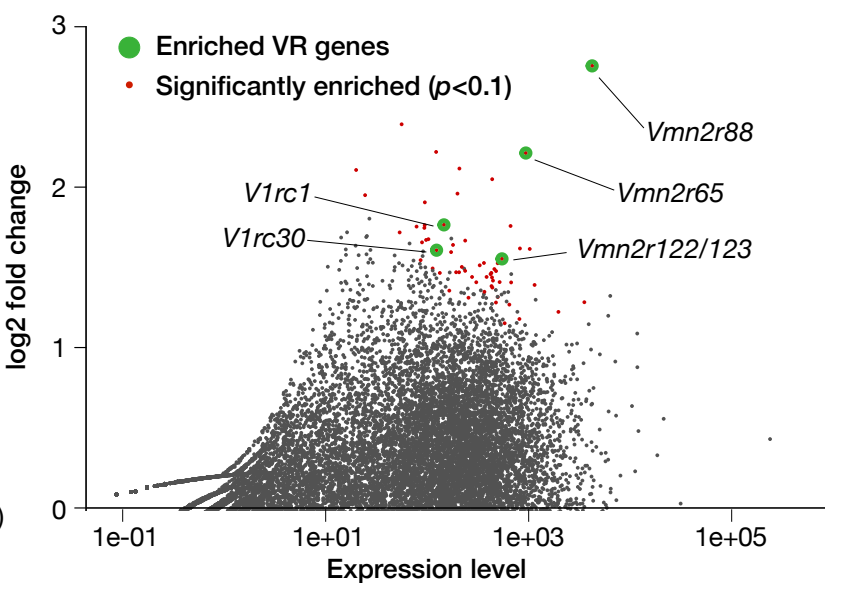

G

Vomeronasal receptor candidates to pup cues by RNA-seq of pS6 pulldown (FDR < 0.05)

Gene Name	Adjusted p-value	log2 Fold Enrichment
Vmn2r88	3.52E-20	2.84
Vmn2r65	2.75E-06	2.22
Vmn1r10 (V1rc1)	1.84E-06	1.86
Vmn1r9 (V1rc30)	1.09E-05	1.7
Vmn2r122/123	6.83E-06	1.6

H

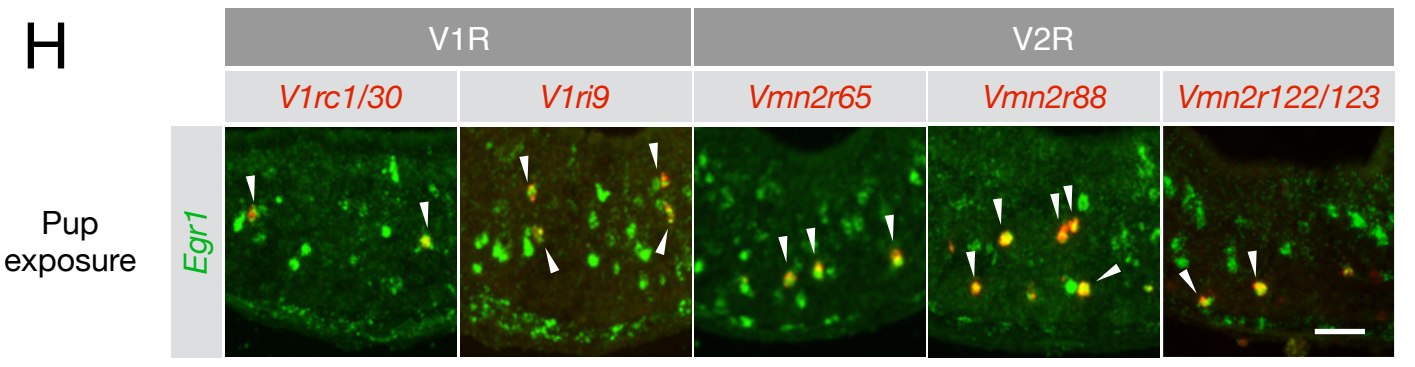

	V1rc1/30	V1ri9	Vmn2r65	Vmn2r88	Vmn2r122/123
% colabel	15.6 ± 1.5 (n = 428)	9.0 ± 1.7 (n = 503)	11.2 ± 1.6 (n = 406)	43.4 ± 0.8 (n = 553)	14.0 ± 2.2 (n = 486)

93.2 ± 7.8 %

I

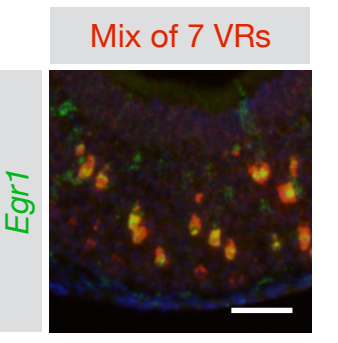

92.2 ± 1.2 %
(n = 425)

J

	V1rc1/30	V1ri9	Vmn2r65	Vmn2r88	Vmn2r122/123
Adult ligand activity	Adult ♀bedding	Adult ♀bedding	Adult ♀bedding	Adult ♂bedding	Adult ♂salivary gland extract

A

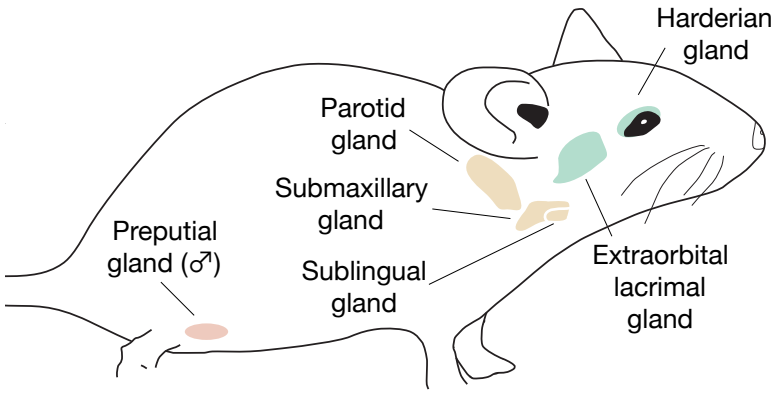

B

Tissue or stimulus	Sex	Vmn2r65	Vmn2r88
Adult salivary gland	♂	-	+
	♀	+	+
Lacrimal glands	♂	n/d	+
	♀	-	n/d
Urine	♂	-	-
	♀	-	-
Pup salivary gland	♂/♀	+	+

C Vmn2r65 ligand activity in C57BL6/J adult ♀ excretions and gland extracts

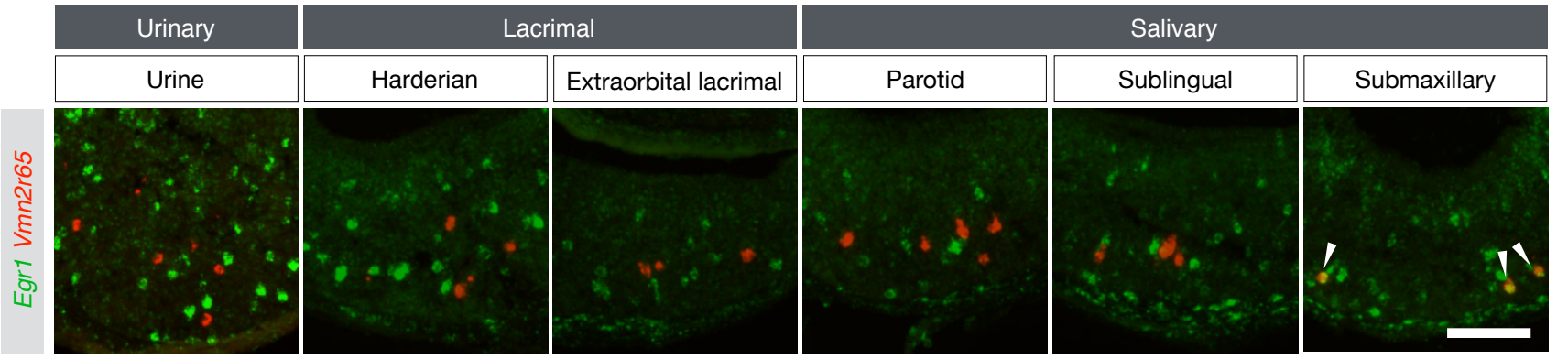

	Urine	Harderian	Extraorbital lacrimal	Parotid	Sublingual	Submaxillary
% colabel	0 (n = 94)	0 (n = 91)	2.8 ± 0.9 (n = 81)	1.0 ± 1.0 (n = 93)	20.4 ± 11.2 (n = 92)	89.9 ± 5.3 (n = 94)

D Vmn2r88 ligand activity in C57BL6/J adult ♂ excretions and gland extracts

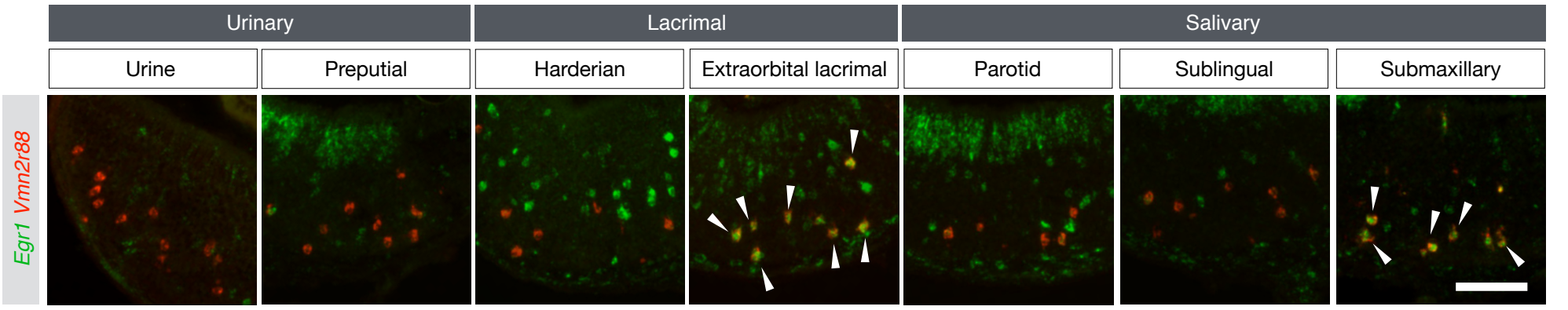

	Urine	Preputial	Harderian	Extraorbital lacrimal	Parotid	Sublingual	Submaxillary
% colabel	0 (n = 139)	31.2 ± 27.0 (n = 109)	9.6 ± 4.4 (n = 153)	76.7 ± 21.6 (n = 105)	29.2 ± 4.2 (n = 130)	23.0 ± 12.4 (n = 183)	93.7 ± 0.29 (n = 126)

E Vmn2r65 and Vmn2r88 ligand activities in C57BL6/J pup salivary gland extracts

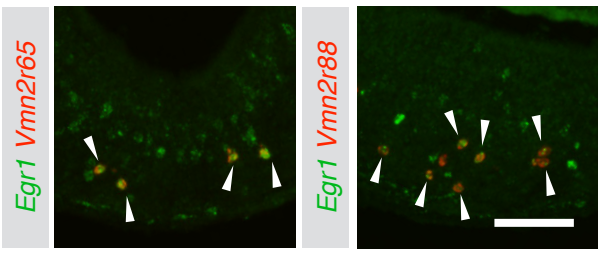

	Egr1 Vmn2r65	Egr1 Vmn2r88
% colabel	85.5 ± 3.0 (n = 75)	85.5 ± 5.7 (n = 147)

F Vmn2r65 and Vmn2r88 ligand activities in C57BL6/J adult submaxillary gland extracts

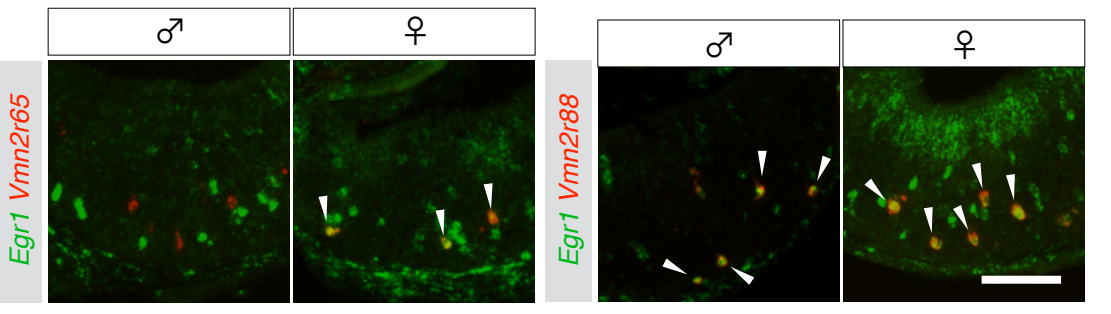

	♂	♀	♂	♀
	Egr1 Vmn2r65		Egr1 Vmn2r88	
	0 (n = 81)	89.9 ± 5.3 (n = 94)	93.7 ± 0.29 (n = 126)	78.5 ± 5.9 (n = 150)

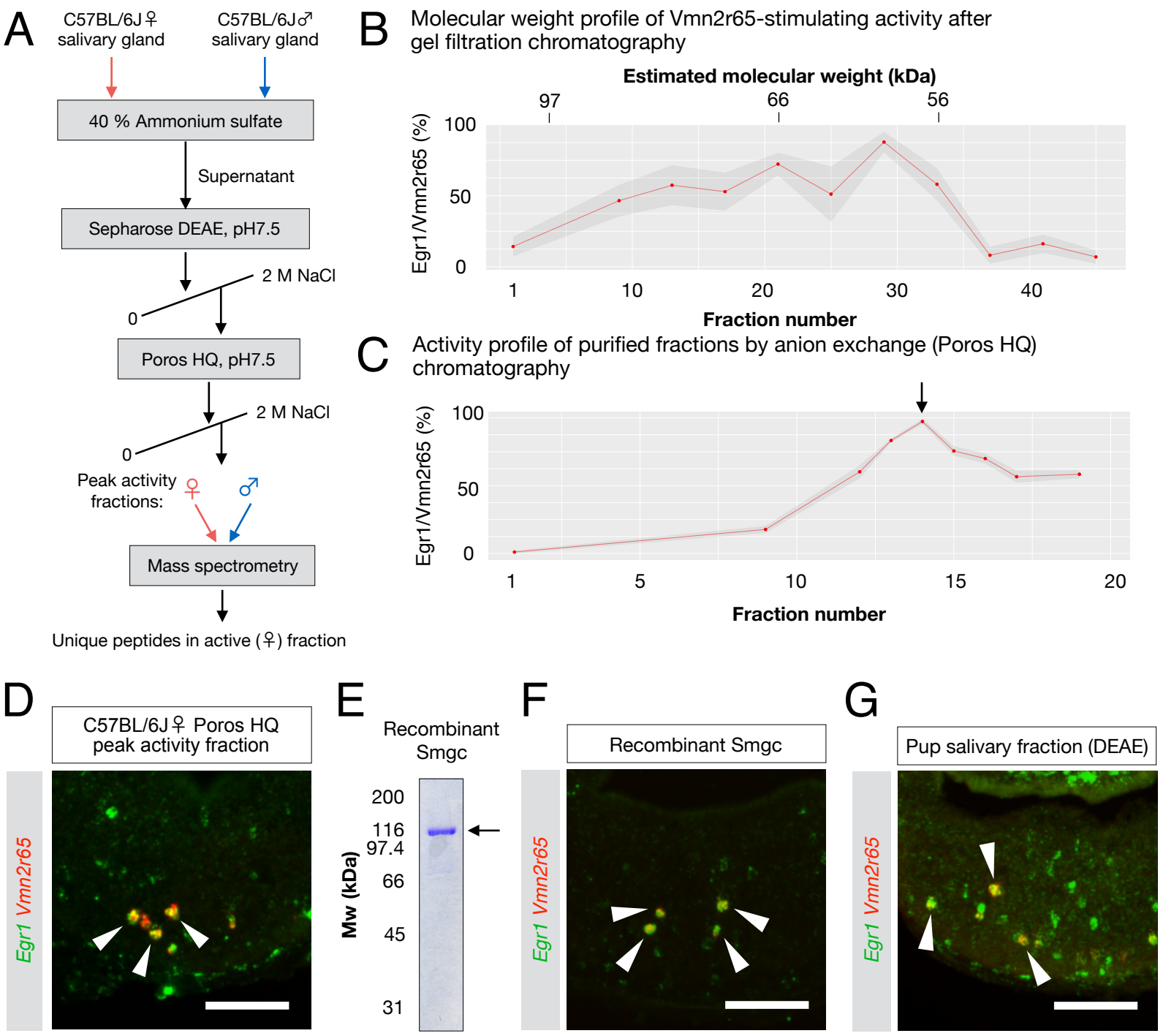
A
C57BL/6J♀ salivary gland
C57BL/6J♂ salivary gland
40 % Ammonium sulfate
Supernatant
Sepharose DEAE, pH7.5
2 M NaCl
0
Poros HQ, pH7.5
2 M NaCl
0
Peak activity fractions:
♀
♂
Mass spectrometry
Unique peptides in active (♀) fraction
B
Molecular weight profile of Vmn2r65-stimulating activity after gel filtration chromatography
Estimated molecular weight (kDa)
97
66
56
Egr1/Vmn2r65 (%)
100
50
0
1
10
20
30
40
Fraction number
C
Activity profile of purified fractions by anion exchange (Poros HQ) chromatography
Egr1/Vmn2r65 (%)
100
50
0
1
5
10
15
20
Fraction number
D
C57BL/6J♀ Poros HQ peak activity fraction
Egr1 Vmn2r65
E
Recombinant Smgc
Mw (kDa)
200
116
97.4
66
45
31
F
Recombinant Smgc
Egr1 Vmn2r65
G
Pup salivary fraction (DEAE)
Egr1 Vmn2r65

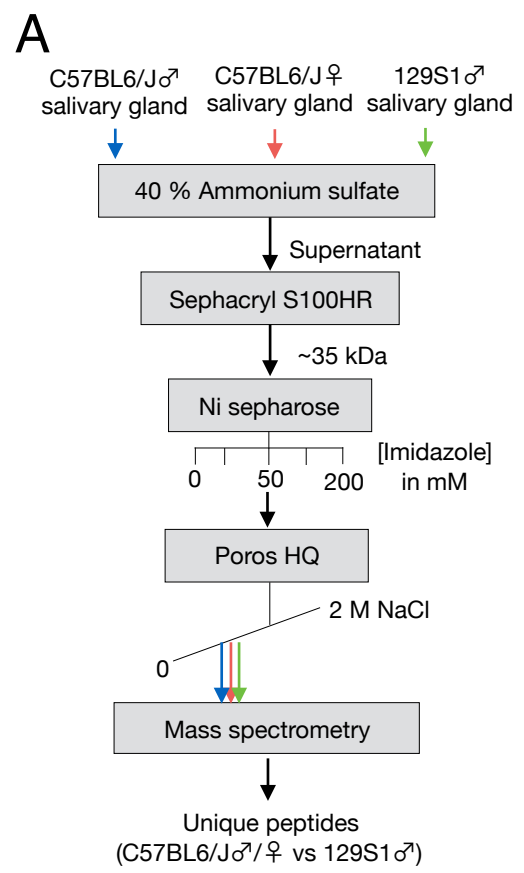

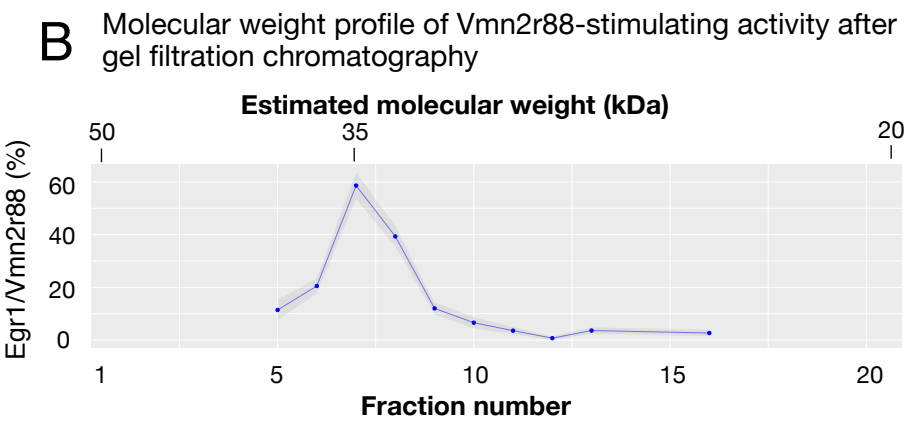

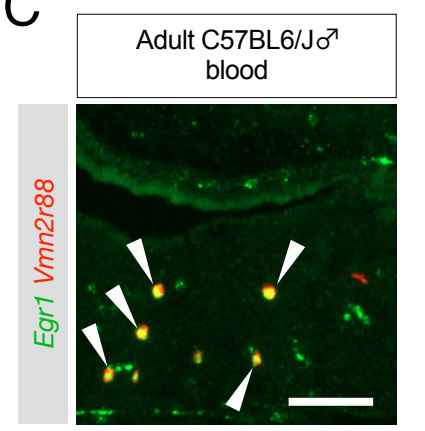

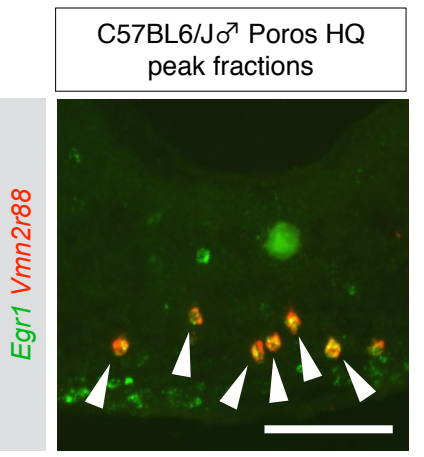

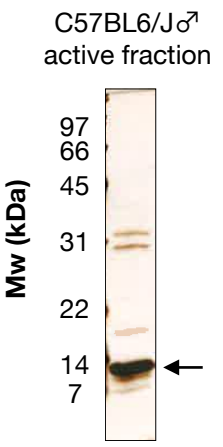

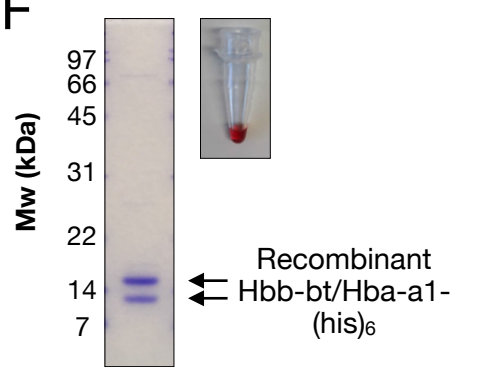

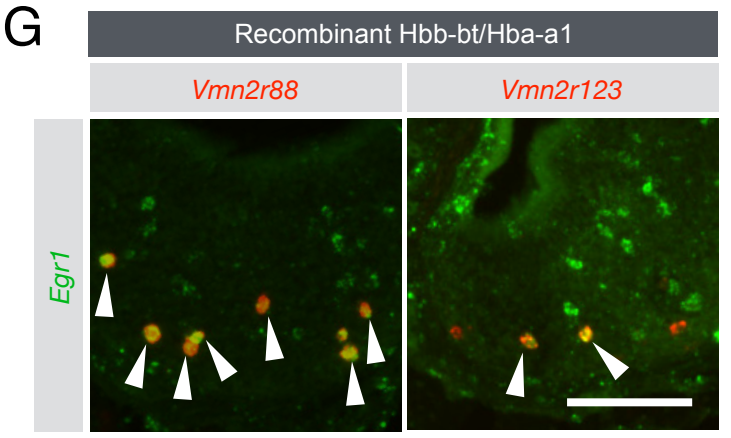

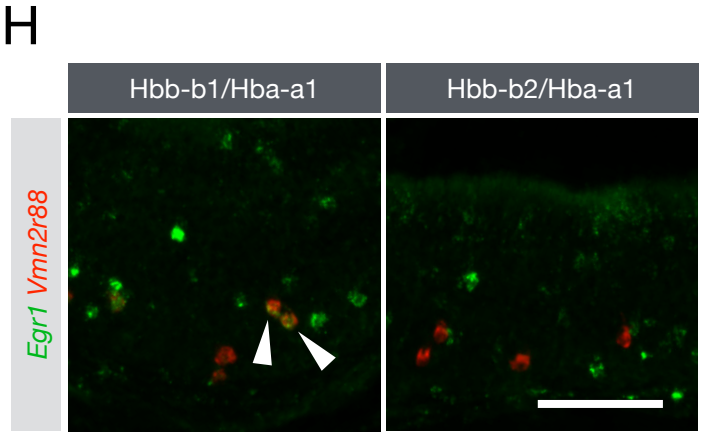

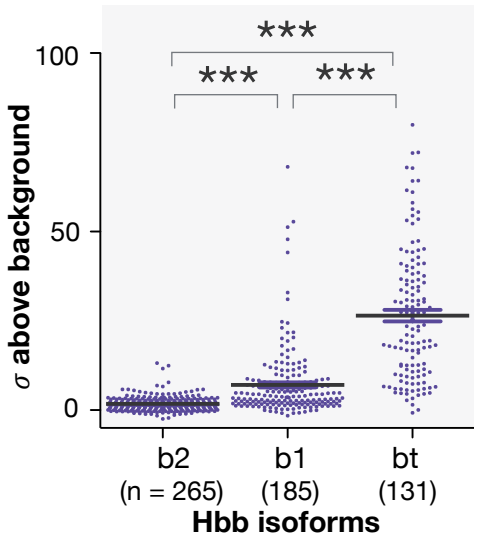

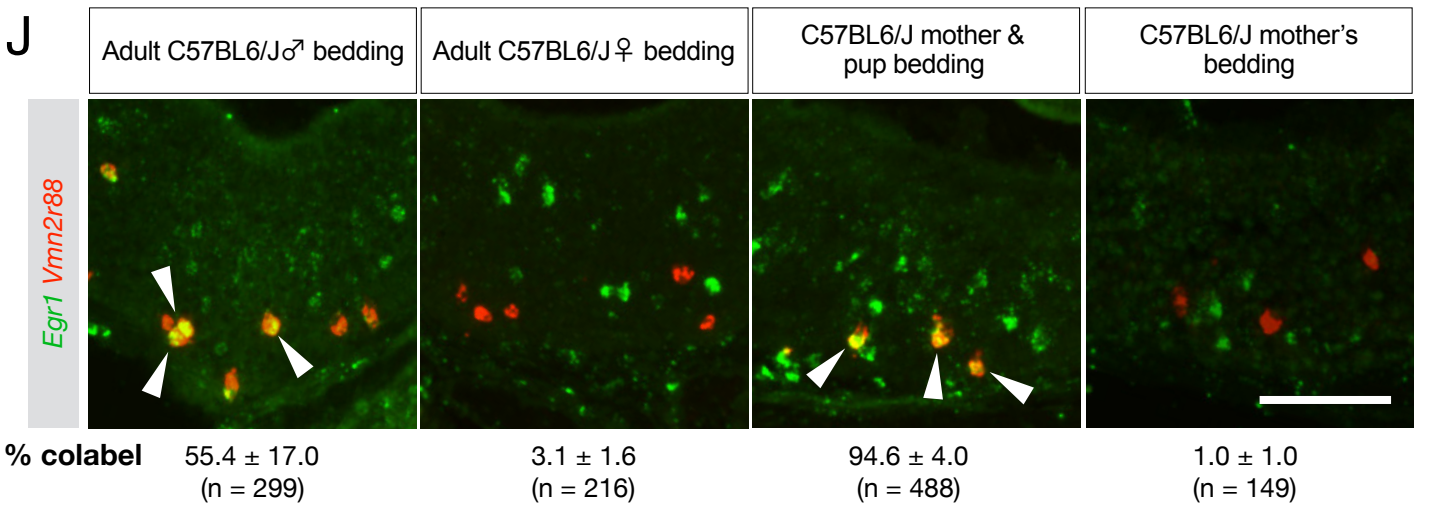

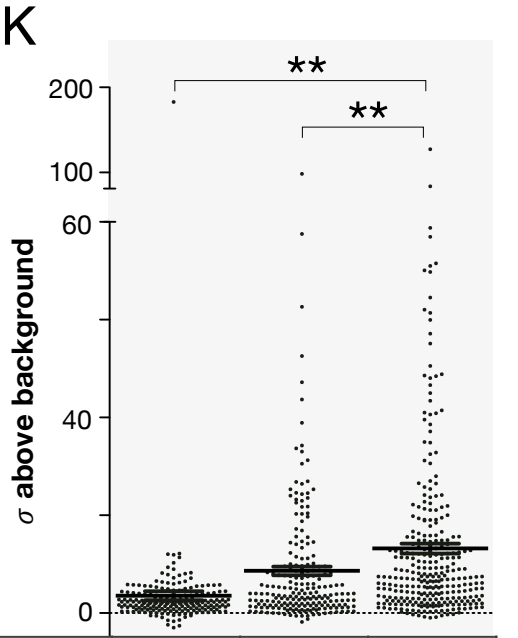

Mother	129	129	B6
Fostered pups	B6	129	129
	(n = 203)	(208)	(297)

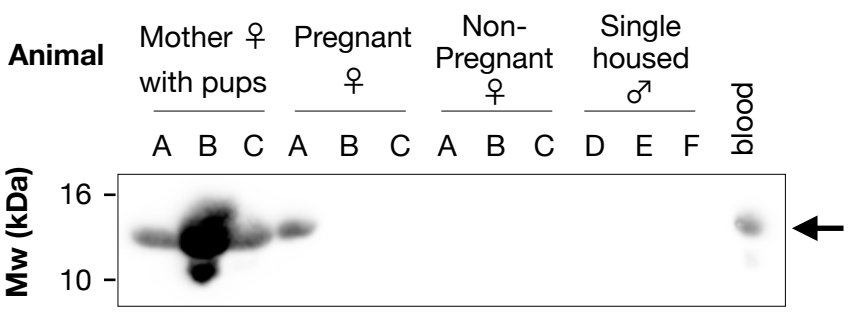

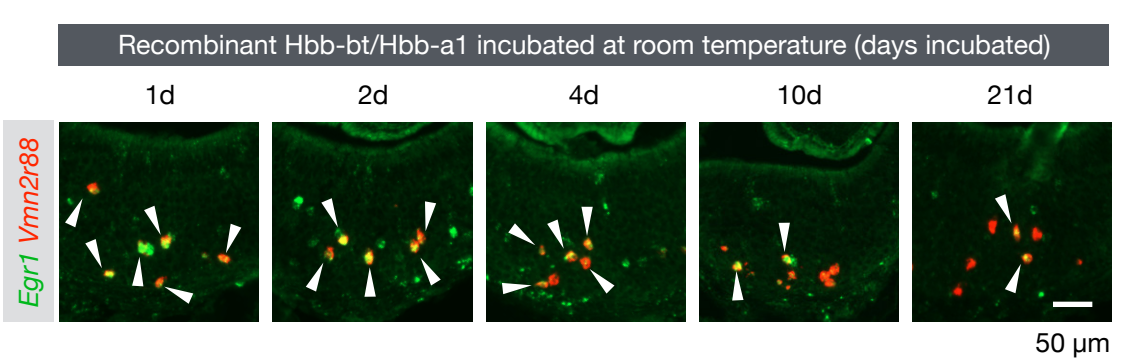

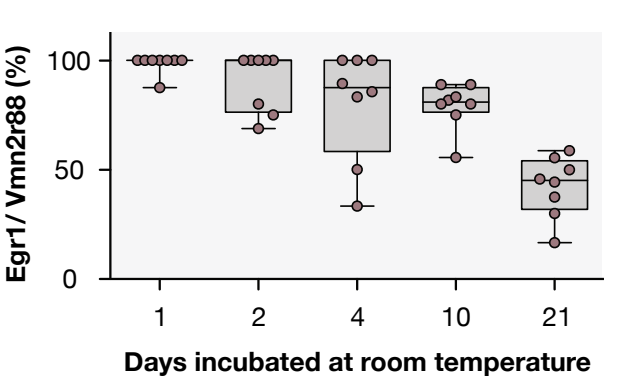

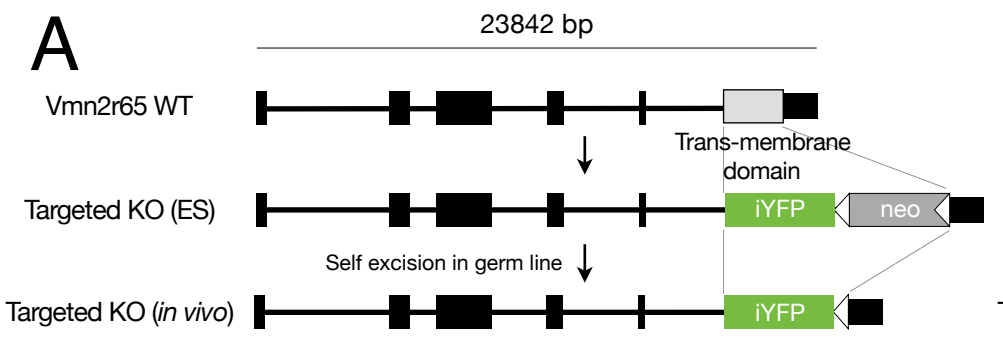
A
23842 bp
Vmn2r65 WT
Trans-membrane domain
Targeted KO (ES)
iYFP
neo
Self excision in germ line
Targeted KO (in vivo)
iYFP

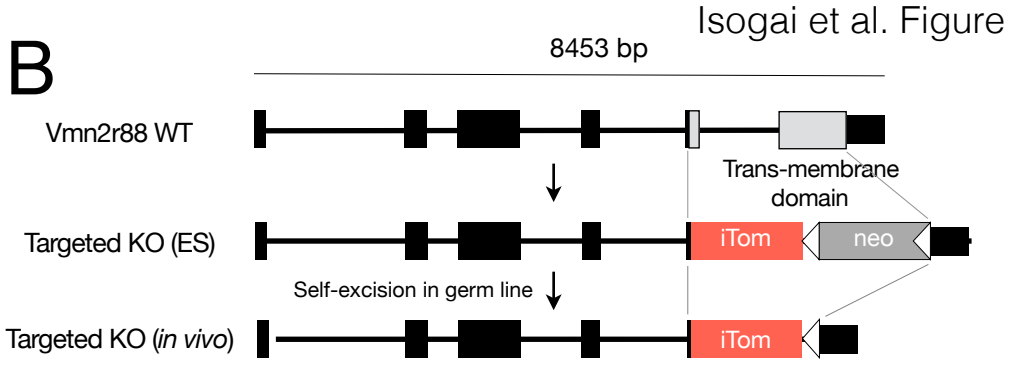
B
8453 bp
Vmn2r88 WT
Trans-membrane domain
Targeted KO (ES)
iTom
neo
Self-excision in germ line
Targeted KO (in vivo)
iTom

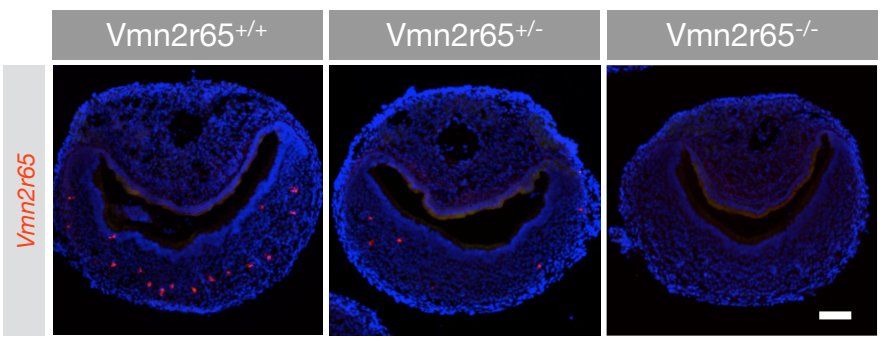
C
Vmn2r65+/+
Vmn2r65+/-
Vmn2r65-/-
Vmn2r65

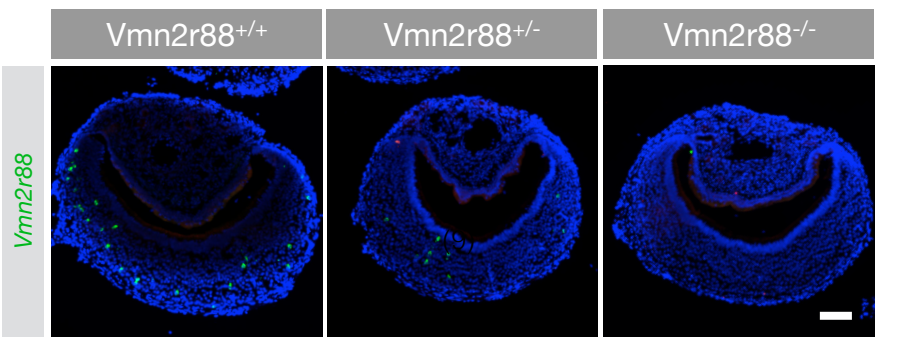
D
Vmn2r88+/+
Vmn2r88+/-
Vmn2r88-/-
Vmn2r88

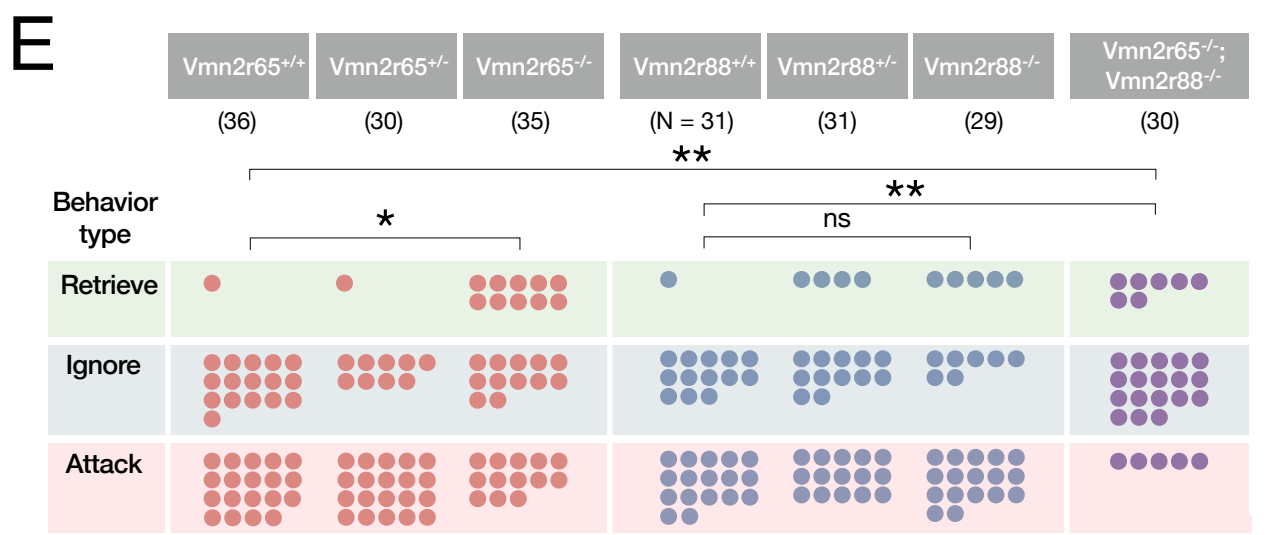
E
Vmn2r65+/+
Vmn2r65+/-
Vmn2r65-/-
Vmn2r88+/+
Vmn2r88+/-
Vmn2r88-/-
Vmn2r65-/-; Vmn2r88-/-
(36)
(30)
(35)
(N = 31)
(31)
(29)
(30)
**
*
**
ns
Behavior type
Retrieve
Ignore
Attack

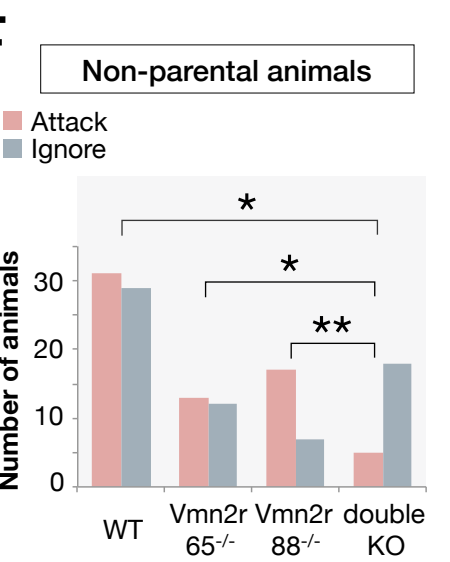
F
Non-parental animals
Attack
Ignore
*
*
**
Number of animals
30
20
10
0
WT
Vmn2r 65-/-
Vmn2r 88-/-
double KO

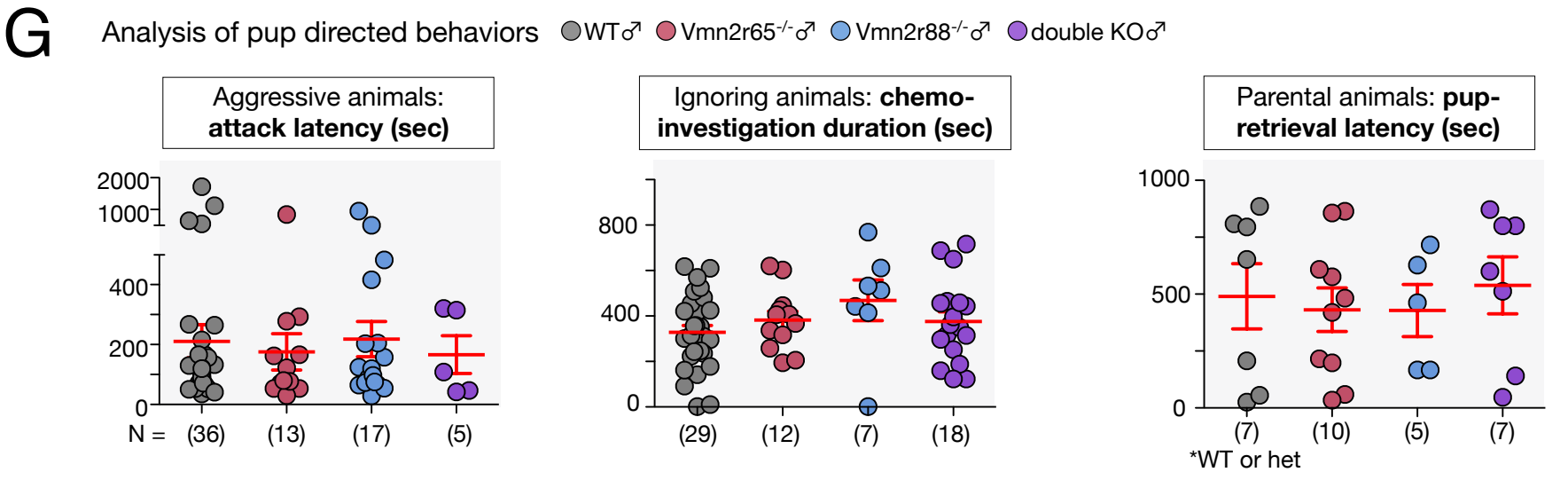
G
Analysis of pup directed behaviors
WT♂
Vmn2r65-/-♂
Vmn2r88-/-♂
double KO♂
Aggressive animals: attack latency (sec)
2000
1000
400
200
0
N =
(36)
(13)
(17)
(5)
Ignoring animals: chemo-investigation duration (sec)
800
400
0
(29)
(12)
(7)
(18)
Parental animals: pup-retrieval latency (sec)
1000
500
0
(7)
(10)
(5)
(7)
*WT or het

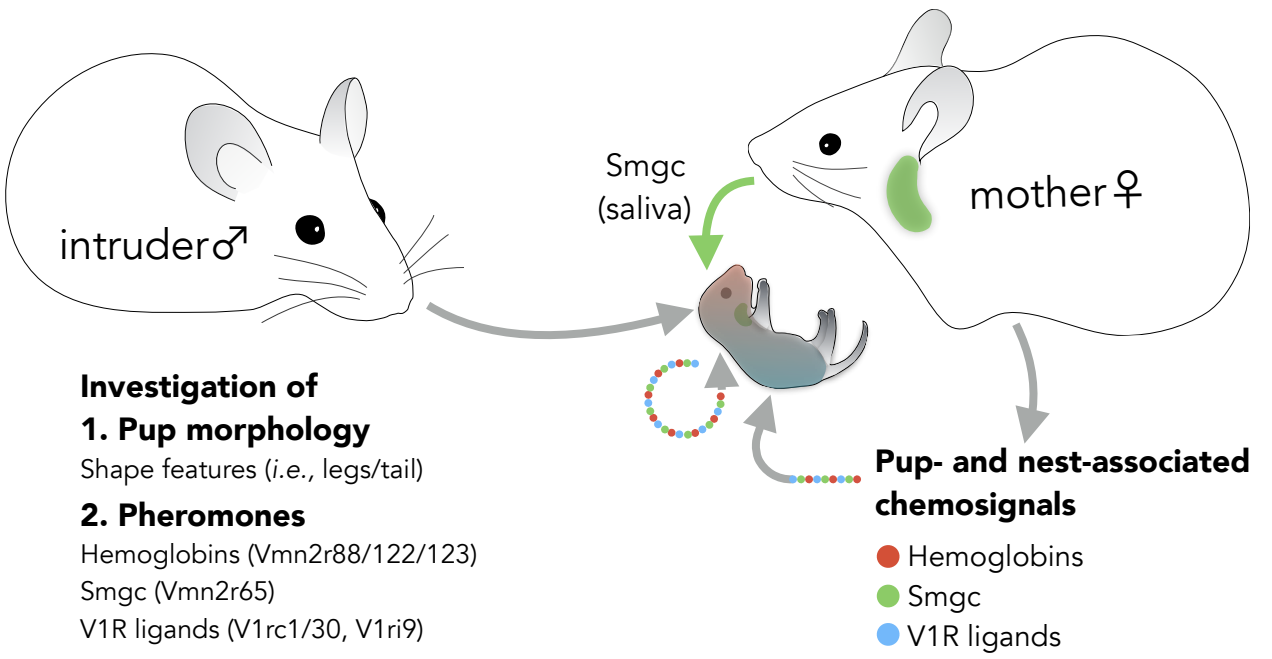
intruder♂
Smgc
(saliva)
mother♀
Investigation of
1. Pup morphology
Shape features (i.e., legs/tail)
2. Pheromones
Hemoglobins (Vmn2r88/122/123)
Smgc (Vmn2r65)
V1R ligands (V1rc1/30, V1ri9)
Pup- and nest-associated chemosignals
Hemoglobins
Smgc
V1R ligands

KEY RESOURCES TABLE

The table highlights the genetically modified organisms and strains, cell lines, reagents, software, and source data **essential** to reproduce results presented in the manuscript. Depending on the nature of the study, this may include standard laboratory materials (i.e., food chow for metabolism studies), but the Table is **not** meant to be comprehensive list of all materials and resources used (e.g., essential chemicals such as SDS, sucrose, or standard culture media don't need to be listed in the Table). **Items in the Table must also be reported in the Method Details section within the context of their use.** The number of **primers and RNA sequences** that may be listed in the Table is restricted to no more than ten each. If there are more than ten primers or RNA sequences to report, please provide this information as a supplementary document and reference this file (e.g., See Table S1 for XX) in the Key Resources Table.

Please note that ALL references cited in the Key Resources Table must be included in the References list. Please report the information as follows:

- **REAGENT or RESOURCE:** Provide full descriptive name of the item so that it can be identified and linked with its description in the manuscript (e.g., provide version number for software, host source for antibody, strain name). In the Experimental Models section, please include all models used in the paper and describe each line/strain as: model organism: name used for strain/line in paper: genotype. (i.e., Mouse: $OXTR^{fl/fl}$: B6.129(SJL)-$Oxtr^{tm1.1Wsy/J}$). In the Biological Samples section, please list all samples obtained from commercial sources or biological repositories. Please note that software mentioned in the Methods Details or Data and Software Availability section needs to be also included in the table. See the sample Table at the end of this document for examples of how to report reagents.

- **SOURCE:** Report the company, manufacturer, or individual that provided the item or where the item can obtained (e.g., stock center or repository). For materials distributed by Addgene, please cite the article describing the plasmid and include "Addgene" as part of the identifier. If an item is from another lab, please include the name of the principal investigator and a citation if it has been previously published. If the material is being reported for the first time in the current paper, please indicate as "this paper." For software, please provide the company name if it is commercially available or cite the paper in which it has been initially described.

- **IDENTIFIER:** Include catalog numbers (entered in the column as "Cat#" followed by the number, e.g., Cat#3879S). Where available, please include unique entities such as RRIDs, Model Organism Database numbers, accession numbers, and PDB or CAS IDs. For antibodies, if applicable and available, please also include the lot number or clone identity. For software or data resources, please include the URL where the resource can be downloaded. Please ensure accuracy of the identifiers, as they are essential for generation of hyperlinks to external sources when available. Please see the Elsevier list of Data Repositories with automated bidirectional linking for details. When listing more than one identifier for the same item, use semicolons to separate them (e.g. Cat#3879S; RRID: AB_2255011). If an identifier is not available, please enter "N/A" in the column.
    - ***A NOTE ABOUT RRIDs:*** We highly recommend using RRIDs as the identifier (in particular for antibodies and organisms, but also for software tools and databases). For more details on how to obtain or generate an RRID for existing or newly generated resources, please visit the RII or search for RRIDs.

Please use the empty table that follows to organize the information in the sections defined by the subheading, skipping sections not relevant to your study. Please do not add subheadings. To add a row, place the cursor at the end of the row above where you would like to add the row, just outside the right border of the table. Then press the ENTER key to add the row. Please delete empty rows. Each entry must be on a separate row; do not list multiple items in a single table cell. Please see the sample table at the end of this document for examples of how reagents should be cited.

TABLE FOR AUTHOR TO COMPLETE

Please upload the completed table as a separate document. ***Please do not add subheadings to the Key Resources Table.*** *If you wish to make an entry that does not fall into one of the subheadings below, please contact your handling editor. (**NOTE:** For authors publishing in Current Biology, please note that references within the KRT should be in numbered style, rather than Harvard.)*

KEY RESOURCES TABLE

REAGENT or RESOURCE	SOURCE	IDENTIFIER
Antibodies		
Phospho-S6 Ribosomal Protein (Ser240/244) Antibody	Cell Signaling Technology	2215BF
Anti-digoxigenin-POD	Roche	11207733910
Anti-fluorescein-POD	Roche	11426346910
Anti-DNP-HRP	Perkin Elmer	FP1129
Anti-rabbit IgG HRP-linked antibody	Cell Signaling Technology	7074P2
Rabbit anti-HBB (, PA5-48233)	Invitrogen	PA5-48233
Donkey anti-rabbit Alexa555 conjugate	Invitrogen	A-31572
Streptavidin-Alexa488 conjugate	Invitrogen or Jackson ImmunoResearch	S11223 or 016-540-084
Bacterial and Virus Strains		
E. coli Rosetta BL2 (DE3)	Novagen	70954
Biological Samples		
Vmn2r65 targeted null mice	This paper	
Vmn2r88 targeted null mice	This paper	
Vmn2r65/Vmn2r88 targeted null mice	This paper	
Chemicals, Peptides, and Recombinant Proteins		
FLAG (DYKDDDDK) peptide	Genscript	RP10586
T7 RNA polymerase	New England Biolabs or Promega	M0251S/L or P2075

Sp6 RNA polymerase	New England Biolabs or Promega	M0207S/L or P1085
T3 RNA polymerase	Promega	P2083
NBT/BCIP	Promega	S3771
Dig RNA labeling mix	Roche	11277073910
Fluorescein RNA labeling mix	Roche	11685619910
DNP-11-UTP	Perkin Elmer	NEL555001EA
Magnetic protein A dynabeads	Invitrogen	10001D
Critical Commercial Assays		
TSA plus biotin kit	Perkin Elmer	NEL749A001KT
TSA plus Cy3 kit	Perkin Elmer	NEL744001KT
SMARTer Ultra Low Input RNA for Illumina Sequencing - HV	Clontech	634826
Low Input Library Prep Kit	Clontech	634947
Deposited Data		
M. musculus reference genome mm10	Ensembl	ftp://ftp.ensembl.org/pub/release-73/fasta/mus_musculus/dna/
RNA-seq raw and analyzed data	This study	GEO: GSE122138
Experimental Models: Cell Lines		
Experimental Models: Organisms/Strains		
Mus musculus, C57BL6/J	The Jackson Laboratory	Stock No:000664
Mus musculus, 129S1/SvImJ	The Jackson Laboratory	Stock No:002448
Mus musculus, CD-1	Charles River	N/A
Mus musculus, TrpC2+/-	Stowers et al. 2002	$Trpc2^{tm1Dlc}$
Oligonucleotides		

Vmn2r65 wild type genotyping primer, forward CTTCATAGCGTTTTTGCCTTC	This study	N/A
Vmn2r65 wild type genotyping primer, reverse TGAGAAGTCGGTTATTCGCC	This study	N/A
Vmn2r65 mutant genotyping primer, forward TAACGGTCCTAAGGTAGCGA	This study	N/A
Vmn2r65 mutant genotyping primer, reverse TCACCCTGAATGCAGGTGTA	This study	N/A
Vmn2r88 wild type genotyping primer, forward GTTTTGTTTGATCAGAAACATAGGTTAATAC	This study	N/A
Vmn2r88 wild type genotyping primer, reverse AGTTCTGTCCTGTTTGTAAGTTCAAATTTGT	This study	N/A
Vmn2r88 mutant genotyping primer, forward TAACGGTCCTAAGGTAGCGA	This study	N/A
Vmn2r88 mutant genotyping primer, reverse TTTTGGTTGAGGACTGGAGT	This study	N/A
Recombinant DNA		
pET28a-hbb-bt-SD-hba-a1-his	This study	N/A
pET28a-his-smgc-flag	This study	N/A
Software and Algorithms		
RNA STAR 2.3.1	Dobin et al. 2013	https://github.com/alexdobin/STAR
DESeq2	Love et al. 2014	https://bioconductor.org/packages/release/bioc/html/DESeq2.html
Rstudio	https://www.rstudio.com/	RRID:SCR_000432
R	http://www.r-project.org/	RRID: SCR_001905
Fiji	http://fiji.sc	RRID: SCR_002285
Samtools	http://samtools.sourceforge.net/	**RRID:SCR_002105**
Prism 5	Graphpad	N/A
Observer XT 14	Noldus	N/A
Other		

Body Double Standard Set	Smooth-On	N/A

TABLE WITH EXAMPLES FOR AUTHOR REFERENCE

REAGENT or RESOURCE	SOURCE	IDENTIFIER
Antibodies		
Rabbit monoclonal anti-Snail	Cell Signaling Technology	Cat#3879S; RRID: AB_2255011
Mouse monoclonal anti-Tubulin (clone DM1A)	Sigma-Aldrich	Cat#T9026; RRID: AB_477593
Rabbit polyclonal anti-BMAL1	This paper	N/A
Bacterial and Virus Strains		
pAAV-hSyn-DIO-hM3D(Gq)-mCherry	Krashes et al., 2011	Addgene AAV5; 44361-AAV5
AAV5-EF1a-DIO-hChR2(H134R)-EYFP	Hope Center Viral Vectors Core	N/A
Cowpox virus Brighton Red	BEI Resources	NR-88
Zika-SMGC-1, GENBANK: KX266255	Isolated from patient (Wang et al., 2016)	N/A
Staphylococcus aureus	ATCC	ATCC 29213
Streptococcus pyogenes: M1 serotype strain: strain SF370; M1 GAS	ATCC	ATCC 700294
Biological Samples		
Healthy adult BA9 brain tissue	University of Maryland Brain & Tissue Bank; http://medschool.umaryland.edu/btbank/	Cat#UMB1455
Human hippocampal brain blocks	New York Brain Bank	http://nybb.hs.columbia.edu/
Patient-derived xenografts (PDX)	Children's Oncology Group Cell Culture and Xenograft Repository	http://cogcell.org/
Chemicals, Peptides, and Recombinant Proteins		
MK-2206 AKT inhibitor	Selleck Chemicals	S1078; CAS: 1032350-13-2
SB-505124	Sigma-Aldrich	S4696; CAS: 694433-59-5 (free base)

Picrotoxin	Sigma-Aldrich	P1675; CAS: 124-87-8
Human TGF-β	R&D	240-B; GenPept: P01137
Activated S6K1	Millipore	Cat#14-486
GST-BMAL1	Novus	Cat#H00000406-P01
Critical Commercial Assays		
EasyTag EXPRESS 35S Protein Labeling Kit	Perkin-Elmer	NEG772014MC
CaspaseGlo 3/7	Promega	G8090
TruSeq ChIP Sample Prep Kit	Illumina	IP-202-1012
Deposited Data		
Raw and analyzed data	This paper	GEO: GSE63473
B-RAF RBD (apo) structure	This paper	PDB: 5J17
Human reference genome NCBI build 37, GRCh37	Genome Reference Consortium	http://www.ncbi.nlm.nih.gov/projects/genome/assembly/grc/human/
Nanog STILT inference	This paper; Mendeley Data	http://dx.doi.org/10.17632/wx6s4mj7s8.2
Affinity-based mass spectrometry performed with 57 genes	This paper; and Mendeley Data	Table S8; http://dx.doi.org/10.17632/5hvpvspw82.1
Experimental Models: Cell Lines		
Hamster: CHO cells	ATCC	CRL-11268
D. melanogaster: Cell line S2: S2-DRSC	Laboratory of Norbert Perrimon	FlyBase: FBtc0000181
Human: Passage 40 H9 ES cells	MSKCC stem cell core facility	N/A
Human: HUES 8 hESC line (NIH approval number NIHhESC-09-0021)	HSCI iPS Core	hES Cell Line: HUES-8
Experimental Models: Organisms/Strains		
C. elegans: Strain BC4011: srl-1(s2500) II; dpy-18(e364) III; unc-46(e177)rol-3(s1040) V.	Caenorhabditis Genetics Center	WB Strain: BC4011; WormBase: WBVar00241916
D. melanogaster: RNAi of Sxl: y[1] sc[*] v[1]; P{TRiP.HMS00609}attP2	Bloomington Drosophila Stock Center	BDSC:34393; FlyBase: FBtp0064874
S. cerevisiae: Strain background: W303	ATCC	ATTC: 208353
Mouse: R6/2: B6CBA-Tg(HDexon1)62Gpb/3J	The Jackson Laboratory	JAX: 006494
Mouse: OXTRfl/fl: B6.129(SJL)-Oxtr$^{tm1.1Wsy}$/J	The Jackson Laboratory	RRID: IMSR_JAX:008471
Zebrafish: Tg(Shha:GFP)t10: t10Tg	Neumann and Nuesslein-Volhard, 2000	ZFIN: ZDB-GENO-060207-1

Arabidopsis: 35S::PIF4-YFP, BZR1-CFP	Wang et al., 2012	N/A
Arabidopsis: JYB1021.2: pS24(AT5G58010)::cS24:GFP(-G):NOS #1	NASC	NASC ID: N70450
Oligonucleotides		
siRNA targeting sequence: PIP5K I alpha #1: ACACAGUACUCAGUUGAUA	This paper	N/A
Primers for XX, see Table SX	This paper	N/A
Primer: GFP/YFP/CFP Forward: GCACGACTTCTTCAAGTCCGCCATGCC	This paper	N/A
Morpholino: MO-pax2a GGTCTGCTTTGCAGTGAATATCCAT	Gene Tools	ZFIN: ZDB-MRPHLNO-061106-5
ACTB (hs01060665_g1)	Life Technologies	Cat#4331182
RNA sequence: hnRNPA1_ligand: UAGGGACUUAGGGUUCUCUCUAGGGACUUAGGGUUCUCUCUAGGGA	This paper	N/A
Recombinant DNA		
pLVX-Tight-Puro (TetOn)	Clonetech	Cat#632162
Plasmid: GFP-Nito	This paper	N/A
cDNA GH111110	Drosophila Genomics Resource Center	DGRC:5666; FlyBase:FBcl0130415
AAV2/1-hsyn-GCaMP6- WPRE	Chen et al., 2013	N/A
Mouse raptor: pLKO mouse shRNA 1 raptor	Thoreen et al., 2009	Addgene Plasmid #21339
Software and Algorithms		
Bowtie2	Langmead and Salzberg, 2012	http://bowtie-bio.sourceforge.net/bowtie2/index.shtml
Samtools	Li et al., 2009	http://samtools.sourceforge.net/
Weighted Maximal Information Component Analysis v0.9	Rau et al., 2013	https://github.com/ChristophRau/wMICA
ICS algorithm	This paper; Mendeley Data	http://dx.doi.org/10.17632/5hvpvspw82.1
Other		
Sequence data, analyses, and resources related to the ultra-deep sequencing of the AML31 tumor, relapse, and matched normal.	This paper	http://aml31.genome.wustl.edu
Resource website for the AML31 publication	This paper	https://github.com/chrisamiller/aml31SuppSite

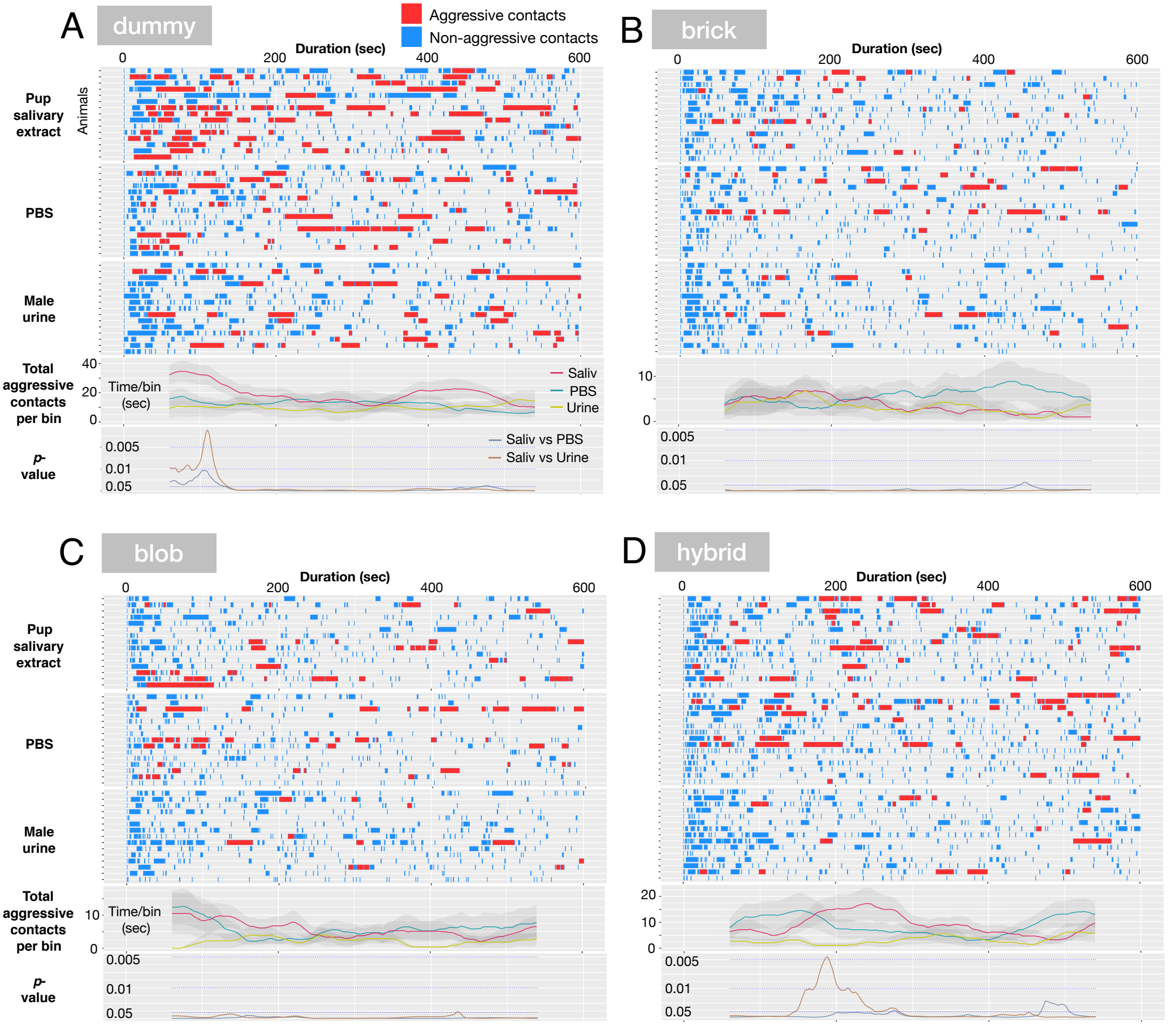
A
dummy
Aggressive contacts
Non-aggressive contacts
Duration (sec)
0
200
400
600
Pup salivary extract
Animals
PBS
Male urine
Total aggressive contacts per bin
40
20
0
Time/bin (sec)
Saliv
PBS
Urine
p-value
0.005
0.01
0.05
Saliv vs PBS
Saliv vs Urine
B
brick
10
0
C
blob
D
hybrid
20
10

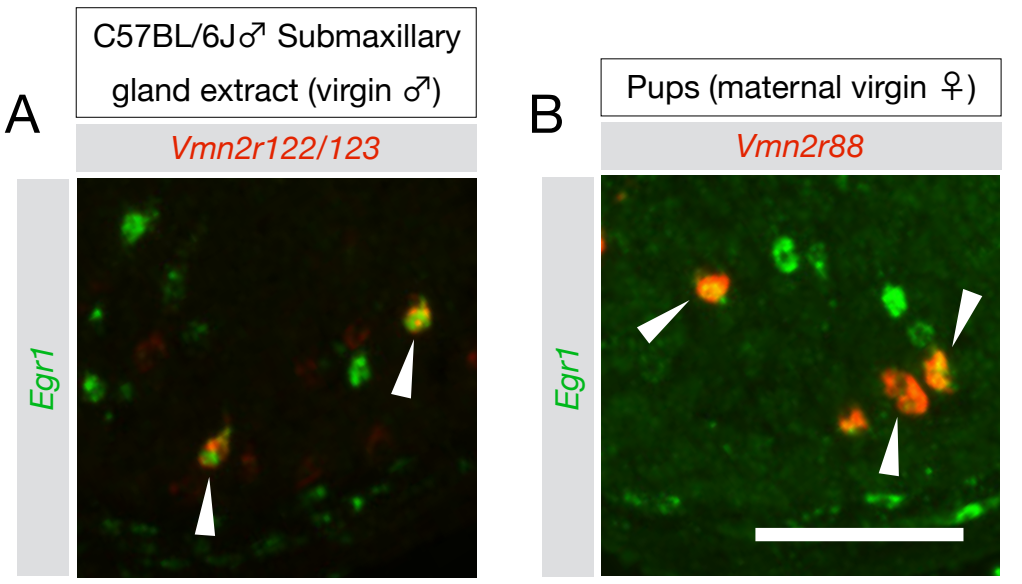
A
C57BL/6J♂ Submaxillary gland extract (virgin ♂)
Vmn2r122/123
Egr1
B
Pups (maternal virgin ♀)
Vmn2r88
Egr1

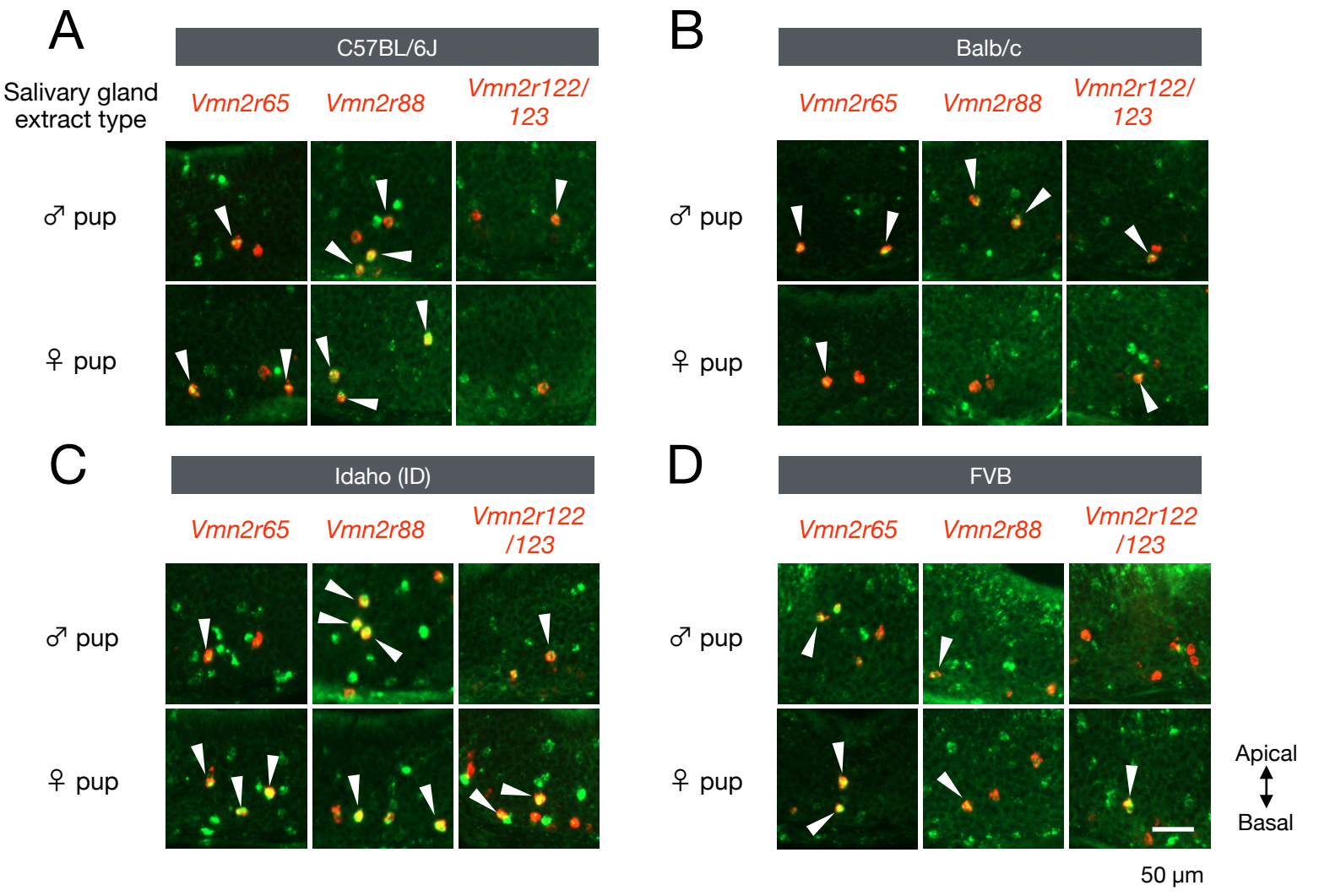

E % *Egr1* positive cells in receptor positive cells
(n = number of receptor positive neurons quantified)

		Vmn2r65			
salivary gland extract type	Strain	**C57BL/6J**	**ID**	**Balb/c**	**FVB**
	♂ pup	51.1±5.6 (n=63)	46.5±22.7 (n=47)	33.6±3.2 (n=47)	58.3±6.2 (n=54)
	♀ pup	57.5±17.0 (n=88)	90.5±0.5 (n=52)	56.8±0.8 (n=77)	71.0±8.5 (n=58)

		Vmn2r88			
salivary gland extract type	Strain	**C57BL/6J**	**ID**	**Balb/c**	**FVB**
	♂ pup	53.7±7.8 (n=113)	58.6±41.4 (n=72)	45.8±20.8 (n=71)	39.4±18.6 (n=55)
	♀ pup	36.2±15.6 (n=128)	95.5±4.5 (n=76)	7.1±7.1 (n=79)	41.0±31.9 (n=70)

		Vmn2r122/123			
salivary gland extract type	Strain	**C57BL/6J**	**ID**	**Balb/c**	**FVB**
	♂ pup	42.2±2.2 (n=28)	53.8±46.2 (n=24)	57.2±29.4 (n=31)	24.8±16.8 (n=62)
	♀ pup	40.6±23.8 (n=54)	65.0±15.0 (n=34)	67.0±9.9 (n=26)	23.4±14.7 (n=44)

A

Description	# Unique Peptides	MW [kDa]	Salivary gland selective ?	Secreted ?
WD repeat-containing protein 1, GN=Wdr1	26	66.4	n	n
Moesin GN=Msn	8	67.7	n	n
Phosphoglycerate mutase 1 GN=Pgam1	10	28.8	n	n
Radixin GN=Rdx	6	68.5	n	n
Isoform 3 of Submandibular gland protein C GN=Muc19/ Smgc	**6**	**70.8**	**y**	**y**
Serine--tRNA ligase, cytoplasmic (Fragment) GN=Sars	6	40.1	n	n
Peroxiredoxin-2 GN=Prdx2	5	21.8	n	n
Triosephosphate isomerase GN=Tpi1	5	18.0	n	n
Androgen binding protein alpha GN=Scgb1b27	4	10.1	y	y
MCG117626 GN=Obp1a	3	18.5	y	y
Ezrin GN=Ezr	1	69.4	n	n
Alpha-1B-glycoprotein GN=A1bg	2	56.5	unknown	y
Protein Obp1b GN=Obp1b	3	19.4	y	y

B

Description	# Unique Peptides	MW [kDa]
Isoform 3 of Submandibular gland protein C GN=Muc19/ Smgc	**19**	64.57

[K].ILEQITSAPGGSVSSAVENLK.[A]
[K].GIVEPITSAAGGSVSSAVENLK.[A]
[R].GSLNVNPLSGLSTK.[S]
[K].ILEQITSAPGGSAERPNAQSSNNLSGK.[L]
[K].KFIEPLTEDHGPTSTSASVSGDSSTSSR.[L]
[K].QNVESSNSSTGSATSNGGGDSNEVR.[G]
[K].QNVEDSTLSTGSATSNEGDDK.[S]
[R].SNVSTGGEPSDKNEPADPGVSGR.[V]
[R].GPSSSAVDSTDSGDRGNLADK.[Q]
[K].SSDNSSNTFREDLEK.[I]
[K].VSGDDPTVQGHDVAASDGSK.[Q]
[R].GPSSSAVDSTDSGDR.[G]
[K].FLEEQYGQTGTDASVSGMSSESSR.[S]
[K].FIEPLTEDHGPTSTSASVSGDSSTSSR.[L]
[K].QGPGFNGPEGVGENNGGSFR.[A]
[K].SDSGSHNLSSGSGSR.[S]
[R].SNVHLSDGFSMESGDDATVQGQQAAASGGPK.[Q]
[K].SGNDATVQGQQAAASGGSK.[H]
[R].LDGHSSDGLSK.[V]

A

Uniprot id	Hits in C57BL6/J male salivary gland (**ACTIVE**)	Coverage (%)	C57BL6/J female salivary gland (**ACTIVE**)	129S1 male salivary gland (**LESS ACTIVE**)
A8DUK4	**Beta-globin GN=Hbbt1**	**100.00**	**y**	**low**
Q91VB8	Alpha globin 1 GN=haemaglobin alpha 2	93.66	y	y
P02089	Hemoglobin subunit beta-2 GN=Hbb-b2	44.90	y	y
P15949	Kallikrein 1-related peptidase b9 GN=Klk1b9	75.48	y	y
P36369	Kallikrein 1-related peptidase b26 GN=Klk1b26 (egfbp-2)	74.71	n	n
P00755	Kallikrein 1-related peptidase b1 GN=Klk1b1	63.98	y	y
P00756	Kallikrein 1-related peptidase b3 GN=Klk1b3	65.90	y	y
P04071	Kallikrein 1-related peptidase b16 GN=Klk1b16	60.92	y	y
P15946	Kallikrein 1-related peptidase b11 GN=Klk1b11	53.26	y	y
Q61759	Kallikrein 1-related peptidase b21 GN=Klk1b21	42.15	n	y
P15948	Kallikrein 1-related peptidase b22 GN=Klk1b22	54.44	y	n
P01132	Pro-epidermal growth factor GN=Egf	26.87	y	y
Q61754	Kallikrein 1-related peptidase b24 GN=Klk1b24	41.83	n	n
Q9JM71	Kallikrein 1-related peptidase b27 GN=Klk1b27	43.35	y	y
P15945	Kallikrein 1-related peptidase b5 GN=Klk1b5	52.87	n	n

B

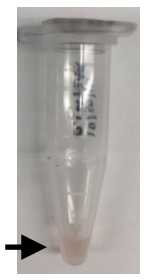

C

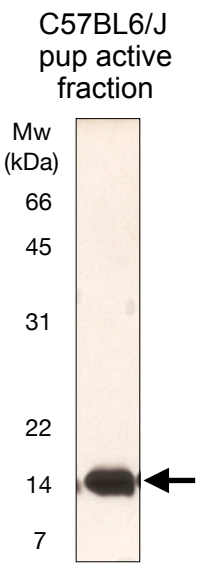

D

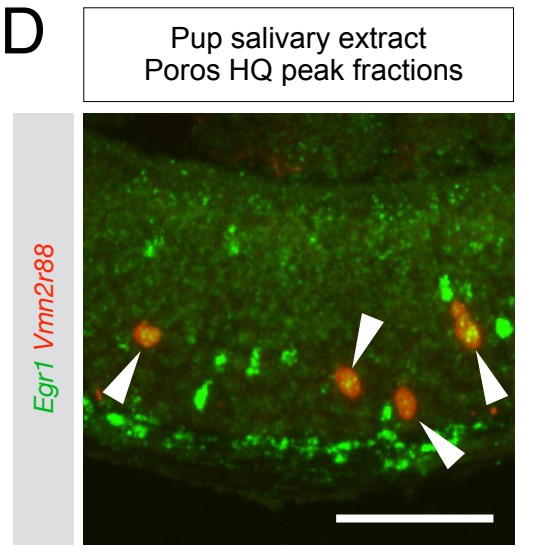

E

Description	# Unique Peptides	MW [kDa]
Beta-globin GN=Hbbt1	**16**	**15.738**
[K].DFTPAAQAAFQK.[V]		
[K].GTFASLSELHCDK.[L]		
[K].AAVSGLWGK.[V]		
[K].KVITAFNDGLNHLDSLK.[G]		
[R].LLGNMIVIVLGHHLGK.[D]		
[R].YFDSFGDLSSASAIMGNAK.[V]		
[K].AAVSGLWGKVNADEVGGEALGR.[L]		
[R].LLGNMIVIVLGHHLGK.[D]		
[K].GTFASLSELHCDKLHVDPENFR.[L]		
[K].KVITAFNDGLNHLDSLK.[G]		
[R].LLVVYPWTQR.[YF]		
[K].VITAFNDGLNHLDSLK.[G]		
Alpha globin 1 GN=haemaglobin alpha 2	**7**	**15.103**
[R].MFASFPTTK.[T]		
[K].TYFPHFDVSHGSAQVK.[G]		
[K].FLASVSTVLTSK.[Y]		
[K].LLSHCLLVTLASHHPADFTPAVHASLDK.[F]		
[K].KVADALANAAGHLDDLPGALSALSDLHAHK.[L]		
[K].IGGHGAEYGAEALER.[M]		
[K].VADALANAAGHLDDLPGALSALSDLHAHK.[L]		

F

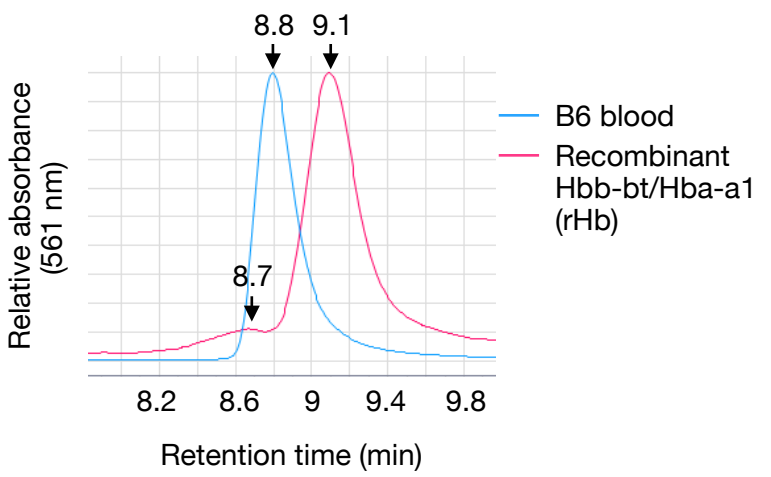

G

	Mean	Std dev	# rep
B6 blood (tetramer)	9.084	0.008	3
rHb (tetramer)	8.636	0.016	3
rHb (dimer)	8.785	0.011	3

*** ***

***$p < 0.0001$ by t-Test

A Analysis of pup-directed behaviors ● WT♂ ● +/-♂ ○ -/-♂ ● double KO♂

Aggressive animals

Attack latency (sec)

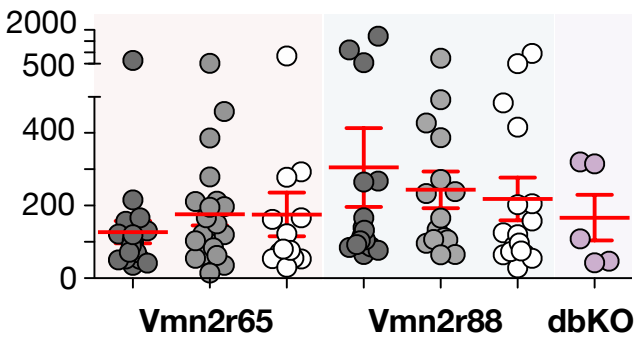

Ignoring animals

Chemoinvestigation duration (sec)

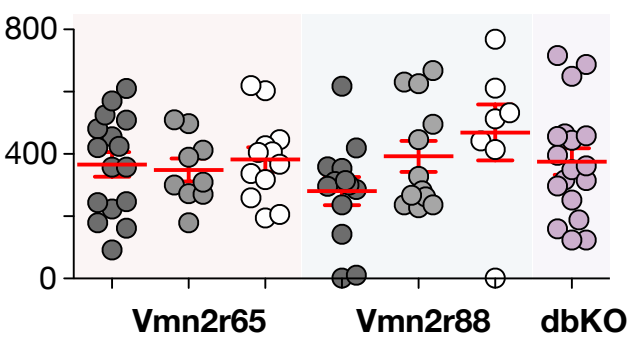

Chemoinvestigation events (number)

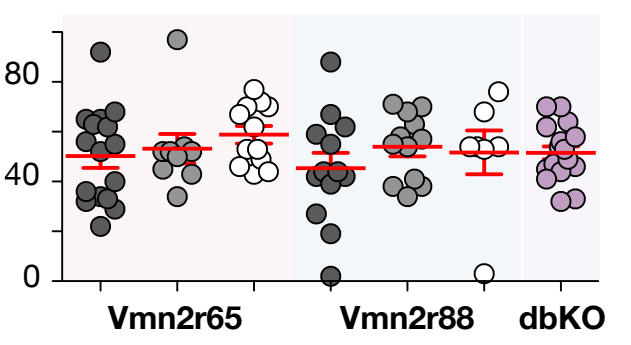

Parental animals

Pup retrieval latency (sec)

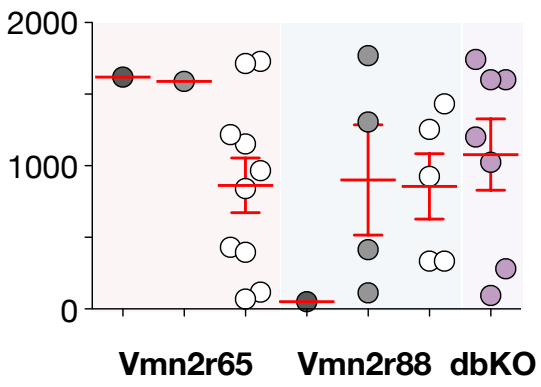

Nest building duration (sec)

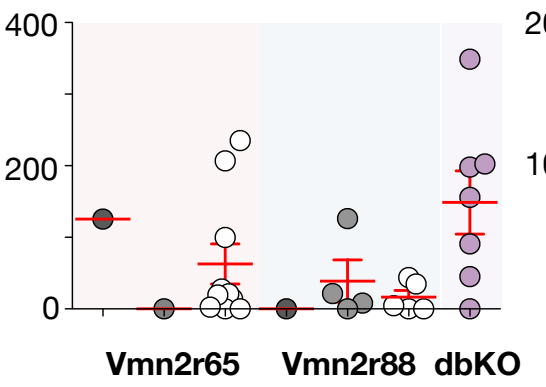

Inside nest duration (sec)

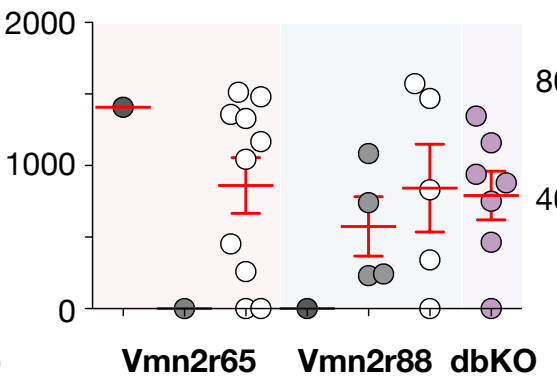

Crouching over pups duration (sec)

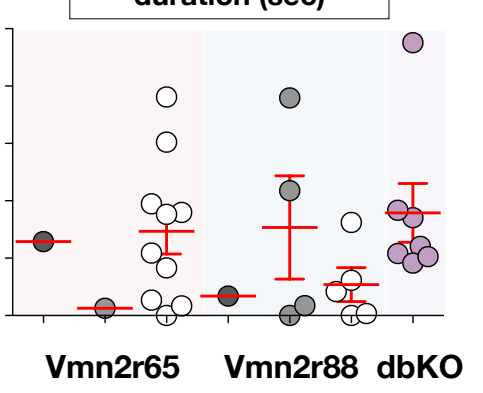

B Analysis of male mating behavior ● WT or Vmn2r65$^{+/-}$♂ ● Vmn2r65$^{-/-}$♂

Latency to mount (sec)

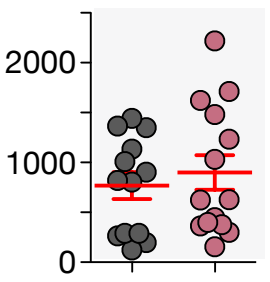

Number of mounts

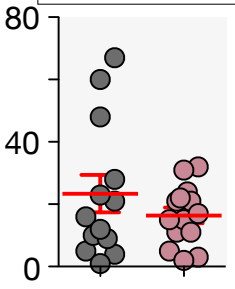

Mounting duration (sec)

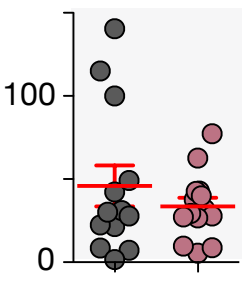

Intromission latency (sec)

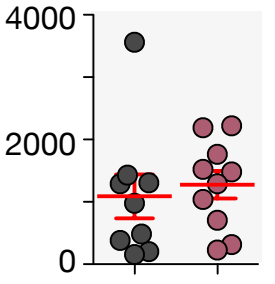

Number of intromission

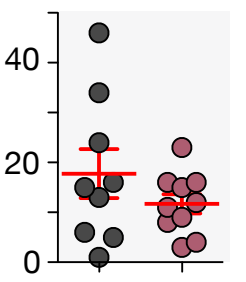

Intromission duration (sec)

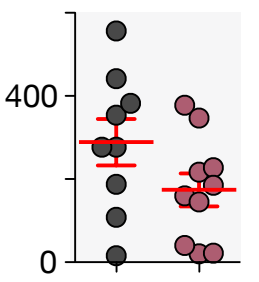

Number of chemoinvesti-gative events

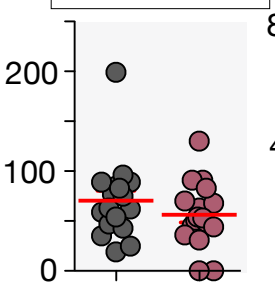

Chemoinvesti-gation duration (sec)

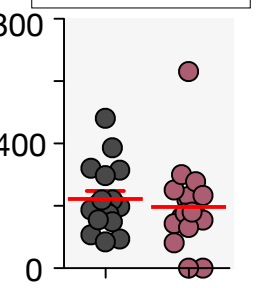

C Analysis of inter-male aggression ● WT♂ ● double KO♂

Total number of attacking animals

Genotype	N	# Attacking	% Attacking
WT	13	12	92.3
Vmn2r65$^{-/-}$; Vmn2r88$^{-/-}$	20	14	70

p = 0.20

Latency to attack (sec)

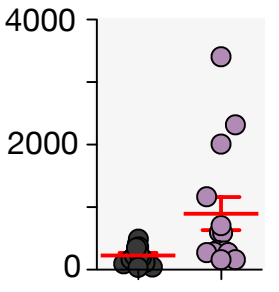

Number of attacks

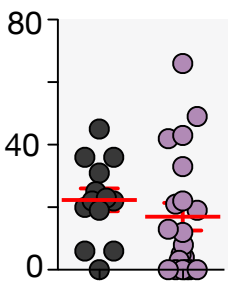

Attack duration (sec)

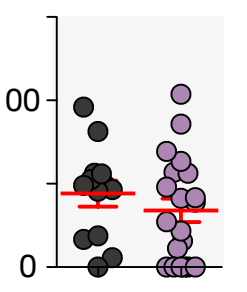

Latency to chemoinvestigate (sec)

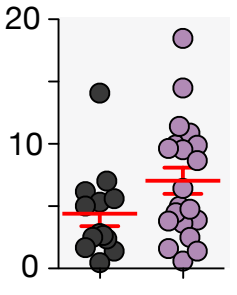

Number of chemoinvestigative events

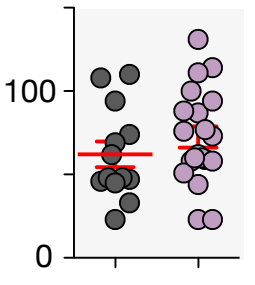

Chemoinvestigation duration (sec)

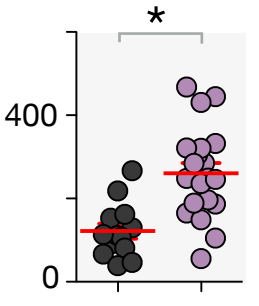

Grooming duration (sec)

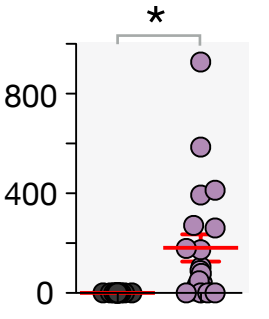

Feature type	Specific stimuli used	Where stimulus is produced	Where stimulus is found	Sensory modality	Receptors
Physical	Pup-like morphology	Shape	pup body, fine features such as limbs and tails	tactile?	not known
Chemical	Smgc	♀ and pup salivary gland	on pup, ♀/pup bedding	VNO	Vmn2r65
	Hemoglobins	erythroid cells others?	on pup, ♂ and ♀/pup bedding	VNO	Vmn2r88,122,123
	V1R ligands	not known	on pup, ♀/pup bedding	VNO	V1rc1, c30, i9